

MULTISPECTRAL PALM VEIN IMAGE
FUSION FOR CONTACTLESS PALM VEIN
VERIFICATION SYSTEM



SOH SHI CHUAN

UMP

Master Of Science

UNIVERSITI MALAYSIA PAHANG

UNIVERSITI MALAYSIA PAHANG

DECLARATION OF THESIS AND COPYRIGHT

Author's Full Name : SOH SHI CHUAN

Date of Birth : 15TH DECEMBER 1992

Title : MULTISPECTRAL PALM VEIN IMAGE FUSION FOR CONTACTLESS PALM VEIN VERIFICATION SYSTEM

Academic Session : SEMESTER 1 2018/2019

I declare that this thesis is classified as:

- CONFIDENTIAL (Contains confidential information under the Official Secret Act 1997)*
- RESTRICTED (Contains restricted information as specified by the organization where research was done)*
- OPEN ACCESS I agree that my thesis to be published as online open access (Full Text)

I acknowledge that Universiti Malaysia Pahang reserves the following rights:

1. The Thesis is the Property of Universiti Malaysia Pahang
2. The Library of Universiti Malaysia Pahang has the right to make copies of the thesis for the purpose of research only.
3. The Library has the right to make copies of the thesis for academic exchange.

Certified by:

(Student's Signature)

(Supervisor's Signature)

921215-06-5749
New IC/Passport Number
Date:

Name of Supervisor
Date:

NOTE : * If the thesis is CONFIDENTIAL or RESTRICTED, please attach a thesis declaration letter.

SUPERVISOR'S DECLARATION

I hereby declare that I have checked **this thesis** and in my opinion, this thesis is adequate in terms of scope and quality for the award of the degree of Master of Science.

(Supervisor's Signature)

Full Name : DR ZAMRI BIN IBRAHIM

Position : SENIOR LECTURER

Date :

(Co-supervisor's Signature)

Full Name : MARLINA BINTI YAKNO

Position : SENIOR LECTURER

Date :

STUDENT'S DECLARATION

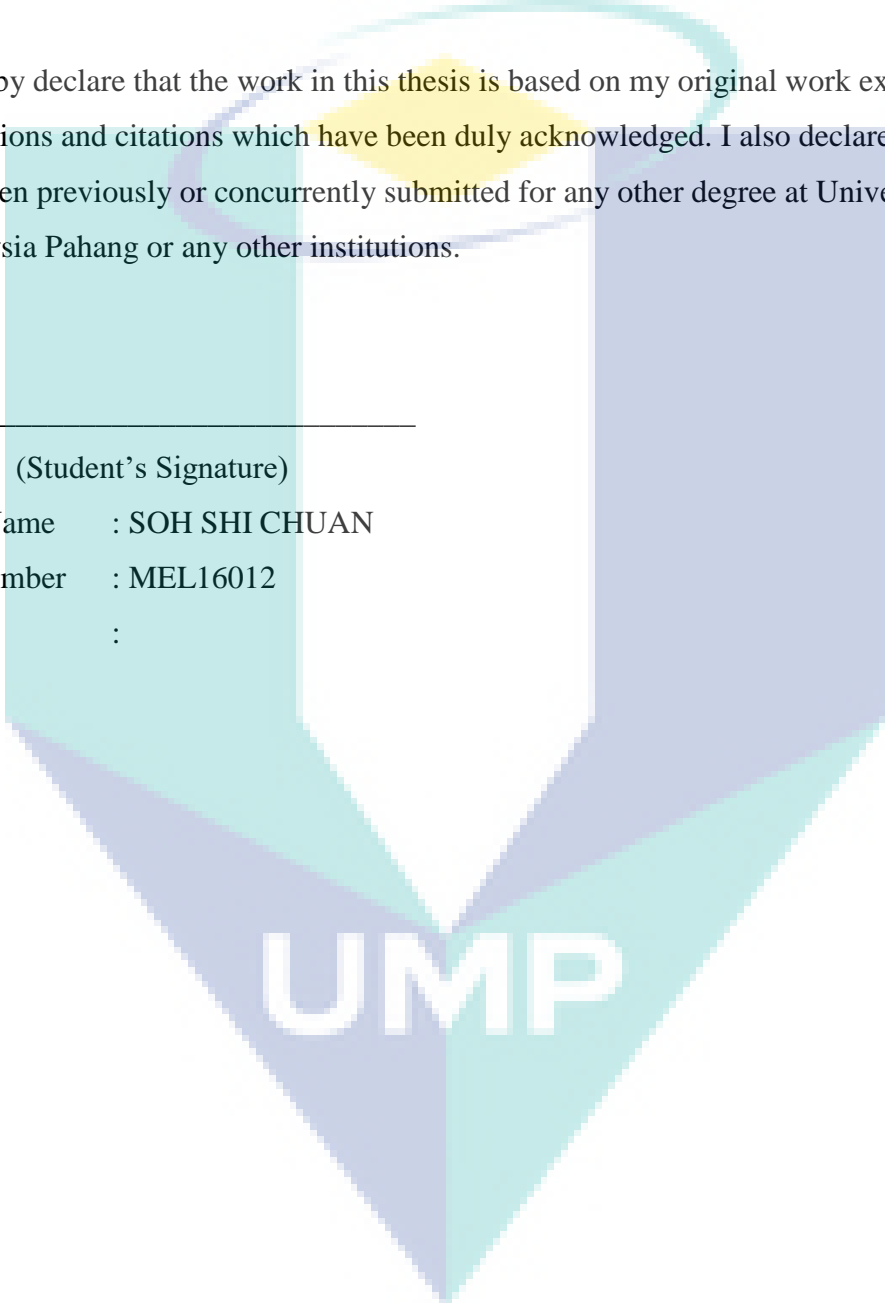
I hereby declare that the work in this thesis is based on my original work except for quotations and citations which have been duly acknowledged. I also declare that it has not been previously or concurrently submitted for any other degree at Universiti Malaysia Pahang or any other institutions.

(Student's Signature)

Full Name : SOH SHI CHUAN

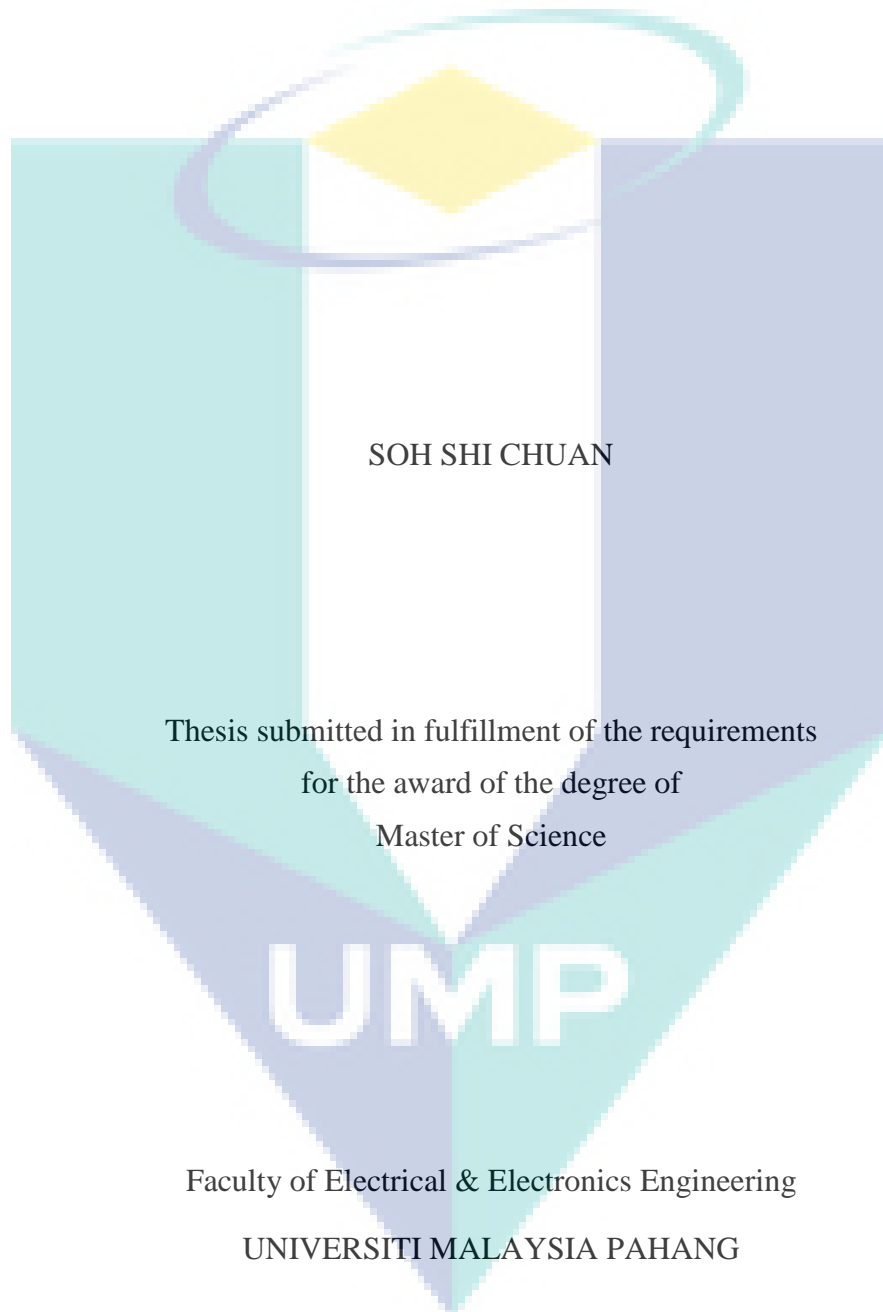
ID Number : MEL16012

Date :



UMP

MULTISPECTRAL PALM VEIN IMAGE FUSION FOR CONTACTLESS PALM
VEIN VERIFICATION SYSTEM



DECEMBER 2018

ACKNOWLEDGEMENTS

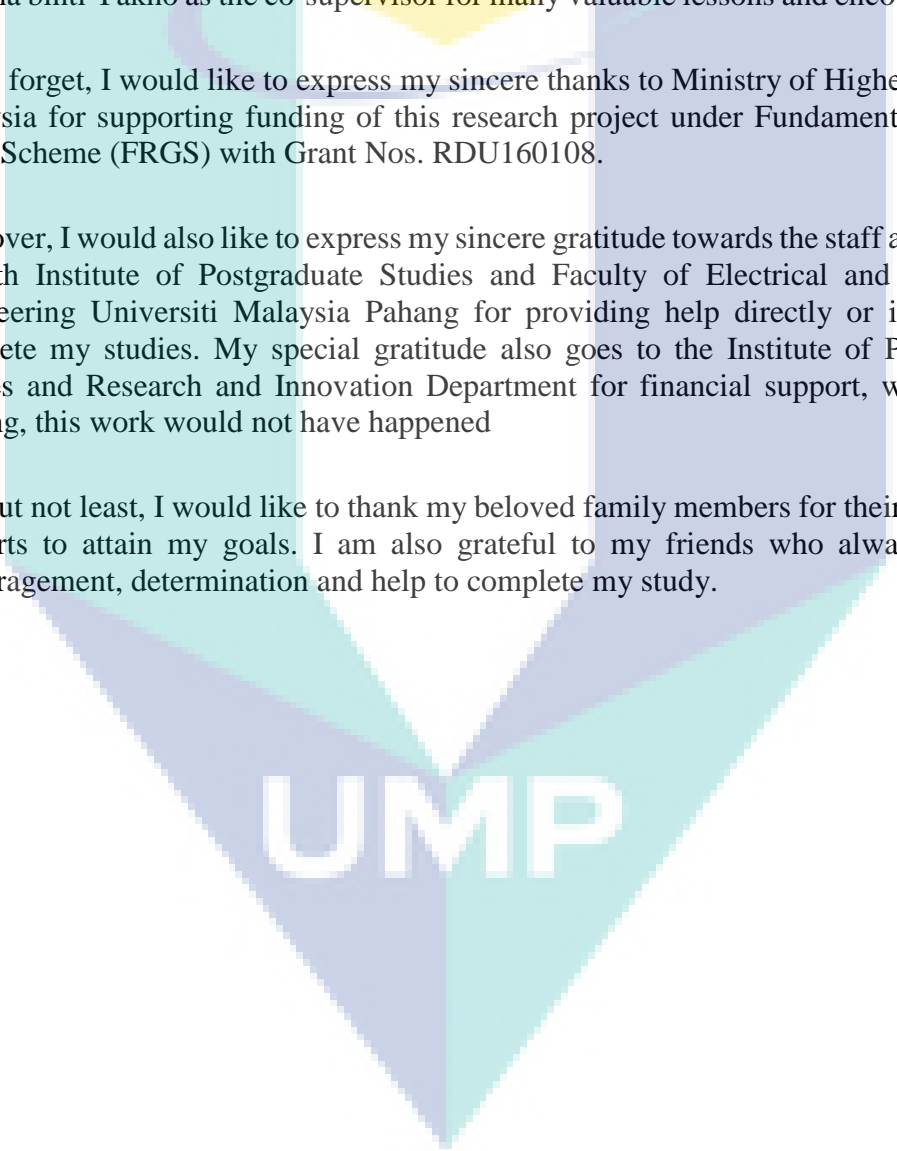
First and foremost, I am very grateful and thankful to God for giving me the strength and wisdom to discover and complete my graduate program. Under His guidance and blessing, I am able to complete my graduate study smoothly.

I would like to express my sincere gratitude to my supervisor, Dr. Mohd Zamri bin Ibrahim for giving me the opportunity and full support to complete my graduate study under his supervision. His continuous guidance, encouragement and relentlessly giving support and ideas, makes this research to be successful. I am also very grateful to Mrs Marlina binti Yakno as the co-supervisor for many valuable lessons and encouragements.

Not to forget, I would like to express my sincere thanks to Ministry of Higher Education Malaysia for supporting funding of this research project under Fundamental Research Grant Scheme (FRGS) with Grant Nos. RDU160108.

Moreover, I would also like to express my sincere gratitude towards the staff and lecturers of both Institute of Postgraduate Studies and Faculty of Electrical and Electronics Engineering Universiti Malaysia Pahang for providing help directly or indirectly to complete my studies. My special gratitude also goes to the Institute of Postgraduate Studies and Research and Innovation Department for financial support, without their funding, this work would not have happened

Last but not least, I would like to thank my beloved family members for their continuous supports to attain my goals. I am also grateful to my friends who always give me encouragement, determination and help to complete my study.



UMP

ABSTRAK

Sistem pengesanan biometrik semakin memberi perhatian dengan usaha untuk melindungi keselamatan dan maklumat kami dalam dunia penyamaran digital ini. Pengesanan urat tapak tangan adalah pengesanan biometrik yang terkenal kerana biometric ini menunjukkan tahap pengesanan yang tinggi. Walau bagaimanapun, kerumitan dan keunikan corak urat tapak tangan menyebabkan pengesanan yang kurang tepat. Imej berkualiti rendah akan memberi kesan kepada proses sistem walaupun proses pengekstrakan ciri urat tapak tangan adalah sempurna. Ini adalah sebab daripada imej kontras yang tidak jelas dan rendah. Terdapat kajian yang dibuat menunjukkan bahawa kemungkinan menggunakan kaedah gabungan imej akan meningkatkan ketepatan pengiktirafan ke tahap yang lebih tinggi. Imej gabungan adalah satu kaedah dengan mengumpulkan maklumat penting dari semua imej dan membuat imej baru yang mempunyai maklumat penting dari semua imej. Gabungan imej dapat memberi maklumat penting dengan meningkatkan kualiti dan kebolegunaan data daripada imej input tunggal sahaja. Dalam tesis ini, Discrete Cosine Transform (DCT) adalah salah satu algoritma gabungan imej yang dicadangkan dalam pengesanan urat tapak tangan. Imej akan dibahagikan kepada blok yang berturut-turut dan akan ubah menjadi pekali DCT. Pekali DCT akan melalui peraturan fusion dan akan diubah kembali ke imej gabungan dengan menggunakan IDCT. Dalam tesis ini, pangkalan data CASIA digunakan untuk memberi tiga jenis spectrum iaitu 700 nm, 850 nm dan 940 nm. Terdapat empat kombinasi gabungan imej yang boleh dibentuk dalam tesis ini iaitu kombinasi dua imej 700 nm dengan 850nm, 700 nm dengan 940 nm, dan 850 nm dengan 940 nm dan juga gabungan tiga imej dengan semua jenis spektrum. Gabungan imej dengan Multi-resolution DCT (MRDCT), DCT Partition Frequency DCT (FPDCT) dan Laplacian Pyramid DCT (LPDCT) diperkenalkan untuk menggabungkan maklumat dari pelbagai jenis spektrum jarak dan memberikan imej output yang lebih jelas dalam corak vein tapak tangan. Dalam tesis ini, gabungan imej antara tiga jenis spektrum mencapai tahap yang lebih baik daripada gabungan imej antara dua jenis spektrum. MRDCT melakukan kadar EER yang terbaik 5.53% berbanding dengan FPDCT dan LPDCT dalam imej gabungan tiga jenis spectrum. Kaedah konvensional seperti Multi-resolution Singular Value Decomposition (MSVD), Wavelet Transform dan Energy of Laplacian (EOL) hanya dapat mencapai kadar EER sebanyak 6.58%, 6.83% dan 8.64% masing-masing. Di samping itu, MRDCT dengan gabungan tiga jenis spektrum menunjukkan penurunan kadar EER sebanyak 9% berbanding dengan imej 700 nm tunggal, 7% berbanding dengan imej 850 nm tunggal, dan 6% berbanding dengan imej tunggal 940 nm. Ia membuktikan bahawa gabungan imej MRDCT sesuai untuk pengesanan urat tapak tangan. Terdapat dua jenis keadah Scale Invariant Feature Transform (SIFT) and Speeded Up Robust Feature (SURF) berdasarkan pengekstrakan ciri urat tapak tangan disiasat. Algoritma SIFT mencapai penurunan kadar EER sebanyak 12% pada 700 nm, 8% pada 850 nm, 7% pada 940 nm berbanding dengan algoritma SURF. Hasilnya menunjukkan bahawa algoritma SIFT mencapai kadar pengesanan yang lebih baik dan mengekstrak lebih banyak maklumat dan pasangan sepadan berbanding dengan algoritma SURF. Sebagai kesimpulan, gabungan imej MRDCT dengan pengekstrakan SIFT sesuai digunakan dalam sistem pengesanan biometric urat tapak tangan tanpa sentuhan sensor.

ABSTRACT

Biometrics recognition system are getting more attention in efforts to protect our security and information in this world of digital impersonation. Palm vein recognition are well-known in biometrics recognition where it shows a high level of authentication. However, there is still an unsolved issued in accuracy due to the complexity and uniqueness of palm vein pattern. Low quality image provides unclear and low contrast image affecting the process although palm vein feature extraction is perfect. There were studies to investigate the possibility that fusion methods would improve or enhance the accuracy to a higher level. Image fusion is a method to collect necessary information from all input image with different sources and create an output image that ideally has information from input image. Fused image can provide more information than single input image that improve quality and applicability of data. In this work, image fusion algorithms based on Discrete Cosine Transform (DCT) in palm vein recognition is proposed. Input image will be divided into consecutive blocks and transformed into DCT coefficients. Fusion rule will be applied within the DCT coefficients and transformed back into fused image using inverse DCT. In this work, CASIA database is used to provide three types of wavelength spectrum which are 700 nm, 850 nm, and 940nm. There are four combination of image fusion that can be formed, dual combination with 700 nm and 850nm, 700 nm and 940 nm, 850 nm and 940 nm and triple combination of all wavelength. Multi-resolution DCT (MRDCT), Frequency Partition DCT (FPDCT) and Laplacian Pyramid DCT (LPDCT) image fusion is introduced on fusing more informative information from different types of wavelength and resulting in an image with finer details of vein patterns in the output image. In this work, triple combination of image fusion achieve better than dual combination of image fusion. By fusing three wavelength spectrums, MRDCT performed the best at 5.53% in EER rate compared to FPDCT and LPDCT. The conventional method such as Multi-resolution Singular Value Decomposition (MSVD), wavelet transform and Energy of Laplacian (EOL), were only able to achieve EER rate of 6.58%, 6.83% and 8.64% respectively. In addition to that, MRDCT with triple wavelength spectrum fusion showed a significant drop in EER by 9% compared with single 700 nm image, 7% compared with single 850 nm image, and 6% compared with single 940 nm image. It proved that MRDCT image fusion is suitable for palm vein recognition. For feature extraction, two types of local invariant feature based method was investigated, Scale Invariant Feature Transform (SIFT) and Speeded Up Robust Feature (SURF). SIFT algorithm achieved a reduction in EER rate by 12% in 700 nm, 8% in 850 nm, 7% in 940 nm compared with the SURF algorithm. The result shows that SIFT algorithm achieved a better recognition rate and extract more information and matching pairs compared to SURF algorithm. In conclusion, MRDCT image fusion with SIFT feature extraction are suitable to use in contactless palm vein recognition system.

TABLE OF CONTENT

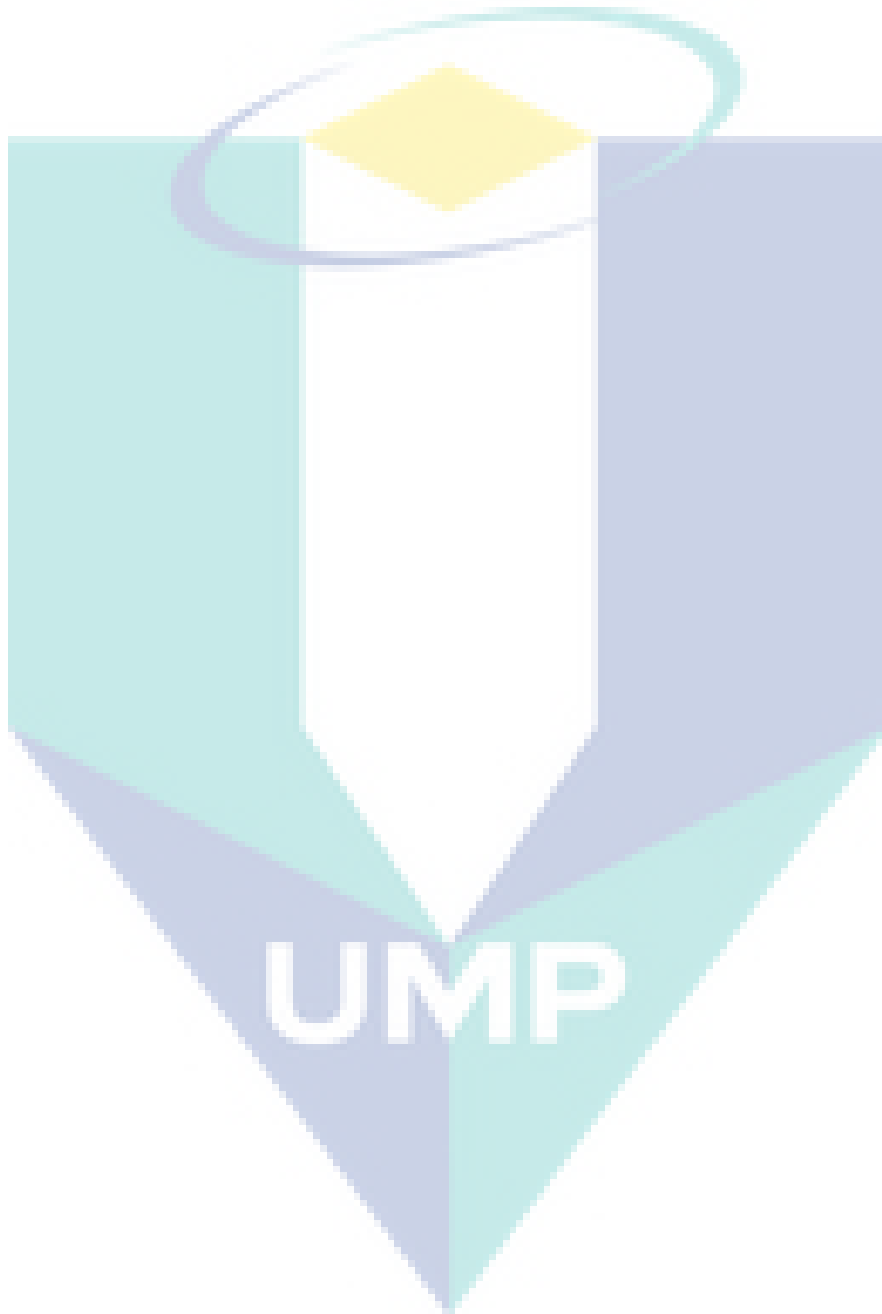
DECLARATION	
TITLE PAGE	
ACKNOWLEDGEMENTS	ii
ABSTRAK	iii
ABSTRACT	iv
TABLE OF CONTENT	v
LIST OF TABLES	ix
LIST OF FIGURES	x
LIST OF SYMBOLS	xii
LIST OF ABBREVIATIONS	xiii
CHAPTER 1 INTRODUCTION	1
1.1 Background of work	1
1.2 Problem statement	3
1.3 Objective	4
1.4 Scope	5
1.5 Statement of contribution	5
1.6 Thesis outline	6
CHAPTER 2 LITERATURE REVIEW	8
2.1 Introduction	8
2.2 Palm vein image acquisition	8
2.3 Image pre-processing	10

2.4	Image fusion	13
2.5	Pyramid based image fusion	15
2.6	Discrete transform based image fusion	16
2.6.1	Discrete cosine transform (DCT)	16
2.6.2	Discrete wavelet transform (DWT)	18
2.6.3	Singular value decomposition based image fusion (SVD)	19
2.6.4	Energy of Laplacian image fusion (EOL)	20
2.7	Feature extraction	20
2.7.1	Geometry based method	20
2.7.2	Statistical based method	22
2.7.3	Local invariant feature based method	25
2.8	Feature matching	27
2.9	Critical review	27
2.10	Summary	29
CHAPTER 3 METHODOLOGY		30
3.1	Introduction	30
3.2	Palm vein image acquisition	31
3.3	Pre-processing	33
3.4	Palm vein image fusion	36
3.4.1	Discrete cosine transform (DCT) fusion	36
3.4.2	Multi-resolution singular value decomposition (MSVD)	41
3.4.3	Energy of Laplacian (EOL)	43
3.4.4	Wavelet transform (WT)	44
3.5	Feature extraction	45
3.5.1	Scale invariant feature transform (SIFT)	45

3.5.2	Speed up robust feature (SURF)	48
3.6	Feature matching	51
3.7	Summary	52
CHAPTER 4 RESULTS AND DISCUSSION		53
4.1	Introduction	53
4.2	Pre-processing	53
4.3	Feature extraction	58
4.3.1	SIFT feature extraction	59
4.3.2	SURF feature extraction	61
4.4	Comparison with the feature extraction method	63
4.5	Image fusion	65
4.6	Comparison with the image fusion method	67
4.7	Comparison with the conventional method	71
4.8	Summary	72
CHAPTER 5 SUMMARY AND FUTURE WORK		74
5.1	Introduction	74
5.2	Summary of the work	74
5.3	Future work	75
REFERENCES		77
APPENDIX A IMAGE FUSION TECHNIQUES IN DUAL COMBINATION OF DIFFERENT TYPE OF WAVELENGTH SPECTRUM		85
APPENDIX B EER AND AUC FOR IMAGE FUSION IN DUAL COMBINATION OF 700 NM AND 850 NM WAVELENGTH SPECTRUM		86
APPENDIX C EER AND AUC FOR IMAGE FUSION IN DUAL COMBINATION OF 700 NM AND 940 NM WAVELENGTH SPECTRUM		88

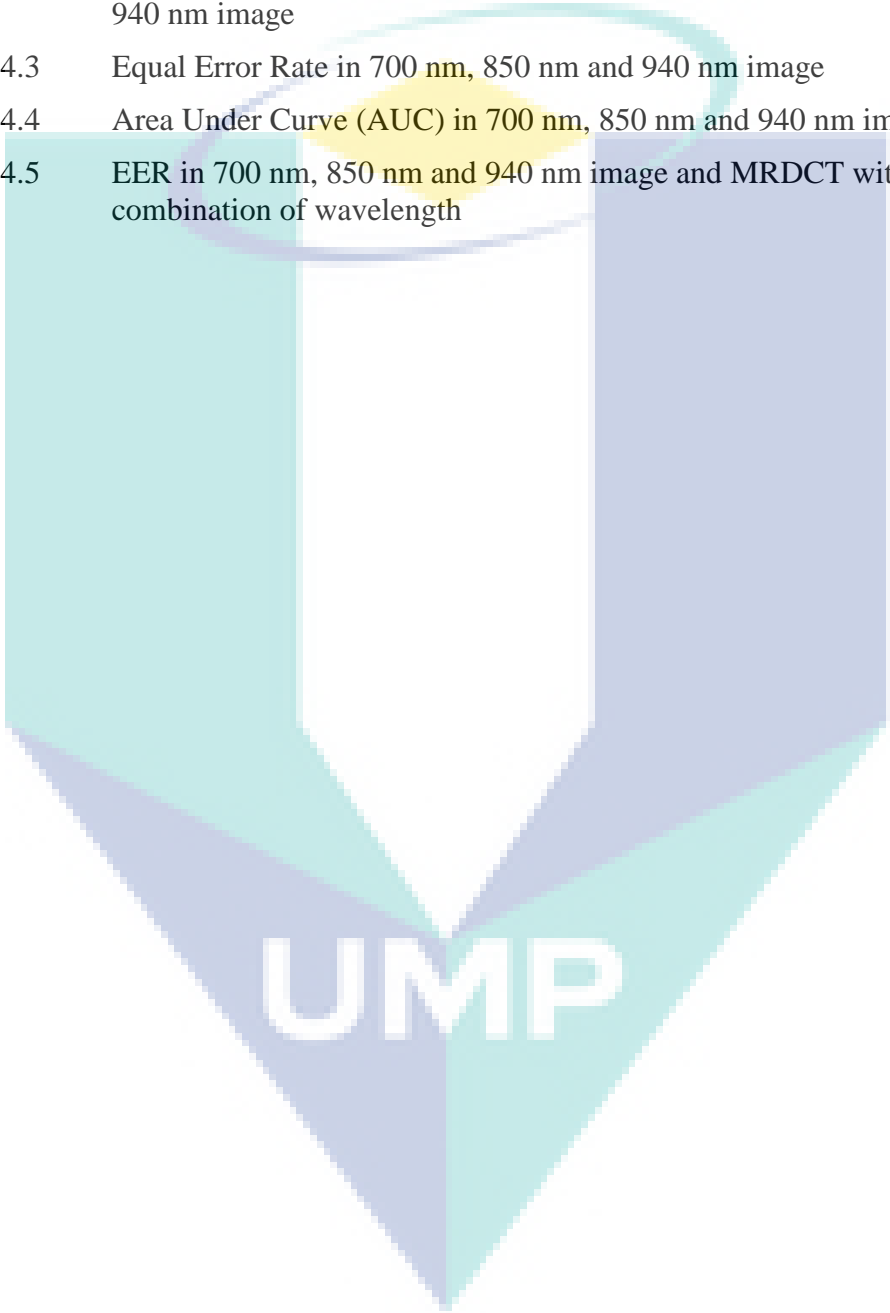
APPENDIX D EER AND AUC FOR IMAGE FUSION IN DUAL COMBINATION OF 850 NM AND 940 NM WAVELENGTH SPECTRUM	90
---	-----------

APPENDIX E EER AND AUC FOR IMAGE FUSION IN TRIPLE COMBINATION OF 700 NM , 850 NM AND 940 NM WAVELENGTH SPECTRUM	92
--	-----------



LIST OF TABLES

Table 4.1	Euclidean Distance of 10 samplers 10°, 20°, and 30° degree of rotation	57
Table 4.2	Equal Error Rate and Area Under Curve for three different wavelength using SIFT and SURF classifier in 700 nm, 850 nm and 940 nm image	64
Table 4.3	Equal Error Rate in 700 nm, 850 nm and 940 nm image	71
Table 4.4	Area Under Curve (AUC) in 700 nm, 850 nm and 940 nm image	71
Table 4.5	EER in 700 nm, 850 nm and 940 nm image and MRDCT with triple combination of wavelength	72



UMP

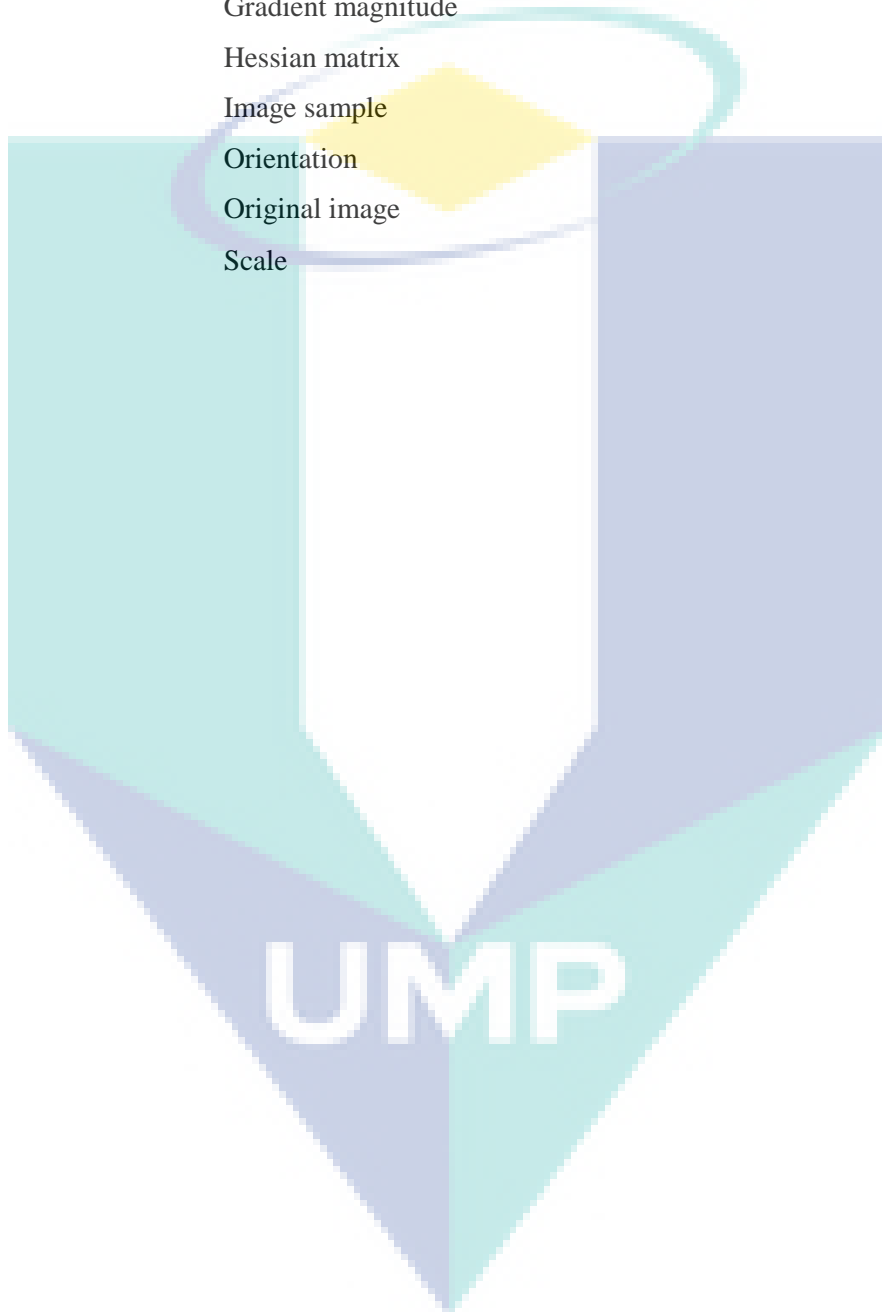
LIST OF FIGURES

Figure 2.1	Basic principle of near infrared camera on capturing palm vein image	9
Figure 2.2	Palm vein ROI extraction, a) ROI extraction, b) Central of boundary point, c) Estimation of center of the web points	11
Figure 2.3	Block diagram for ROI extraction in palm vein images.	11
Figure 2.4	Block diagram for palm vein recognition system.	12
Figure 2.5	Process of CHVD algorithms, (a) 4 valley points, (b) ROI for left palm, (c) ROI for right palm.	13
Figure 2.6	Overall fusion in different fusion level.	14
Figure 2.7	Image fusion based on discrete transform function	16
Figure 2.8	Process flow of DCT based image fusion in JPEG format.	17
Figure 2.9	Generic framework of DWT based image fusion in palm print recognition system	19
Figure 2.10	Coordinate system of LBP operator	23
Figure 2.11	LDP operator with the radius of 6 from the center position	24
Figure 3.1	Overall process of palm vein recognition system	30
Figure 3.2	Process flow of palm vein recognition system	31
Figure 3.3	Multispectral Imaging Device in CASIA database	32
Figure 3.4	Different types of wavelength (a) 460nm, (b) 630nm, (c) 700nm, (d) 850nm, (e) 940nm, (f) Natural Light.	33
Figure 3.5	Block diagram of pre-processing stage	33
Figure 3.6	The main steps of coordinate systems, (a) Original image, (b) Binary image, (c) boundary tracking, (d) Coordinate system with tangent line, (e) Subimage extracted in center part, (f) ROI extraction in palm	35
Figure 3.7	Block diagram for image fusion	36
Figure 3.8	Computation of 2-D DCT in column and row wise.	37
Figure 3.9	Image fusion process using DCT	37
Figure 3.10	Separation of LF and HF coefficients with the coefficient factor.	38
Figure 3.11	Multi resolution image analysis using DCT.	39
Figure 3.12	(a) Downsampling from 8x8 blocks to 4x4 blocks. (b) Upsampling from 4x4 blocks to 8x8 blocks.	40
Figure 3.13	Laplacian Pyramid Construction and Reconstruction	41
Figure 3.14	MSVD decomposition structures with three level of decomposition.	42
Figure 3.15	MSVD fusion scheme	43
Figure 3.16	Schematic diagram of EOL based image fusion	43

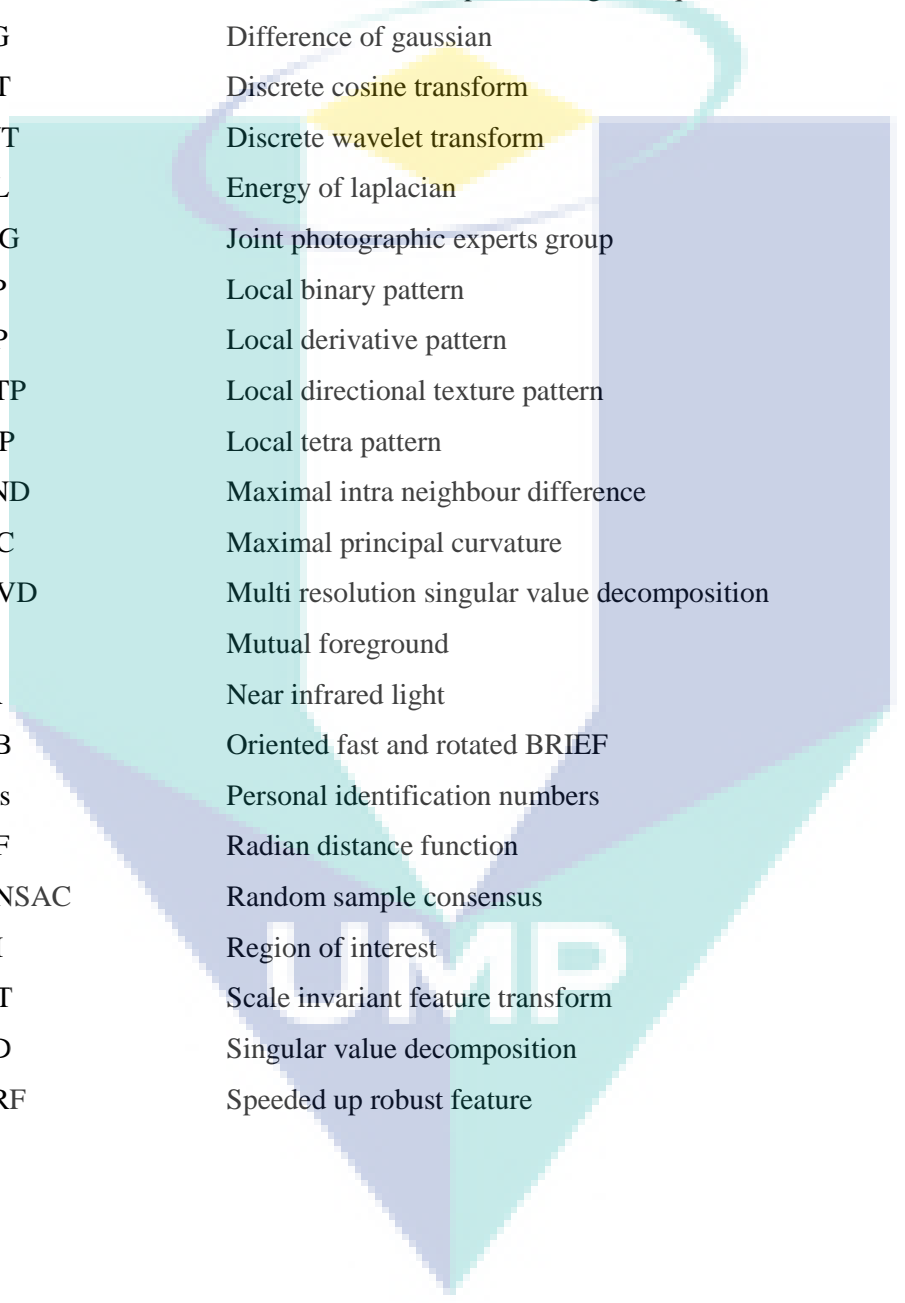
Figure 3.17	Block diagram of Wavelet based image fusion	44
Figure 3.18	DoG obtained by using the simple subtraction of different scale Gaussian level	46
Figure 3.19	Key points located by comparing pixel with its neighbors.	47
Figure 3.20	The key point descriptor generated by summarizing the contents in image gradients with the length of the arrow in eight directions.	48
Figure 3.21	Gaussian second order derivative from left to right in x and y direction and approximations using box filters.	49
Figure 3.22	Interest point detected in left picture and orientation is assign in the right picture with Haar wavelet response in the middle.	50
Figure 3.23	Diagram for building the descriptor in every interest points.	50
Figure 4.1	(a) Original Image, (b) Otsu Threshold, (c) Morphological Operation, (d) Centroid of the palm.	54
Figure 4.2	(a) ROI extraction in wavelength 700 nm, (b) ROI extraction in wavelength 850 nm, (c) ROI extraction in wavelength 940 nm.	55
Figure 4.3	Artificial rotation in one sampler (a) 10 degree of rotation, (b) 20 degree of rotation, (c) 30 degree of rotation.	56
Figure 4.4	CLAHE filter (left) and Median Filter (right) in ROI extraction, (a) 940 nm palm vein image, (b) 850 nm palm vein image, (c) 700 nm palm vein image.	58
Figure 4.5	SIFT feature extraction with feature points for few sampler for 700 nm in the left, 850 nm in the middle and 940 nm in the right, a) sampler number 38, b) sampler number 88, c) sampler number 89	60
Figure 4.6	SIFT matching in genuine and imposter pair, (a) without RANSAC mismatching point removal, (b) after RANSAC mismatching point removal.	61
Figure 4.7	SURF feature extraction with feature points for few samplers for 700 nm in the left, 850 nm in the middle and 940 nm in the right, a) sampler number 38, b) sampler number 88, c) sampler number 89.	62
Figure 4.8	SURF matching in genuine pair, (a) without RANSAC mismatching point removal, (b) after RANSAC mismatching point removal.	63
Figure 4.9	Equal Error Rate (EER) of SIFT and SURF matching in three different wavelength spectrum	64
Figure 4.10	FPDCT image fusion for several types of combination	66
Figure 4.11	Effect of number of matching points before and after one of the image fusion applied.	67
Figure 4.12	EER for dual type combination of wavelength spectrum, (a) 700 nm with 850 nm image, (b) 700 nm with 940 nm image, (c) 850 nm with 940 nm image	69
Figure 4.13	EER for triple combination of wavelength spectrum	70

LIST OF SYMBOLS

X	Determinant of hessian
I_{FU}	Fused image
ϕ	Fusion strategy
m	Gradient magnitude
H	Hessian matrix
A	Image sample
θ	Orientation
I	Original image
σ	Scale



LIST OF ABBREVIATIONS



AC	Alternating current
CCD	Charge-coupled device
CHVD	Competitive hand valley detection
CLAHE	Contrast limited adaptive histogram equalization
DoG	Difference of gaussian
DCT	Discrete cosine transform
DWT	Discrete wavelet transform
EOL	Energy of laplacian
JPEG	Joint photographic experts group
LBP	Local binary pattern
LDP	Local derivative pattern
LDTP	Local directional texture pattern
LTrP	Local tetra pattern
MIND	Maximal intra neighbour difference
MPC	Maximal principal curvature
MSVD	Multi resolution singular value decomposition
MF	Mutual foreground
NIR	Near infrared light
ORB	Oriented fast and rotated BRIEF
PINs	Personal identification numbers
RDF	Radian distance function
RANSAC	Random sample consensus
ROI	Region of interest
SIFT	Scale invariant feature transform
SVD	Singular value decomposition
SURF	Speeded up robust feature

CHAPTER 1

INTRODUCTION

1.1 Background of work

The development of security systems are attracting more attention in recent years with increasing financial activities and security awareness in the society. The requirement of information security keeps increasing in view of the constant development of society in the aspect of technology, science, and economic. There is a real risk for everyone that their information can be accessed by other people anytime and everywhere. Hence, information security plays a significant role in access control system, either access to buildings or computer systems. Several security systems have been introduced such as password, ID cards, or Personal Identification Numbers (PINs). These traditional personal verification methods offer only limited security. Traditional personal verification methods are prone to be forgotten, lost, or stolen. They do not meet other requirements such as convenience, reliability, and security in a wide range of applications such as high security government buildings, banking systems, or hospitals. In consideration of those factors, majority users have adopted the use of biometrics technology which can fulfil the need of accurate recognition systems and as access control methods.

Biometrics is the technology of identifying and recognizing a person by using the intrinsic physiological and extrinsic behavioural characteristics of humans. Biometric recognition systems include face recognition, palm prints, finger prints, iris, and handwriting have been proposed and become a powerful alternative to improve the security of personal verifications. Face and fingerprint recognition have now been fully utilized in financial and security domains. However, most of them have pros and cons and none of those approaches are perfect in all application scenarios. For example, there

are certain segment of the population which cannot activate their fingerprints and palm prints on extraction on high quality image, for example manual workers. Manual workers have damages on the fingerprints which may affect recognition (Elnasir &Shamsuddin, 2014). On the other hand, face recognition will face degradation once the face is obstructed by hair or lighting conditions and viewpoints. Face recognition now still lack the robustness against pose and illumination variance (X.Zhang &Gao, 2009).

To address those issues, new biometrics properties have been identified and received attention for use in identification and verification techniques. Vein patterns method has been introduced to overcome the aforementioned method by using the blood vessels underneath the skin to perform the verification techniques. Currently, many R&D resources have conducted research on the topic of vein pattern recognitions. From several vein methods studied, palm vein gained more attention from researchers due to more abundant texture information and simple acquisition of images. Palm vein has a great level of recognition accuracy due to the uniqueness and complexity of vein patterns of the palm. Vein patterns are the network structure of the blood vessels lying under the human skins that are unable to be observed by naked eyes. Vein patterns has its own uniqueness and distinctiveness even among identical twins. Vein recognition becomes highly reliable and secure due to the differences of vessels network among individuals.

Furthermore, palm vein will not vary during the person's lifetime and impossible to read or copy since it lies under the skin. But, the most important advantage is that the vein exist only for living humans. Vein pattern will also stabilize over a period of time. Accuracy is improved for the palm vein image acquisition since there is no contact with the sensor which means no contamination on the image (MacGregor & Welford, 1991). Palm vein is the technology which is more secure as it is present internally to the body, so it is quite difficult to be forged which effectively protects against all possible spoof attacks. Besides, palm vein is an ideal part of all biometrics method because it does not have hair as an obstacle, hence the palm vein image acquisition is not obstructed. Palm vein recognition is being developed which provides a good prospect. It has become increasingly attractive to researchers in biometric research field compared to other biometrics methods.

A typical vein recognition systems have four main stages which are image acquisition, pre-processing, vein pattern feature extraction, and matching stages. Vein

patterns are usually captured by using near infrared (NIR) camera. This is because vein patterns are most visible under the near infrared light (NIR). Hence, palm vein images are normally acquired by CCD camera that is sensitive to light. After acquiring the palm images, the images are then segmented from the background by using Region of Interest (ROI) extractions. The image with the background removed will be used to extract the features to obtain the shape representation of patterns. Finally, the system will recognize the vein patterns and determine whether the vein image is genuine or imposter.

1.2 Problem statement

A lot of work has already been done on the palm vein recognition method but there is still a scope of further improvement. Erroneous extractions due to bad quality of the palm vein pattern images may lead to fatal errors in the process. Low quality image such as unclear and low contrast will result the low recognition rate of the system although the processing method is perfect. Low quality image will produce noise which make the extraction of vein pattern difficult because of the degradation of performance of the systems. Although the texture is represented as uniformed appearance, lack of uniformity of brightness and colour could cause problems on efficiency of progress on the systems.

Several methods have been introduced to solve low quality image issues. One of the methods is image fusion which is done by fusing multi-spectral image into one image by obtaining more features on the vein patterns. Image fusion are able to recover the source images since the system cannot guarantee on capturing high quality images. However, some of the methods may be the best in terms of preserving vein but they produce blurry images that may cause wrong judgements on the genuine and imposter matches (Sharma, 2016). Some of the images are present with intensity distortions and illumination noises.

In the view of aforementioned problem, contactless design palm vein recognition system are one of the most challenging and promising areas in vein biometrics. Contactless design palm vein recognition system presents their problems as projection transformation, uneven illumination, and also difficulties in extracting ROI in pre-processing stage. It is hard because the palm images have limitations of using the natural lights. It is required to use near-infrared light on palm acquisition on either produced a

palm print or palm vein images. On those factors, it could lead to blurry boundaries and also inhomogeneous thickness of the image. The difficulties to extract palm vein is increased once the image have different hand position or substantial change of hand positioning of the same person. Especially for palm vein image recognition under remarkable posture changes, it will show that the proposed method is superior in terms of the recognition performance.

Complexity of vascular patterns and irregularities in subsequent samplers of the same person is also one of the most challenging part of the process. Since each individual have their own unique patterns, it is challenging to make sure that the system can recognize the system input for every individual. A powerful processing technique or method should be introduced to make sure that any error will not happen. From the aforementioned issues, providing accurate palm vein readings has remained an unsolved issues in this biometrics method. The real problem which occurs is how to produce a real life biometrics system that is able to detect and recognize the system input accurately and robustly. Several researchers have researched on several methods to produce an accurate and fast recognition method or algorithms in the systems. However, most of the methods which could ensure on accuracy have slow algorithms or vice versa. Hence, it still an open topic on research until now.

1.3 Objective

The purpose of this work is to propose the palm vein recognition technique by using fusion method to recognize the vascular pattern which is complex and irregular in subsequent samplers of the same person.

- To investigate and implement image fusion technique using different wavelength spectrum for a palm vein recognition system.
- To develop features extraction algorithms that is able to handle orientation changes in palm vein pattern.
- To evaluate and validate the effectiveness of image fusion technique and the robustness of the proposed feature extractions in this work.

1.4 Scope

This work is focused on a specific scope. There are four main stages in vein recognition system which are image acquisition, pre-processing, feature extraction, and matching stage. The main focus of this studies is on the pre-processing stage which is the image fusion techniques on pre-processing. After several pre-processing methods were applied, image fusion by fusing multispectral image into one image to recover some bad quality image by preserving vein pattern and reducing noise. This technique contributes to other techniques that are able to works on real time application. Several types of image fusion techniques will be evaluated, and the performance investigated, and the drawback of the image discussed after image fusion applied.

. Vein pattern extraction techniques can be categorized into four which are geometrical based, statistical based, local invariant featured based and appearance based feature extraction method. In CASIA database, the users are allow to do some movement when capturing on the images. Among all the study on vein extraction, the most suitable method for vein recognition systems is the local invariant based methods. Hence, this studies will be focusing on the local invariant feature based methods and will be investigated between some of the local invariant feature based methods.

In vein image acquisition, vein image will be considered by using the image database which exist online. The palm vein image will be obtained from the CASIA multispectral palm vein database which is especially for research and development. This database has different types of wavelength spectrum which is 700 nm, 850 nm and 940 nm that can be applied to the image fusion techniques in this study. Besides, CASIA database were mostly used in other related studies. During pre-processing and matching techniques, the most suitable method is identified and applied in this study.

1.5 Statement of contribution

The contribution of the work is the development of palm vein recognition system using the image fusion techniques by fusing different types of wavelength spectrum. There are three different types of wavelength 700 nm, 850 nm and 940 nm which enable the test for dual combination image fusion and triple combination image fusion for palm vein recognition systems. It is proven that triple combination image fusion perform more effectively compared to dual type combination image fusion using the same database.

Besides that, image fusion also improved the recognition rate of palm vein recognition system. From previous works, most of the works applied are only the basic processing stage in palm vein recognition systems. However, this work have applied the fusion techniques to the palm vein recognition systems to analyse the impact of image fusion techniques to the recognition rate. Image fusion techniques has been proved to be able to fuse several images with different types of wavelength spectrum and form a fused image with more finer detail of vein pattern with less generating of noises. Fused image with finer detail of vein pattern are able to generate more feature points or feature pattern when feature extraction method is applied.

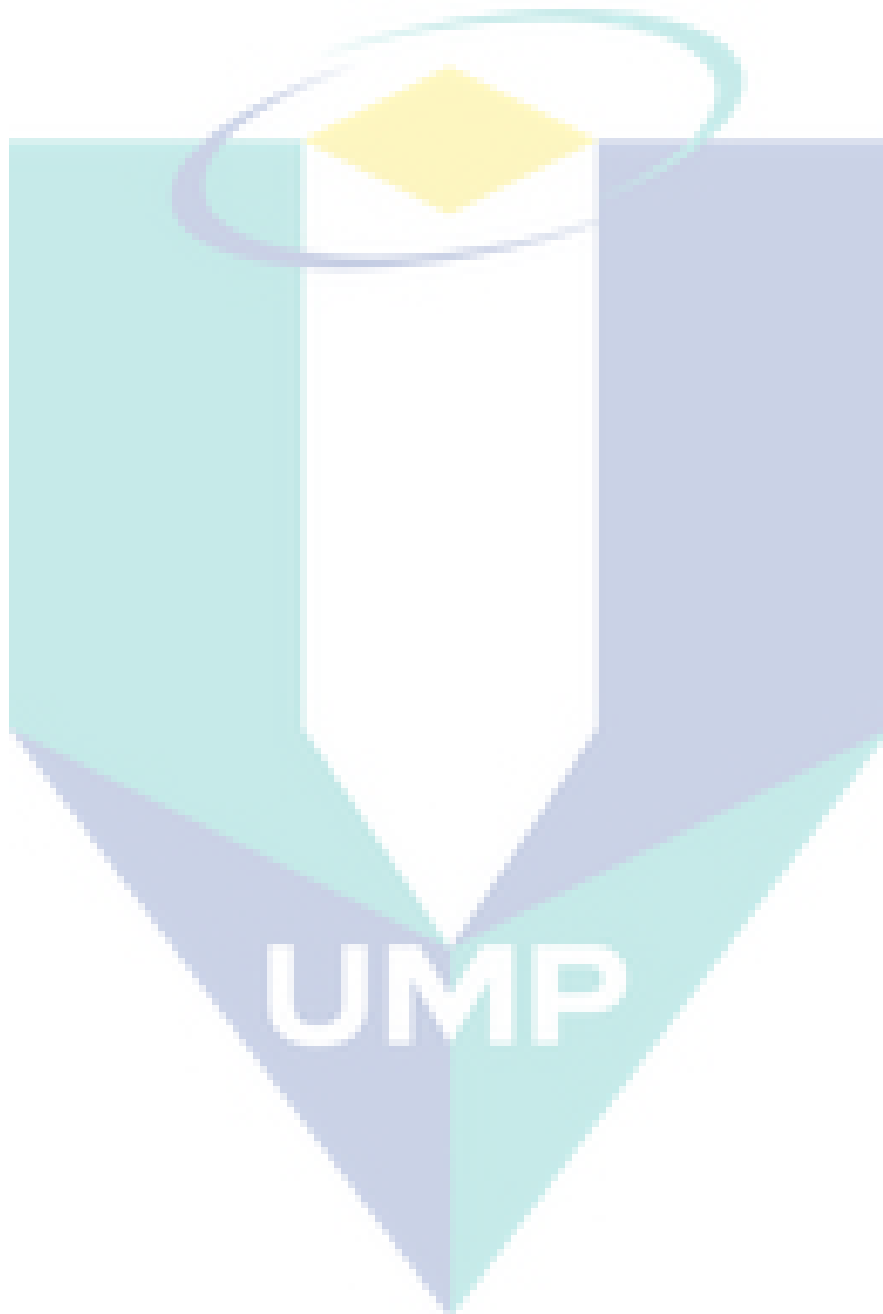
1.6 Thesis outline

This thesis consists of five chapters. The first chapter will be discussing the introduction, background study, problem statement, objective, and scope. In this chapter, the overall work will be explained to ensure the reader understand this study by referring to the chapter one. The objective is stated to ensure that this work has achieved the objectives. Chapter 2 will discuss more on theory and literature review of studies that has been done. The overall process from pre-processing until matching stage will be discussed. However, the focus and scope of this research is still the image fusion techniques. Hence, image fusion techniques will be the priority on this research.

The methodology of this work will be discussed in chapter 3. Palm vein recognition system with image fusion techniques will be shown in this chapter. This chapter will include the process of this work. The database used in this work will be discussed in this chapter. This chapter will also discuss on the method used in this research. Every method will be discussed for every image fusion techniques and feature extraction techniques.

As for chapter 4, each of the results will be discussed and analysed. The effect after image fusion techniques to the picture will be discussed in visual inspection. The efficiency or usage of image fusion which contributes to recognition rate will be discussed. The image fusion techniques with highest performance will be compared with the conventional method to prove that the effectiveness of image fusion techniques in palm vein recognition system. Last but not least, conclusion and future work will be

discussed in chapter 5. In this chapter, future improvement or other methods that can be used to increase the efficiency and accuracy will be discussed.



CHAPTER 2

LITERATURE REVIEW

2.1 Introduction

This section will discuss about previous research on the process of the recognition systems. Recognition that is used for other biometrics application will be reviewed as a reference to the palm vein recognition techniques. Full process from the image acquisition to the matching stage will also be reviewed in this section. Other than that, image fusion techniques will be discussed in this section. A few of image fusion techniques have been introduced to tackle the problems which occurred in contactless design recognition system.

2.2 Palm vein image acquisition

Palm vein image are normally taken under infrared light. This is because vein patterns will be more visible under infrared light compared to natural light. Most of the images taken under natural light are unable to obtain the discriminative information which makes the recognition not possible. Multispectral image that was captured in near-infrared light sources make it possible to obtain more multifarious information to improve the extraction of image features. In order to recognize the vein pattern in the palm image, NIR with wavelength of more than 760 nm is the minimum requirement. This is because the light can only penetrate through the human tissue in that wavelength or above. Therefore, it will be very easy for the image processing to recognize the superficial veins and deep veins.

Fusion method by fusing palm print and palm vein images based on ‘‘Laplacianpalm’’ features has been proposed (J.-G. Wang, Yau, & Suwandy, 2015). In their works, they developed their own IR camera to capture both palm print and also palm

vein image. The IR camera developed had emitted in the wavelength range of between 300 to 1200 nm. In another work, a digital noise reduction with NIR charge-coupled device (CCD) camera was developed for the palm vein recognition systems (Lee, 2012). Near IR illumination (LEDs) has been added surrounding the camera. By adding this LEDs, the effect of surrounding light which is uneven illumination can be reduced and this adding effect will also act as an infrared filter for the palm vein image. This camera are able to capture the palm vein NIR image on about 1100 nm. Figure 2.1 shows the basic principle of Near Infrared camera on capturing the palm vein image.

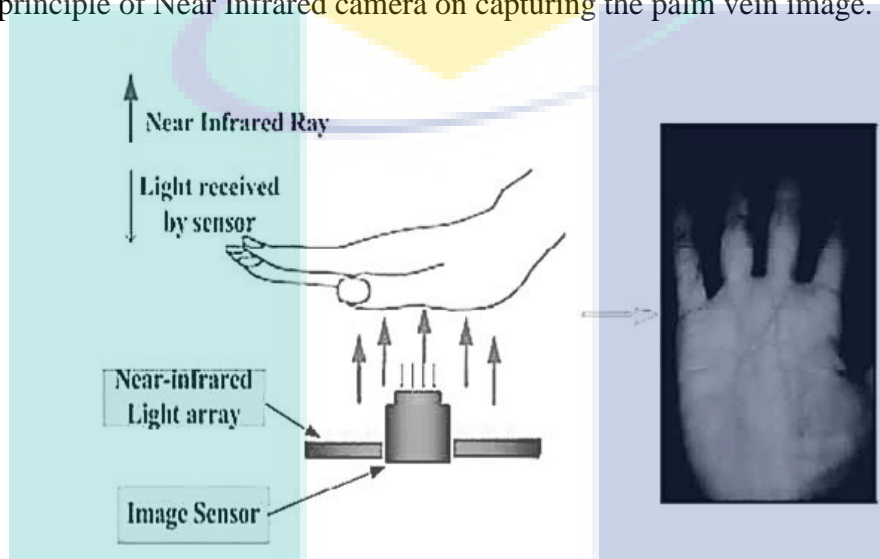


Figure 2.1 Basic principle of near infrared camera on capturing palm vein image
Source: Xu (2015)

The palm vein image can also be obtained using the open database which is open for the researchers to research on this section. CASIA Multispectral Palmprint Image Database contains 7200 palm images from 100 samplers. Each sample contains six palm images at the six different wavelength which are 460 nm, 630 nm, 700 nm, 850 nm, and 940 nm (Palmprint & Database, 2012). Different type of wavelength spectrum will be capturing by using the control circuit that built-in the capturing system. In this database, samplers are allowed to make some certain degree of variations on hand postures. Vein image will be captured by using the device that supplies an evenly distributed illumination using a CCD camera. By using this CASIA database, it is possible to use this database on either palm vein or palm print and also a fusion of palm vein and palm print image on recognition techniques. In PolyU multispectral palm vein images, 250 participants were involved in palm image acquisition. It contains 6000 images from 500 different palms with left hand and right hand. The clipped ROI image was also provided for every image.

2.3 Image pre-processing

Image pre-processing is essential by obtaining a clear image in order to extract vein pattern easily. In palm vein recognition systems, image pre-processing can be separated into two steps which are ROI extraction and image enhancements. ROI extraction is the step where an image of the area located at the middle of the palm is extracted. This step is to obtain a fixed size ROI which is normalized to minimize the rotational, scales, and translational changes. By undergoing image enhancement, a clear palm vein image will be obtained so that the vein pattern can be extracted correctly.

Zhou and Kumar (2011) have introduced the pre-processing stage which is suitable for contactless design for palm vein recognition systems. By extracting the ROI extraction in the middle of the palm, two web points is generated in between the index finger and middle finger, as well as between the ring finger and little finger as shown in Figure 2.2(a). Binarization will be adopted by converting the image into black and white. This is to separate the palm and the background region. Central position or centre image is estimated from the boundary of palm as shown in Figure 2.2(b). The distance is computed by finding the local minima in between the two web points. Estimation of centre to the web points is estimated and will be drawn as shown in Figure 2.2(c). Figure 2.3 shows the process of pre-processing stage adopted in their works.

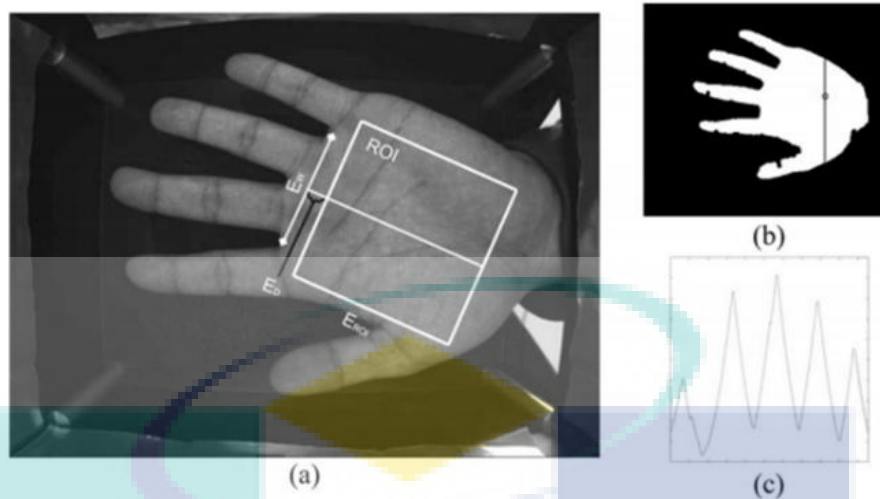


Figure 2.2 Palm vein ROI extraction, a) ROI extraction, b) Central of boundary point, c) Estimation of center of the web points

Source: Zhou & Kumar (2011)

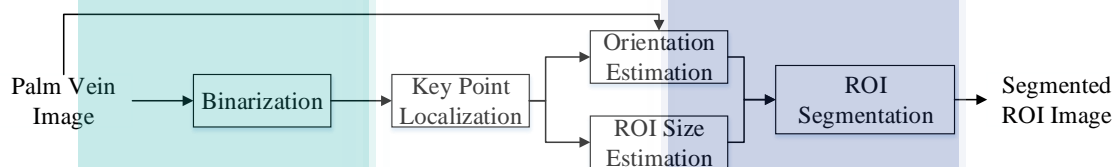


Figure 2.3 Block diagram for ROI extraction in palm vein images.

Source: Zhou & Kumar (2011)

This approach is similar to another study conducted earlier (Hao, Sun, Tan, & Ren, 2008). However, this work has achieved a computational efficiency with no additional process required. Figure 2.4 shows the process for the palm vein recognition systems. By using background estimation algorithms, image is divided into 32x32 non-overlapping blocks and the average grey level pixels in every block are computed. Finally, the ROI images extraction will be scaled in a fixed size adopted with histogram equalization by achieving an enhanced image. This method are normally employed by most of the researchers either for palm vein or palm print recognition (Y.-B. Zhang, Li, You, & Bhattacharya, 2007).

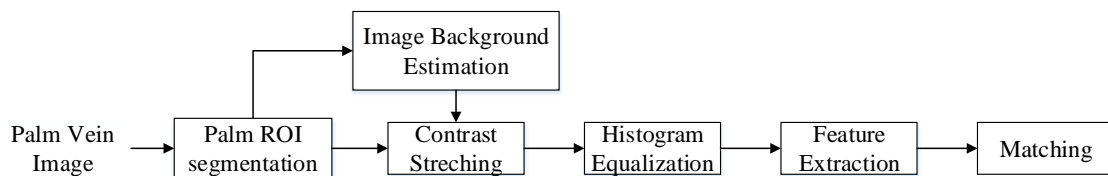


Figure 2.4 Block diagram for palm vein recognition system.

Source: Zhou & Kumar (2011)

In this research paper (W. Kang, Liu, Wu, & Yue, 2014), the authors had done some modification on the pre-processing. This is because a lot of issues need to be addressed on the palm vein image. Near Infrared images are generally shown in non-uniform illumination and also darker with low contrast mode. This create difficulties on extracting the palm vein pattern in contact free recognition systems. This work had applied the ROI extraction with the entire palm region including five fingers. However, by extracting the entire palm region including fingers, it shows that the vein extraction includes the area in between finger veins and palm veins. Besides, the computational efficiency will be impacted once there was more vein extraction to be extracted.

Otsu threshold is a fixed threshold which is normally adopted before ROI segmentation because it is simple and fast. Otsu threshold is to segment the entire palm region with the background of the images. By obtaining the enhanced image, histogram equalization is adopted to the entire palm regions. This method will successfully increase the global contrast where the distribution of grey levels of image is concentrated in the narrow intervals. Vein will be highlighted once the contrast level of the image has been improved. In this work (Zhou, Kumar, & Member, 2011), CLAHE is employed to obtain the normalized and enhanced palm vein images. The works shows that this method is successfully improve the details and contrast of the ROI images. In (W.Kang, Liu, Wu, & Yue, 2014a) and (Smorawa & Kubanek, 2015), the palm vein images enhanced by using CLAHE. Upon the CLAHE adopted to the images, their work proved that the vein pattern can be observed clearer after CLAHE adopted to the palm vein images.

Radian Distance Function (RDF) has been used in the work that was published by Rahul and Cherian (2015). In the beginning, Otsu method was used to extract hand contours from grayscale palm vein image. RDF will function to set the peak and valley points as a reference point and contour point. Finally, final palm vein ROI will be

obtained by using scaling and rotation normalization for the scaling, rotational and translational problems.

Perwira et al. has introduced Competitive Hand Valley Detection (CHVD) to determine the ROI of the palm (Perwira, 2014). CHVD is an algorithm which can identify the palm region by determining the valley point of the palm. Several condition check will be done by finding the points in between each finger. Four valley points will be plotted by using the pixel distance. The pixel will generate and draw a line once the valley point is located in each gap between the finger (G.K.O. Michael, Connie, & Teoh, 2008). By locating the ROI regions, rules in between left and right palm will be applied. Different rules will be applied in either left or right palm for both cases. Figure 2.5 shows the process for CHVD in ROI extraction on the middle of palm images.

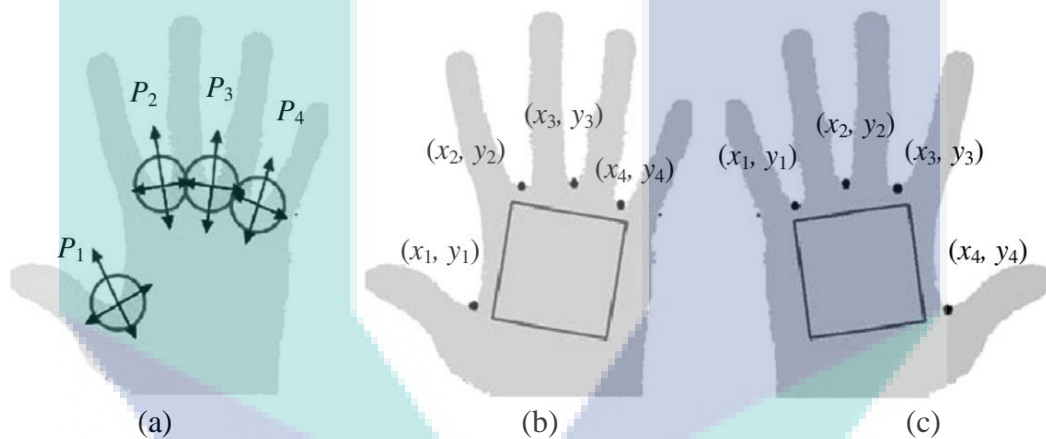


Figure 2.5 Process of CHVD algorithms, (a) 4 valley points, (b) ROI for left palm, (c) ROI for right palm.

Source: Perwira (2014)

2.4 Image fusion

Image fusion is one of the popular techniques which can recover and retrieve important information by fusing several images into a single output image. The output image provides more information than any single input image which improves quality and applicability of data. There are four ways in which image fusion could be introduced which is multi-view, multi-modal, multi-temporal and multi-focus image. Multi-view is fusing the images that are captured at the same time but from different viewpoints into a single image. Images captured by using different sensors are fused by using multi-modal

fusion. The same image captured but in different times is the multi-temporal fusion, while multi-focus fusion is performed on images captured with different focal length.

Image fusion can be performed at four different stages which are signal level, pixel level, feature level and decision level. The images are fused from different sensors to create a new image output with a better signal-to-noise ratio than the original signals. In pixel level fusion, the fusion is formed by using pixel by pixel basis. This method improves performance of image processing where the output image has the information associated with each pixel from a set of pixels in source images. Feature based fusion are the fusion occurring at feature level that requires the objects to be recognized in data sources first. The images are fused by using the extraction of salient features depending on the environment such as pixel intensity, edges, or textures. In decision level fusion, the information or the results is merged to yield a final fused decision. The result obtained is combined by applying decision fusing to reinforce common interpretation. Figure 2.6 shows the concept for different fusion levels (Dong Jiang & Dafang Zhuang, 2011).

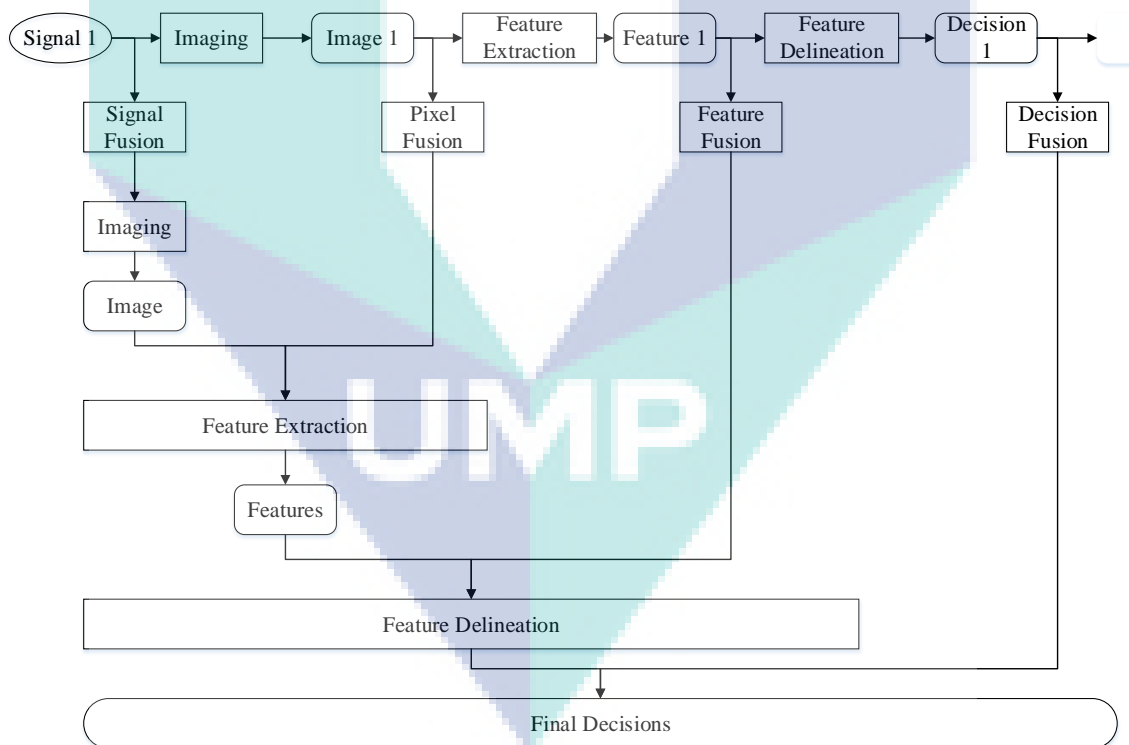


Figure 2.6 Overall fusion in different fusion level.

Source: Dong Jiang & Dafang Zhuang (2011)

There are several works on image fusion application in biometrics field including palm vein recognition system (L.Lu, Zhang, Xu, & Shang, 2017). This work introduced

multi-modal feature level fusion for biometrics identification system (Xin et al., 2018). The study showed the before and after fusion that impacted the biometrics identification systems. Experimental results showed that fusion method achieves an excellent recognition rate and provides higher security compared to single biometrics system used. In addition, the work also proved that DCT algorithm results in higher accuracy and effectiveness in security capability for person identification.

2.5 Pyramid based image fusion

Image fusion by using pyramid based decomposition has been proposed in several works. A pyramid based fusion is the fusion between several images at different scales in single images. Pyramid based fusion has three stages. The level of stages of pyramid is predefined based on the image size. In Sadjadi et.al (2005) and Sanju Kumara et al. (Kumari, Malviya, & Lade, 2014), they adopted and explained image fusion based on pyramid decomposition. Both images will be convolved with a predefined filter of the corresponding level and form a pyramid in the first level. The image will be decimated to half of its sizes. The decimated input images will generate matrices either by selecting maximum or minimum or else taking average in the second stage. In the last stage, input image matrix is undecimated and convolved with the transpose of the predefined filter in first stage. Process of pixel intensity value by applying addition to merge the filtered matrix with the pyramid formed at the respective level in stage one. The resultant image will proceed to the next level.

Besides that, Burt and Adelson (1983) had explained the image fusion techniques based on Laplacian Pyramid. S.M. Mukane et al. (Mukane, Ghodake, & Khandagle, 2017.) also adopted the image fusion based on Laplacian Pyramid. The pyramid construction is equivalent to the convolution of the input image with a set of Gaussian weight functions. The convolution theorem acts as a low pass filter with band limit for each level. In that paper, five levels of Laplacian Pyramid were computed. They explained that the pyramid method provides good image quality in resultant image for multi-focus image. They also explained that the fusion image would be affected by different number of decomposition levels (Mishra, 2015).

2.6 Discrete transform based image fusion

In discrete transform type image fusion, the process is similar with each other. The difference is the type of algorithms used in discrete transform image fusion. First, 2D operations will be performed on the input image. If the image is coloured, RGB components will be separated into each component. The various techniques will be applied here such as Discrete Cosine Transform (DCT) and Discrete Wavelet Transform (DWT). The coefficients obtained from the transformed values will be computed using the average of corresponding pixels. Inverse Transform will be applied to convert the fused transform components back into images. If the input image is coloured, the fused component with RGB value will be combined. Figure 2.7 shows the process of image fusion based on discrete transform techniques.

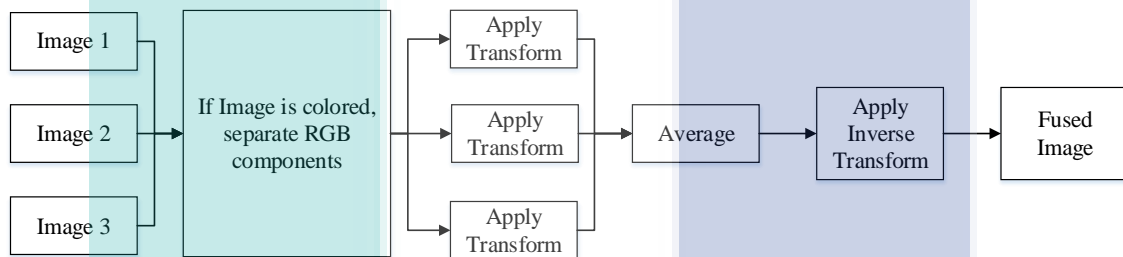


Figure 2.7 Image fusion based on discrete transform function

2.6.1 Discrete cosine transform (DCT)

Discrete Cosine Transform (DCT) has been widely used in image processing techniques. Naidu et al. has come out with different types of techniques using DCT functions. Image will be divided into $N \times N$ non-overlapping block of size. The following process will be repeated in every non-overlapping block. DCT coefficients will be computed using DCT algorithms. Fusion rules will be applied to obtain a new DCT fused coefficients. IDCT will be applied to obtain the image by inverse transform of fused coefficients.

In the study, Naidu et al. stated that DCT type image fusion does not perform well if using the block size of less than 8×8 and also if the block size is similar to the image itself (Naidu et al., 2010). Other than that, DCT based image fusion are suitable for real time application due to its characteristics of fast processing and simplicity of the algorithms.

Nirmala Paramanandham and Kishore Rajendiran had presented and proposed an image fusion techniques for surveillance application using DCT and swarm intelligence (Paramanandham & Rajendiran, 2018). This work was presented for integrating visible and infrared images. Particle Swarm Optimization act as a weight optimizer with DCT as the fusion techniques. Weight optimizer are used to fuse the DCT coefficient of visible and infrared images. By comparing DCT with DWT and SWT, fused image are zoomed in detail for parts of the images and it was found that it achieved better subjective assessment.

Liu Cao et al. presented DCT based multi-focus image fusion in wireless visual sensor network system (Cao et al., 2015). This experiment was conducted using multi-focus image coded in Joint Photographic Experts Group (JPEG) standard format image. DCT with block size of 8x8 was used to decode and dequantize the image which is similar with the works that was discussed above. In this study, they concluded that DCT domain is superior to the other techniques such as DWT techniques in terms of visual inspection and quantitative parameters. Moreover, DCT domain is suitable and efficient when the input images are coded with JPEG format. Figure 2.8 shows the process flow of DCT type image fusion in JPEG format.

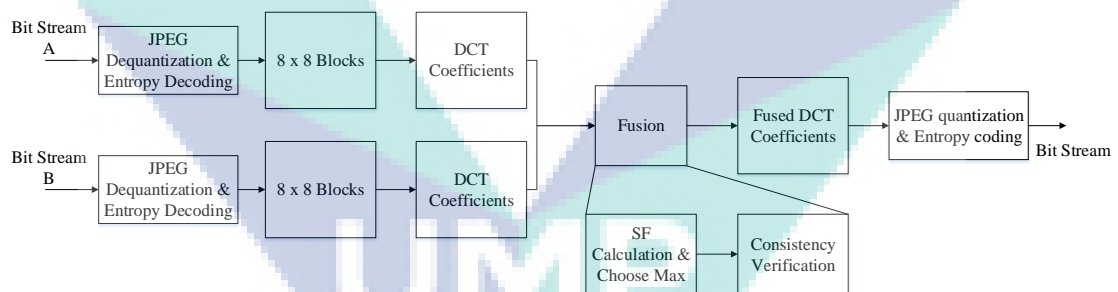


Figure 2.8 Process flow of DCT based image fusion in JPEG format.

Source: Cao et al., (2015)

Y. Asnath and R. Amutha had also presented DCT based image fusion in visual sensor network system (Victy & Amutha, 2014). The method proposed in this work is to investigate the image quality and computation energy of the fused images. Fused image produced was based on higher valued Alternating Current (AC) coefficients in DCT domain. The resultant image had proven that the proposed method in this works had better image quality than the other method which was DWT. The proposed fusion method selected the most informative area that were corresponding to the higher value number

of AC coefficients. It also stated that DCT type image fusion is simple and extremely fast in processing since it does not have any complex arithmetic floating points.

M. Amin-Naji and A. Aghagolzadeh presented the same image fusion in visual sensor network system (Aghagolzadeh, 2018). They stated that DCT based image fusion methods is efficient in terms of transmission and can achieve images that are based in JPEG format. In this work, they added 3x3 mask filter directly to the 8x8 non-overlapping block. Gaussian low pass filter was added to filter the artificial blurring in the input of the multi-focus image. DCT type image has been claimed to outperform other techniques using various evaluation performance metrics.

2.6.2 Discrete wavelet transform (DWT)

Discrete Wavelet Transform (DWT) is a method where the original image will pass through a series of filters before fusion rule is applied. Low pass filter impulse response will be passed through first, followed by decomposition using high pass filter. The output will produce the detail coefficient obtained from high pass filter and approximation coefficient that is obtained from low pass filter (Mishra, 2015). The process will be repeated once the frequency resolution and the approximation coefficients is obtained until maximum level. The 'Haar' wavelet is the first known wavelet that was used by Krishnamoorthy et al. that was applied in fusion techniques to minimize the spectral distortion. This method has been proved to provide better signal-to-noise ratio but the fused images have the effect of lower spatial resolution (Mallat, 1999).

Dong Han et al. also adopted DWT based image fusion in palm print recognition (D.Han, Guo, &Zhang, 2008). The work had applied DWT based image fusion in between RGB component in the source image. According to the results, the red component in the source image obtained the highest verification rate compared to others. The experimental result also showed that DWT based image fusion is effective on blurred images which is a good simulation of unmonitored image capturing. However, this type of fusion will degrade the level of recognition in unblurred image fusion.

Dakshina et al. also presented DWT wavelet based fusion in palm print recognition system (Kisku, 2010). In this work, decomposition of DWT was done by using high resolution palm print image. Decomposition generates a set of low resolution images with wavelet coefficients for each level. Mother wavelet will be shifted and scaled

to obtain basis functions. Mother wavelet replaces a low resolution image with multispectral image with the same spatial resolution level. Finally, the coefficient will convert to the original resolution level. Figure 2.9 shows the generic framework for DWT based image fusion in palm print recognition system.

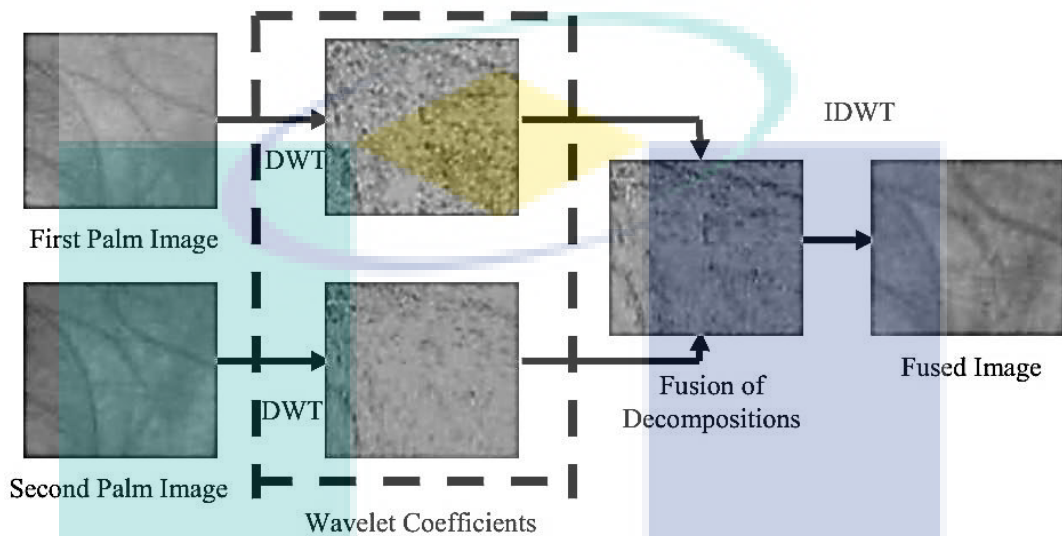


Figure 2.9 Generic framework of DWT based image fusion in palm print recognition system

Source: Kisku (2010)

Ying Hao et al. adopted pixel level fusion in contactless palm print recognition (Institute of Automation, CAS, 2008). This work had adopted the generic framework that was proposed by Zhang et al. Multiscale decomposition are suitable for extracting line-like patterns (Z.Zhang &Blum, 1999). Based on the works, line-like pattern such as vein pattern is the most discriminative features in palm vein images. Multiscale decomposition has been proved to be suitable for preserving directional information. This work had proven that the fusion in between different wavelength has improved the performance of contactless biometrics systems. The advantages of pixel-level fusion are shown in the memory consumption and the image representations.

2.6.3 Singular value decomposition based image fusion (SVD)

Singular Value Decomposition (SVD) is a linear algebra with a matrix factorization method. Image fusion method based on multi-resolution singular value decomposition (MSVD) has been presented and evaluated (Laboratories, 2011). Image fusion based on MSVD has proved that the result is similar with the wavelet transform.

It does not have any vector sets such as DCT or wavelets. Its vectors are based on its datasets. Hence, this technique is simple and suitable for any real time applications (Roopa &Manvi, 2014).

2.6.4 Energy of Laplacian image fusion (EOL)

Several focus measurements for the multi-focus image fusion has been presented in this paper. Huang and Jing mentioned some of the multi-focus image fusion that include the energy of Laplacian of the image (EOL) (W.Huang &Jing, 2007). Energy of Laplacian of the image is applied with the Laplacian operator shown in the equation below. This method is the method that analyses high spatial frequency associated with image border sharpness. This type of image fusion is focused in the spatial domain and it is also suitable for real time application. In the paper, the experiment conducted showed that the Energy of Laplacian had achieved the highest performance compared to the other methods. Besides that, the works conducted in this paper also shows that EOL has better results than other spatial frequency methods in spatial domains (Aghagolzadeh, 2018).

$$EOL = \sum_x \sum_y \left(-f(x-1, y-1) - 4f(x-1, y) - f(x-1, y+1) - 4f(x, y-1) + 20f(x, y) - 4f(x, y+1) - f(x+1, y-1) - 4f(x+1, y) - f(x+1, y+1) \right)^2 \quad 2.1$$

2.7 Feature extraction

Recently, studies of palm veins have focused more on the palm vein extraction. There were several reviews on the type of methods used in palm vein recognition system. It can be categorized into three which are the geometry based method, statistical based methods, and local invariant feature based methods (Soh, Ibrahim, &Yakno, 2018).

2.7.1 Geometry based method

Geometry based method are the method which typically uses vascular structure information. The palm vein pattern are extracted using spatial methods such as Gabor filter, vector grams of maximal intra-neighbour difference, repeated line tracking, and maximum curvature points. These types of methods are not without problems in extraction, representation and matching. It induces information loss on tiny and blurred pixels which occurred on low quality image. This kind of methods are highly dependent

on the chosen coordinate systems. Once there were issues present on the image, it would affect the recognition rate of the systems. Hence, those methods are sensitive to scaling, rotation and translational problems. It also causes poor distinguishing ability (W.Kang &Wu, 2014).

Gabor filter has been adopted in the feature extraction stage (Lee, 2012; Thamri, Aloui, & Naceur, 2018). This method is useful in 2D image due to its variation to 2D spatial position. Gabor filter has been proven to be useful in the texture analysis because of its characteristics on spectral specificity of texture and its variation with 2D spatial position. Gabor filter are able to extract edge information of the images that widely act as a tuneable filter. Gabor filter is also applied in either finger or palm vein images (Bharathi &Sudhakar, 2018).

In addition, it also has an advantage against near infrared images which cause brightness and contrast problem on the images (D.Zhang, Kong, You, &Wong, 2003). It was able to achieve high speed performance in either frequency or space domains. The application of this method has been tried on other recognition techniques such as iris recognition (Daugman, 1993). In other types of application, Gabor filter acts as a band pass filter that uses a multi-channel filter theory for image processing for human visual systems. Different types of Gabor filter have also been proposed to identify which Gabor filter is suitable for palm vein recognition (W. Y.Han &Lee, 2012).

For other methods, Miura et al. (Miura, Nagasaka, &Miyatake, 2004) proposed the palm vein extraction by using repeated line tracking algorithm. This method is able to locate the vein patterns even from the low quality images. The tracking lines will be based on the dark line detection that will move along the line or by pixel. Once there was no dark line detected, the tracking operation will automatically start at another position. In the end, the dark lines will keep on repeating to recover the vein patterns. However, this method is highly sensitive to uneven illumination in the images. This method has been found that it highly unable to recognize the person in cold weather due to the unclear vein pattern in the fingers. This system design in this works have limitation in the same placement of finger image. Thin vein will be another issue that tracking point will be moving on thin veins to be small statistically.

Miura et al. (Miura, Nagasaka, & Miyatake, 2007) proposed another technique which was local maximum curvature to extract vein patterns. This algorithm will be applied on cross-sectional profiles on vein images. Cross-sectional profiles help on extracting the vein with various length and brightness. Cross-sectional profiles will look like a dent because vein is darker than the surrounding area. By referring to the cross-sectional profiles, curvature profiles will be computed. Detection of vein and the centre positions will be assigned. Maximum curvature points will be found from four directions and finally will be calculated using the weighted sum of the all points.

Kang and Deng (W. X. Kang & Deng, 2009) used a different method which was maximal intra neighbour difference (MIND) to extract the vein features. MIND image will be obtained once the neighbour information vein extracted. This MIND image will be processed by histogram modification. By comparing the weighted sum of MIND image and mean image, the vein pattern images will be obtained. Key parameters can be set according to the user to improve results.

2.7.2 Statistical based method

Statistical based method is the method which typically uses various statistical data in the image such as Local Binary Pattern (LBP), Local Derivative Pattern (LDP), Local Tetra Pattern (LTrP) and Local Directional Texture Pattern (LDTP). However, the use of these methods is effected on axis or scale change which is the reason of using block-based strategies on feature extraction.

Local Binary Pattern (LBP) has been proposed for facial recognition, finger recognition, and palm print recognition. This method compares the grey level neighbourhood pixel values. LBP is an image texture descriptor that is able to differentiate the spatial structure of the image components (Ojala, Pietikainen, & Maenpaa, 2002). LBP will describe the image in direction forms where direction of LBP is an important property to the texture. The direction of LBP reflects the characteristic of image textures. The original operator 3x3 neighbourhood consists of 8 pixels in between a middle pixel. Figure 2.10 shows the coordinate system of the LBP descriptor.

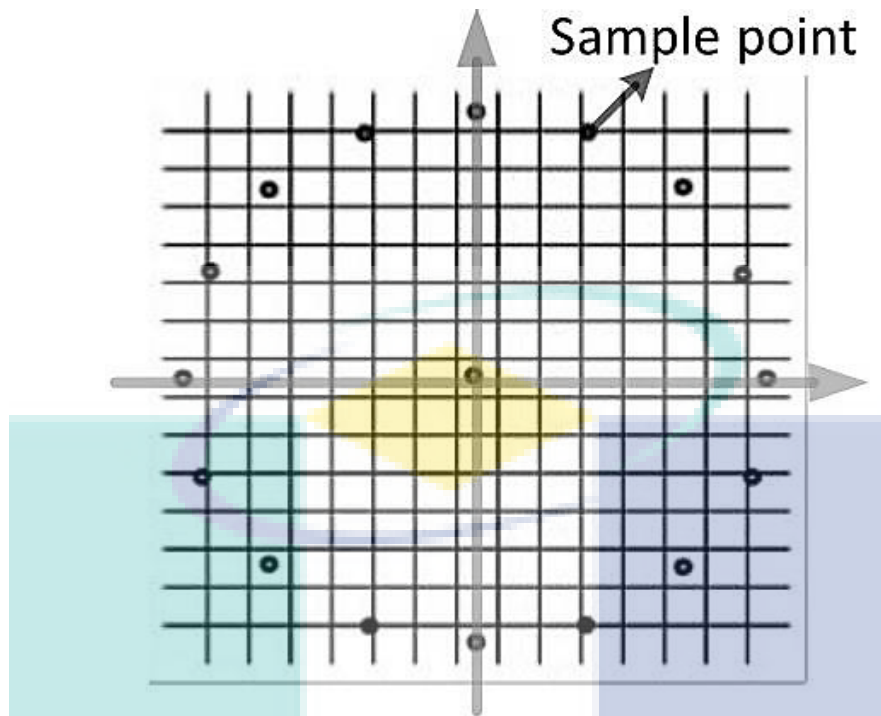


Figure 2.10 Coordinate system of LBP operator
 Source: W. Lu, Li, & Zhang (2016)

By using Directional Features from Local Binary Pattern (W.Lu et al., 2016), palm vein features extraction will be represented as a binary value therefore those value can be computed efficiently using binary operations. Directional activities of vein patterns and fusion with the multi-resolution analysis by the LBP is proposed on this feature extraction methods. Directional features are proved to be effective in extracting vein patterns either in texture based or structure based methods. A new LBP descriptors is developed by extracting more directional information for palm vein representation (W.Lu et al., 2016).

From this work (W.Kang & Wu, 2014), mutual foreground fusion with LBP for palm vein identification has been proposed. Maximal Principal Curvature (MPC) algorithm and k-mean are adopted for the feature extraction. Noise will be minimized and the accuracy has been improved which gives a good foundation to the following processing steps. In this experiment, LBP was matched with the mutual foregrounds (MF) of vein image. MF method extracted texture and its neighbourhood points only in grayscale image that include majority of useful distinctive information and eliminate the background pixels.

Local Derivative Pattern (LDP) have large order texture descriptor (Piciucco, Maiorana, & Campisi, 2017). It is an evolution of the LBP that LDP operator can extract the derivative direction which is in second order pattern information. In order to obtain the LDP descriptor, own suitable parameter have to be set or adjusted. In another paper (Mirmohamadsadeghi & Drygajlo, 2011), the best operator for extracting the palm vein features is within the size of 236x236 with veins of 2 to 10 pixel thick at a radius of 6 from the centre point. Figure 2.11 shows the neighbourhood for LDP operator at the radius of 6. The output histogram will be generated by the LDP once all the characteristics and features are obtained. The image descriptor will be in length of 16384 for an image divided into 16 sub images. It results in four grades according to the four directional features (Akbar, Wirayudha, & Sulistiyo, 2016).

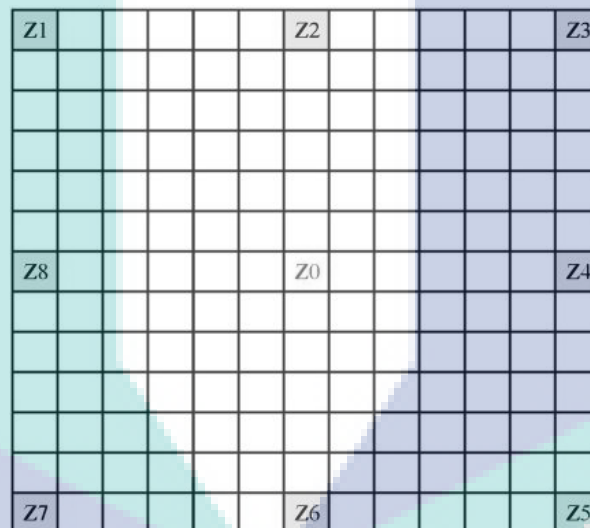


Figure 2.11 LDP operator with the radius of 6 from the center position
 Source: Mirmohamadsadeghi & Drygajlo (2011)

Local Directional Texture Pattern (LDTP) is a local feature descriptor that works especially for contactless design recognition systems. It is able to encode contrast and directional information of texture vein patterns (Rahul & Cherian, 2015; Rivera, Castillo, & Chae, 2015). 7 binary code will be computed in the input image. Distinctive information with 8 directions will be gathered by using the mask techniques with edge response of neighbourhood. Kirsch masks is to reveal vein pattern structure and it is robust against noise. In this work (Rahul & Cherian, 2015), Local Directional Texture Pattern (MF-LDTP) also works with the mutual foreground and it is used for palm vein recognition. Similar method of MF-LBP method that was discussed above and a new

technique of MF-LDTP is developed which has undergone the same process with the MF-LBP method.

Local Tetra Pattern (LTrP) uses four direction on the texture descriptor which created more information on the image. LTrP achieve higher order derivative in texture descriptors (Saxena, Tec, Travieso, &Alonso-hernández, 2015). Similar trend theory is the same with the LBP and LDP method above. The difference between those methods is the order derivative in the equation used. Thirteen binary patterns is represented in one image and those images will be combined together and become a single image.

2.7.3 Local invariant feature based method

Local invariant feature based methods are the methods where image features which exists are extracted as a point. These methods are not sensitive to rotation, scale, and axis changes. This method are mostly used for the contactless design system. However, due to the loss of useful feature information, binarization will not be used in pre-processing stage (P.-O.Ladoux, Rosenberger, &Dorizzi, 2009). Some research have directly extracted invariant features from the vein image without any pre-processing process.

Gurunathan et al. (Gurunathan, Sathiyapriya, &Sudhakar, 2016) used Speeded Up Robust Feature (SURF) feature invariant based method on multimodal palm vein and palm print recognition system. In the beginning of this work, they tested SURF by using rotated sampled. The result showed that it is able to match correctly even though the sample image had been rotated. Expected result was obtained and concluded with the merit of rotation invariant. In this paper, feature level fusion is applied to obtain the multimodal recognition systems. Fusion in between palm print feature extraction with palm vein feature extraction after SURF extraction is combined. Fusion method push the recognition rate to the higher level compared to only one or when conventional method is used. Distance measures is used for this kind of local invariant feature based methods (Pan &Kang, 2011). These methods have their own key point identifier and descriptor.

Scale Invariant Feature Transform (SIFT) has also been proposed in this paper (P.-O.Ladoux et al., 2009). SIFT has also been proposed in palm vein recognition system (Soh, Ibrahim, Yakno, & Mulvaney, 2018; Li, 2018). Key point of SIFT are located in the gradient of the image (Mikolajczyk &Schmid, 2005). Difference of Gaussian (DoG)

is used as the descriptor which has the difference plane of Gaussian layer. Descriptor is created to read the key points which can be understood by the algorithm (Lowe, 2004). In this paper (W.Kang, Liu, Wu, &Yue, 2014b), RootSIFT has been developed with the Hellinger kernel. RootSIFT and SIFT adopt the same methods on feature extraction for vein patterns. They obtain the similarity measurement with Euclidean distance that only brings improvement on the computational efficiency. Euclidean distance is used to maintain invariant features which are normalized to a Euclidean unit vector (Pan &Kang, 2011). In this work, they also tested SIFT algorithms by manually rotating the sample images. The result also showed that the rotation would not affect the SIFT techniques.

Yan, Deng, and Kang had proposed a score level fusion techniques between SIFT and Oriented Fast and Rotated BRIEF (ORB) used for palm vein pattern extraction (Yan, Deng, &Kang, 2015). Both features are able to extract a different type of feature which motivates this score level fusion to adopt vein pattern extraction techniques. SIFT are able to extract blob feature while ORB are able to extract corner feature. SIFT points are placed in the image and ORB feature points are placed along the vein pattern which means that the two features have different features point placement.

This study also performed the fusion level in between fusion of left and right palm images by using SIFT algorithms (Aishwarya &Devipriyanga, 2016). Left and right palm image will undergo SIFT algorithm and also Radon transform technique. The feature obtained from these two techniques will be combined and the left and right palm images will be fused. The recognition rate showed that it achieved better performance. However, by visual effect on the image it can be clearly shown that there was left and right palm image that overlapped each other's.

SIFT has also been applied in feature fusion level in palm vein recognition method (Yan, Kang, Deng, &Wu, 2015b). A similarity based feature fusion strategy has been proposed to streamline and optimize the feature vector sets. This is because it contains redundant information or vector sets by identifying the several vector sets that belongs to the same individuals that affect the speed and precision of matching. Hence, this works had proposed a method that improved the speed by lowering down the computational cost on the systems. Once there was similar feature vector sets found, the feature vector sets will keep one in the template. Else, if not similar, the feature point will be labelled until

all feature vectors are depleted. Finally, a new label points or vector sets will be computed and this vector sets will be registered as a new template.

2.8 Feature matching

Feature matching is the final stage to evaluate the method impact to the recognition rate. These matching method in general can be classified into two categories which are geometry and feature based matching (Michael, Connie, Teoh, Connie, &Teoh, 2011). Geometry based matching is the method that compares geometrical primitives like points and line features on the vein patterns. Point matching are used to compute the similarity in between two feature sets. Point features that are located by using interesting point detector (You, Li, &Zhang, 2002) always adopted distance metric like Cosine Similarity Distance (Manmohan et al., 2015), Hamming Distance (W. Y.Han &Lee, 2012), and Euclidean Distance (W. Kang et al., 2014; P. O. Ladoux, Rosenberger, & Dorizzi, 2009). Line-based matching is also computed using Euclidean distance measure that computes the similarity and dissimilarity between two line segments that are represented in coordinate systems (D.-S.Huang, Jia, &Zhang, 2008).

Feature based matching works well in either appearance or texture based techniques. PCA, LDA and ICA are among the subspace methods which are normally adopted with Euclidean distances on matching scores (G.-M. Lu, Wang, & Zhang, 2004; G. Lu, Zhang, & Wang, 2003). Other distance measures like chi square distances or city block distance were applied as well (X. Wu, Wang, & Zhang, 2004a; X. Wu, Wang, & Zhang, 2004b; X. Wu, Zhang, & Wang, 2003). Feature based method has a great advantage on low resolution image than geometry based method. This is because geometry based method requires precise location and orientation of geometrical features that are normally easier to obtain in high resolution image.

2.9 Critical review

This section will discuss the method and database used in this work after review of previous works is done. CASIA multispectral palm image database is focused in this work. A publicly available database is chosen to standardize the result and also available to compare with previous works. CASIA multispectral palm image database has 6 different types of wavelength spectrum that are able to propose an image fusion techniques by fusing several image into a single fused image. Several types of wavelength

spectrum in each individual will be fused to become one single image. This database is also popular among other database such that most of the previous studies are using this database to make comparison to each other.

Image pre-processing has played its role on enhancing the image by improving the contrast of image to obtain a finer detail of vein pattern in the images. According to the works that discussed above, palm vein recognition usually paired with the ROI extraction techniques. Otsu threshold is applied first to separate the region between palm and background region. The middle of the palm is taken for the computational process because the palm vein is all focused in the middle of the palm area. CLAHE is the popular technique to adjust the contrast so that vein pattern can be obtained easily. Median filter is used to filter the little noise beside or at the edge of the vein patterns.

Among all those featured extraction methods, local invariant feature based method has been focused in this work. Local invariant feature based method has been proven that it is not sensitive to rotation, translational, and scale changes. Because CASIA database are allowed to make some rotation changes on capturing the image, this type of method is the most suitable by applying in this database. SIFT and SURF methods will be used on this study where local invariant feature based method is suitable to be adopted in CASIA database.

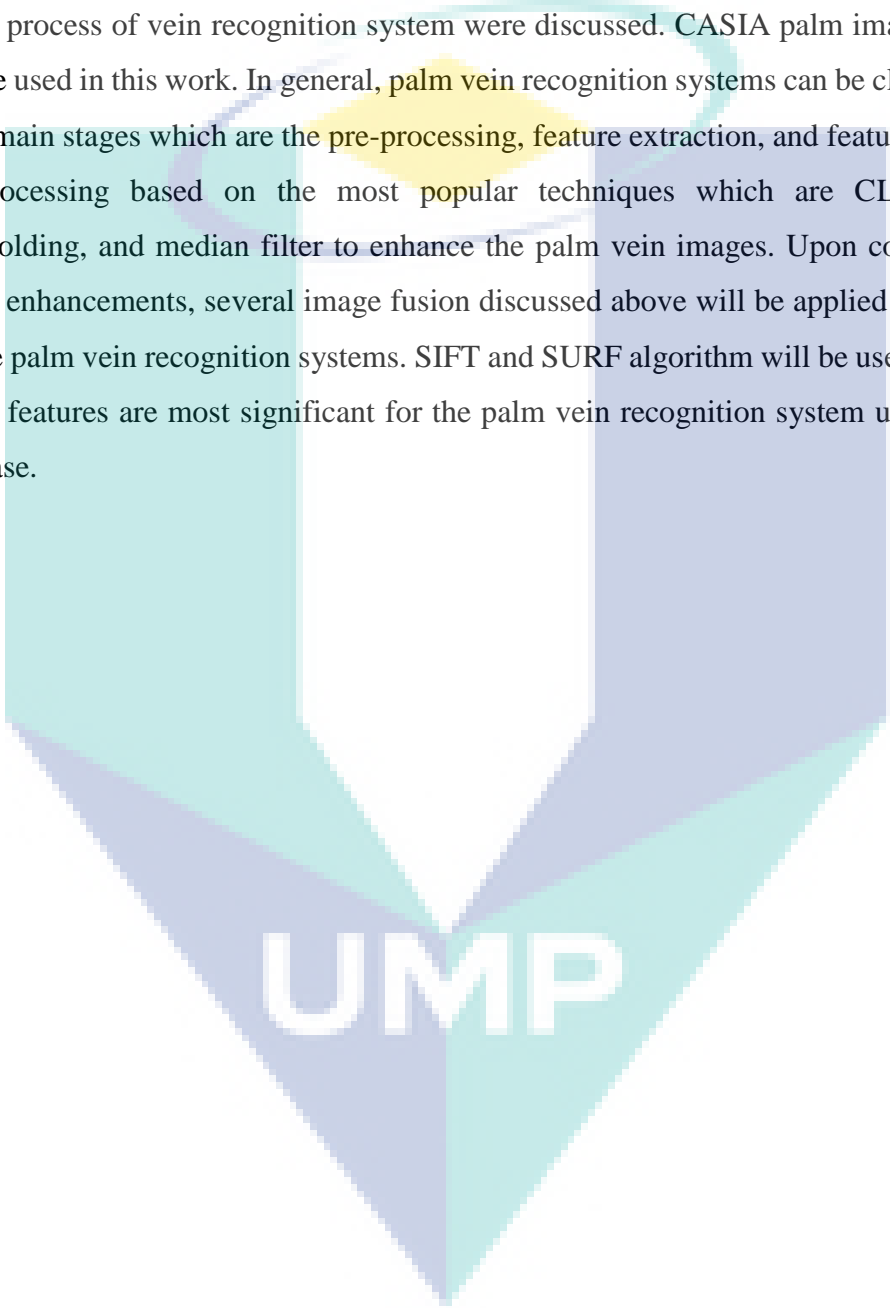
Point matching method will be used to classify the genuine and the imposter. Among those similarity distance measure, Euclidean distance is the popular method. Euclidean distance is used to compute the similarity and dissimilarity between two feature sets. Normalization of feature sets will be applied to normalize the vector in between [0, 1].

In this full process of palm vein recognition systems, image fusion techniques has been proposed by fusing palm image with different types of wavelength spectrums. According to the previous works, the fusion method are proven to be able to push the recognition rate to higher levels compared to the existing techniques used. Several image fusion will be used and compared to each other to identify which types of image fusion are suitable for the palm vein recognition systems. Image fusion in different type of wavelength are less proposed in those previous works. Image fusion techniques is

proposed to be used for the palm vein recognition system. It is believed that image fusion techniques can obtain a better recognition rate compared to the existing techniques used.

2.10 Summary

In this chapter, the previous methods of image fusion and techniques used in the whole process of vein recognition system were discussed. CASIA palm image database will be used in this work. In general, palm vein recognition systems can be classified into three main stages which are the pre-processing, feature extraction, and feature matching. Pre-processing based on the most popular techniques which are CLAHE, Otsu thresholding, and median filter to enhance the palm vein images. Upon completion of image enhancements, several image fusion discussed above will be applied in this work for the palm vein recognition systems. SIFT and SURF algorithm will be used to analyse which features are most significant for the palm vein recognition system using CASIA database.



UMP

CHAPTER 3

METHODOLOGY

3.1 Introduction

This chapter discussed in details all the methods used for the palm vein recognition system. This chapter will include the steps from the beginning which is palm vein acquisition until the end of the process which is the feature matching methods. Few of image fusion techniques will be discussed here to identify the effectiveness of image fusion techniques impact to the palm vein recognition systems. Figure 3.1 and 3.2 shows the overall process of palm vein recognition system used in this work and the general process of palm vein recognition respectively.

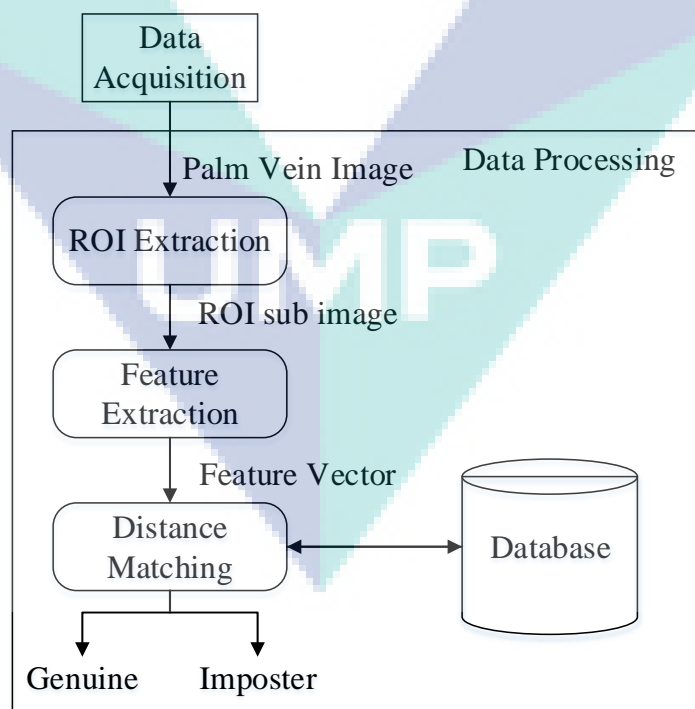


Figure 3.1 Overall process of palm vein recognition system

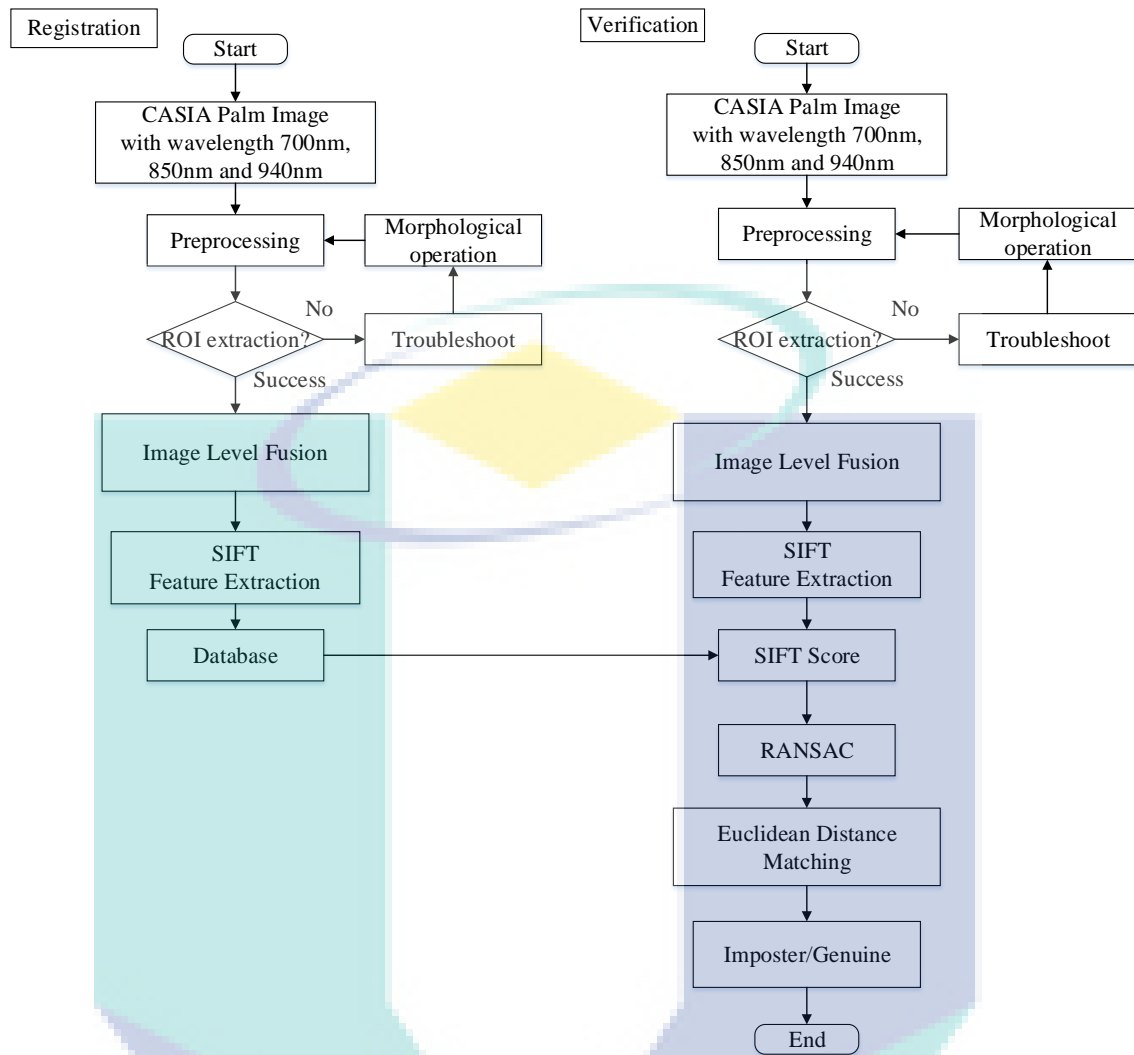


Figure 3.2 Process flow of palm vein recognition system

3.2 Palm vein image acquisition

In this work, palm image will be obtained from an open database which is the CASIA database. It contains 7200 palm images from 100 samplers by using self-design multispectral imaging device. The self-design multispectral device is shown in Figure 3.3. Two sessions were captured for each hand with time interval of more than one month. Three palm images were captured for each hand, with a total of six palm images taken for each sample. Each sample contains six palm images taken at six different electromagnetic spectrum which are 460 nm, 630 nm, 700 nm, 850 nm, and 940 nm and also natural light, for left and right palm images (Palmpoint & Database, 2017.). In between each image taken, samplers were allowed to make a certain degree of variation of hand postures. There was no restriction on postures and position of palms when

capturing because there was no pegs on the devices. Palm image were captured by capturing devices that supplied evenly distributed illumination.

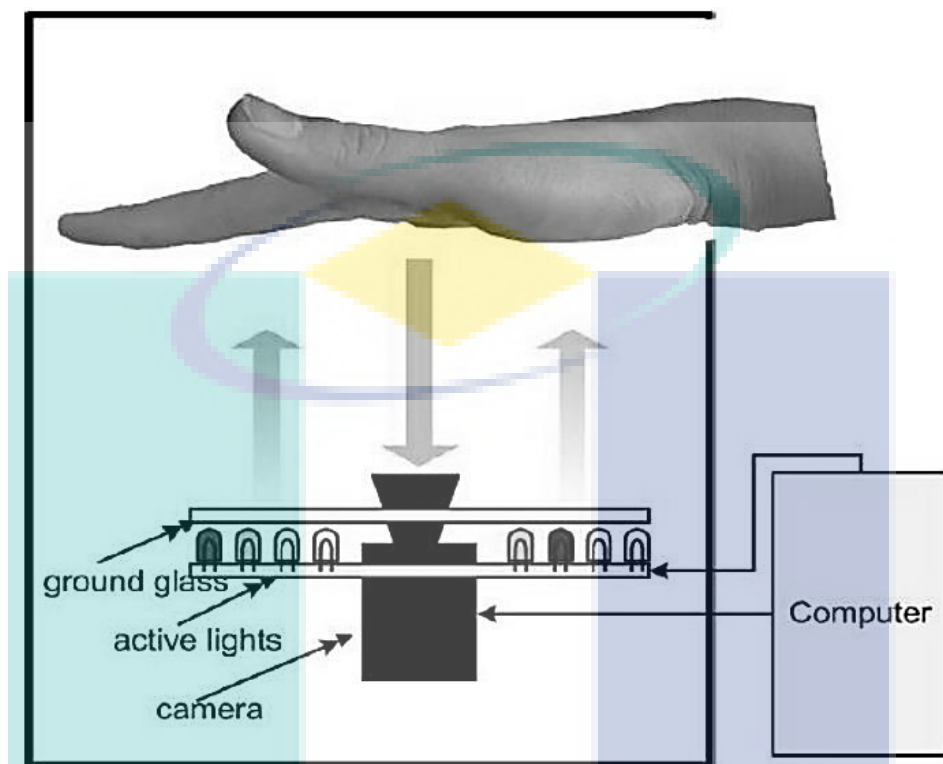


Figure 3.3 Multispectral Imaging Device in CASIA database
Source: Kisku, Rattani, Gupta, Sing, & Hwang (2012)

There are several reasons why this database was used on this study. First, this work used the open database because of the image capturing device and the scope of this studies. In order to develop an infrared imaging capture device, the cost has to be included in this study. Besides, it could delay this research while developing an image capturing device. By using own developed capturing device, it could produce some problems or noises which could affect the important parts of studies. This database was released and the public can download it for research and educational purpose Therefore, this research opted to use the open database which is available since the scope is focused more on the image fusion techniques.

There are several database that is open and available for the research studies. CASIA database was selected on this research because several methods have been using this database on evaluate the performance. By using the same database, this study are able to compare with existing methods to investigate the performance. By using this CASIA database, it is possible to use this database on fusion of different type of

wavelength spectrum for multimodal biometrics analysis because the different types of wavelength spectrum are available in CASIA database. In Figure 3.4, there are 6 different types of wavelength are available in CASIA database.

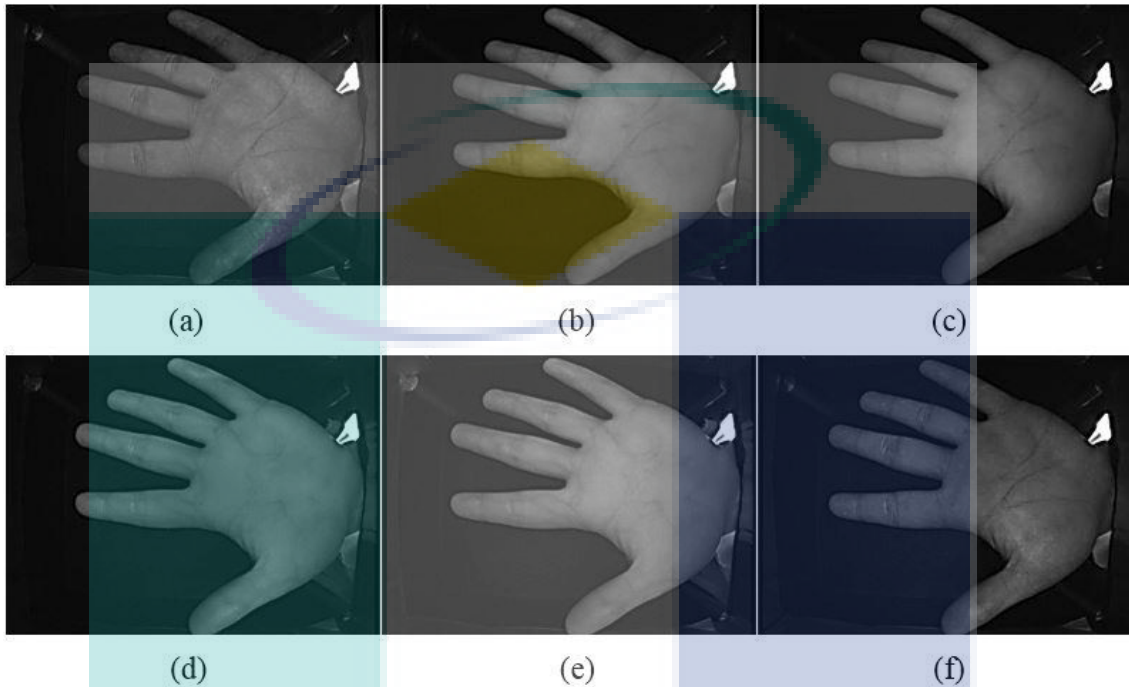


Figure 3.4 Different types of wavelength (a) 460nm, (b) 630nm, (c) 700nm, (d) 850nm, (e) 940nm, (f) Natural Light.

3.3 Pre-processing

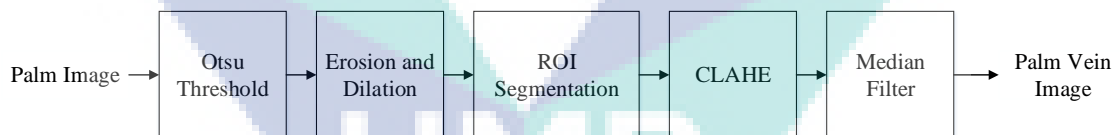


Figure 3.5 Block diagram of pre-processing stage

Figure 3.5 shows the overall block diagram in pre-processing stage. Palm vein image may carry some kind of noise caused by camera, weather, or other external stimuli e.g. salt and pepper noise. Hence, palm vein image is required to be pre-processed to remove the noise to produce reliable results. Before all those pre-processing method is applied, Region of Interest (ROI) extraction will be adopted first. ROI extraction was used to align different palm vein image for matching. Hence, it is important to extract only the centre part of palm vein images, otherwise more processing is required on the feature extraction stage. Besides that, rotational, translational and scale changes can also be normalized to minimize those problems.

Gaps between the fingers as reference points were to determine and extract the central part of palm vein images for reliable feature measurements. There were five main steps in this coordinate systems. Low-pass filter such as Gaussian smoothing was applied in whole palm images (C.Wang, Zeng, Sun, Dong, &Zhu, 2017). Threshold was used to convert RGB image into binary image. The palm images were binarized to separate the palm region from the background region. In other words, it was done to remove the background or unwanted region from the palm images. Figure 3.6(b) shows the binary images after it was converted from RGB images. Morphological filtering was done to reduce the small white area beside the palm region. The boundaries of the gaps between fingers were obtained by using a boundary tracking algorithms. The boundaries of the gap in between index and middle finger together with the ring and little finger were built up using the tracking algorithms. Between ring and middle fingers, the boundaries were not extracted since they were not important or useful for tracking algorithms. Figure 3.6(c) shows the two points utilized as the reference point on build up this algorithms. In the following steps, tangent in between two gaps were computed. This were the steps by using the estimation of the distance from centre position of the palm to the boundaries of the palms. Two points were searched using the corresponding local minima from the calculated distance. The image was smoothed by using Gaussian filter and then the centroid of the image was identified. The distance to the centroid and minimum and maximum peak were determined. In order to get the Y-axis of the coordinate system, a line was drawn by passing through the midpoint of these two points that was perpendicular to the Y-axis. Figure 3.6(d) shows the tangent line drawn in between two gaps. Finally, the image with a fixed size was extracted using the coordinate system and it then proceed to the next stage for feature extraction. A rectangular shape can be drawn using the distance of the centroid and the maximum and minimum peak. Fixed size of 192x192 rectangular shape was drawn at the palm for recognition. Figure 3.6(e) and (f) show the sub image extracted using the fixed size of coordinate system. This coordinate system made sure every palm image was rotated to a fixed degree rotation and extracted on the palm region which made the system invariant on rotation change (D.Zhang et al., 2003).

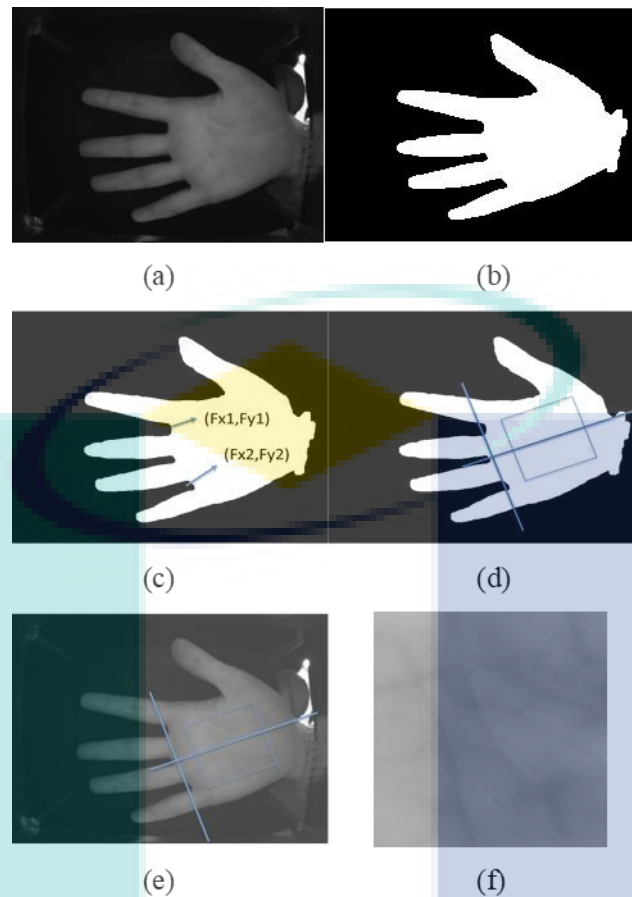


Figure 3.6 The main steps of coordinate systems, (a) Original image, (b) Binary image, (c) boundary tracking, (d) Coordinate system with tangent line, (e) Subimage extracted in center part, (f) ROI extraction in palm

By using the sub image extracted, Otsu threshold was applied first to convert into binary image and able to extract hand contours from the grayscale image. Low pass Gaussian filter and Otsu threshold were adopted to eliminate the image with high frequency and background noise that required short processing time (Article, 2014). Otsu threshold was performed to find the optimal threshold value from the gray level histogram and segment image with uneven illumination (Lee, 2012). Erosion and dilation will be applied after OTSU threshold in order to make sure the ROI extraction will be exactly on the palm.

Image adjustment had corrected the brightness on the ROI images. In the following step, Histogram Equalization was adopted to maximize the quality of features (Pan & Kang, 2011). ROI image was divided into 8x8 blocks and stretched to a histogram distribution with limited and uniform contrast (Hengyi Zhang, Tang, Li, Wai, & Kong, 2017.). Contrast-limited adaptive histogram equalization (CLAHE) is a popular method

on limited over amplify noise with minimizing unevenly distributed contrast on image (Sun et al., 2017). By using this method, the details on the palm vein patterns will be improved. CLAHE are able to magnify the visibility of blood vessels by aligning the image components.

In this step, CLAHE improved the contrast but it produced some noise due texture that created salt and pepper noise. Noise removal was then performed using median filter. The median filter was applied to remove the noise, hence improving the palm vein image quality. The median filter is a non-linear digital filtering technique, often used to remove the noise (L.Wang, Leedham, &Siu-Yeung Cho, 2008). The median filter ran through part by part of an image and replaced each entry with the median of neighbouring values. Finally, small speckles noise that appeared beside the vein patterns were removed by using median filter, such that this filter was able to conserve edges by eliminating noises.

3.4 Palm vein image fusion

Image fusion is used to combine different types of wavelength spectrum to become a fused image which provides more important information. Fused image is produced by integrating multiple image sources and then processed for the verification engine to make performance evaluation. Image fusion is the focus in this works to analyse the impact of fusion techniques to the recognition rate. There will be several techniques testing for the fusion to evaluate which techniques outperform the recognition rate among others. Figure 3.7 shows the block diagram on image fusion applied in the process.

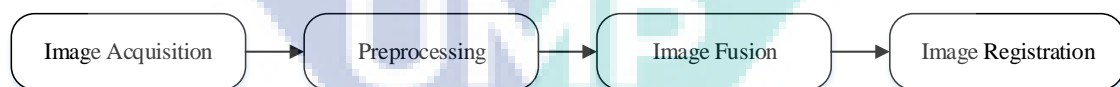


Figure 3.7 Block diagram for image fusion

3.4.1 Discrete cosine transform (DCT) fusion

Discrete Cosine Transform (DCT) was used to express an order of image data points at different frequencies by using sum of cosine functions. It was an essential technique mostly applied in digital image processing. Most of the DCT coefficients focused in low frequency area due to its excellent energy compactness properties at different frequency (Naidu, 2013). It compacted more image values and edges, contributing to high frequency coefficients. 2D DCT and IDCT are shown in Equations

3.1 and 3.2 respectively. Figure 3.8 shows the computation of 2D DCT required to operations columns coefficients first and process to row coefficients. X is the DCT coefficients and $N \times N$ is the length of the signal. Since, 2D DCT is a direct extension of 1D DCT, 2D DCT involve in x and y direction. In equation 3.1 and 3.2, $\alpha(k_1) = \sqrt{\frac{1}{N}}$ when k equal to 0 or $\alpha(k_1) = \sqrt{\frac{2}{N}}$ when k not equal to 0.

$$X(k_1, k_2) = \alpha(k_1)\alpha(k_2) \sum_{n_1=0}^{N_1-1} \sum_{n_2=0}^{N_2-1} x(n_1, n_2) \cos\left(\frac{\pi(2n_1+1)k_1}{2N_1}\right) \cos\left(\frac{\pi(2n_2+1)k_2}{2N_2}\right) \quad 3.1$$

$$X(k_1, k_2) = \sum_{n_1=0}^{N_1-1} \sum_{n_2=0}^{N_2-1} \alpha(k_1)\alpha(k_2)x(n_1, n_2) \cos\left(\frac{\pi(2n_1+1)k_1}{2N_1}\right) \cos\left(\frac{\pi(2n_2+1)k_2}{2N_2}\right) \quad 3.2$$

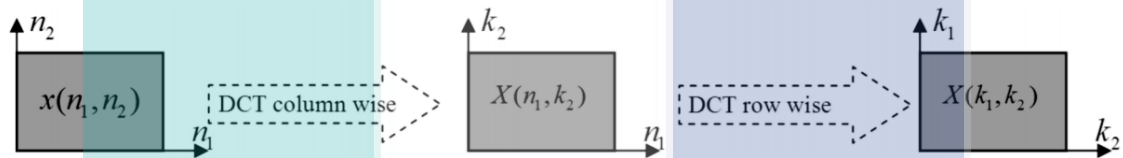


Figure 3.8 Computation of 2-D DCT in column and row wise.

Source: Naidu (2010)

Input image was divided into non-overlapping blocks of size 8×8 and then transformed into DCT coefficients. Fusion rule was applied within the DCT coefficient in each block with more number of higher value of AC coefficients. The consecutive 8×8 DCT domain blocks will be converted into spatial domain by applying inverse DCT (Naidu, Aerospace, &Naidu, 2015). Figure 3.9 shows the simple image fusion process using DCT and inverse DCT.

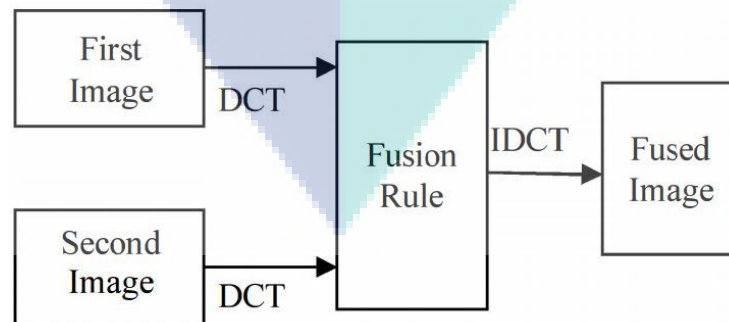


Figure 3.9 Image fusion process using DCT

3.4.1.1 Frequency partition discrete cosine transform (FPDCT)

Frequency Partition Discrete Cosine Transform will partition the DCT coefficients into low frequency (LF) and high frequency (HF) region. Partition was done according to the partition factor f by using energy compaction property of DCT coefficients. Partition factor f was expressed from 0 to 1 with intervals of 0.1 thereby creating 10 distinctive levels. Image was downsampled by selecting frequency level according to the pixel intensity. The fused image was then upsampled to the original size using inverse DCT. Figure 3.10 shows the partition method on partition DCT coefficients into LF and HF region (Kaur &Kaur, 2015).

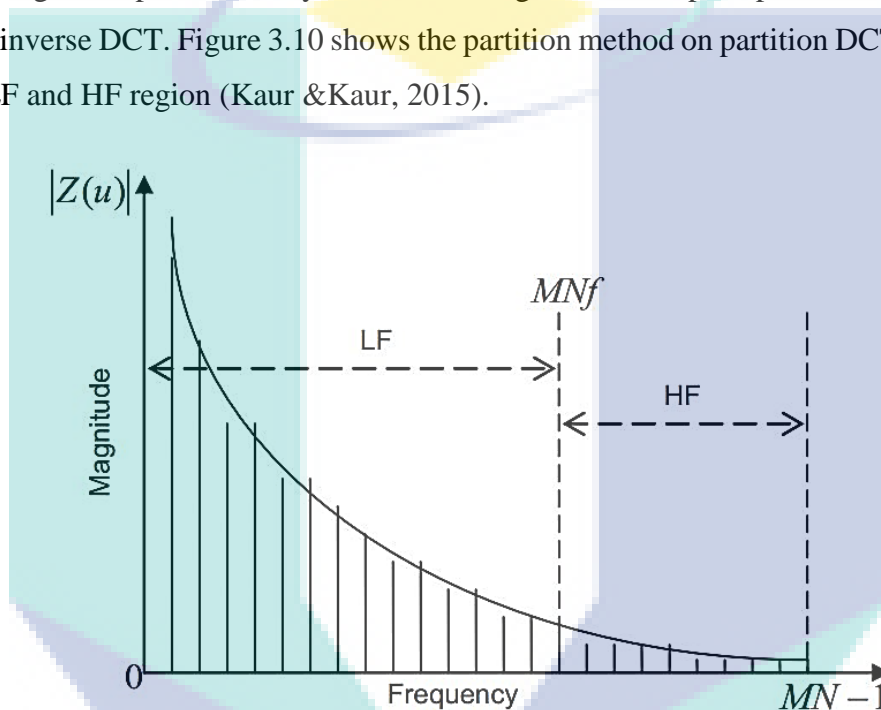


Figure 3.10 Separation of LF and HF coefficients with the coefficient factor.

Source: Kaur & Kaur (2015)

3.4.1.2 Multi-resolution DCT (MRDCT)

In multi-resolution DCT, DCT coefficient was filtered by low pass and high pass finite impulse filters (FIR). DCT coefficient was separated into halves and each half of coefficient was filtered by high and low pass filters. The output filter was decimated to the factor of two to achieve first level decomposition. Second level decomposition was repeated by using the decimated output high pass and low pass coefficient filtered by high and low pass filters. The level of decomposition was achieved successively by repeating the procedure in low pass and high pass filter (Naidu et al., 2015). Figure 3.11 shows the DCT coefficient passing through low pass, L and high pass, H in each level. Multi-resolution DCT had the similar characteristics with the wavelet transform in the field on

proper reorganization and representation of its coefficients (B . K . Shreyamsha Kumar , M . N . S . Swamy, 2013).

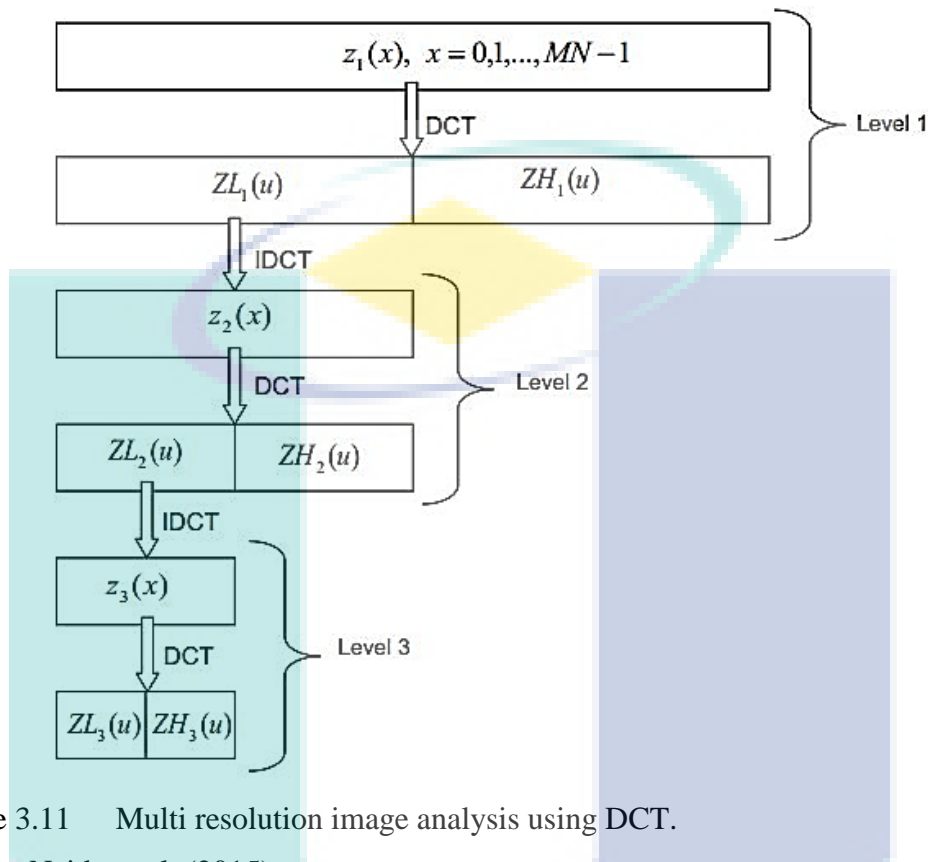


Figure 3.11 Multi resolution image analysis using DCT.
Source: Naidu et al. (2015)

3.4.1.3 Laplacian Pyramid (LPDCT)

In Laplacian Pyramid, level of decomposition was set at 5 to ensure the high detail fusion at pixel level. Both input images were upsampled to level 5 before fusion techniques were applied. Both images were fused and would be downsampled to original image using inverse DCT.

In downsampling or reduction function, images were divided into non-overlap block of 8x8. Every block was converted into DCT coefficients. 4x4 out of 8x8 non-overlap block would be treated as low frequency (LF) and this low frequency (LF) region would be applied IDCT to obtain downsampling. By using this downsampling method, four consecutive 8x8 blocks had become four consecutive 4x4 blocks in spatial domain. Same procedure was repeated to the rest. Figure 3.12(a) shows the downsampling process that converted four consecutive 8x8 blocks to four consecutive 4x4 blocks.

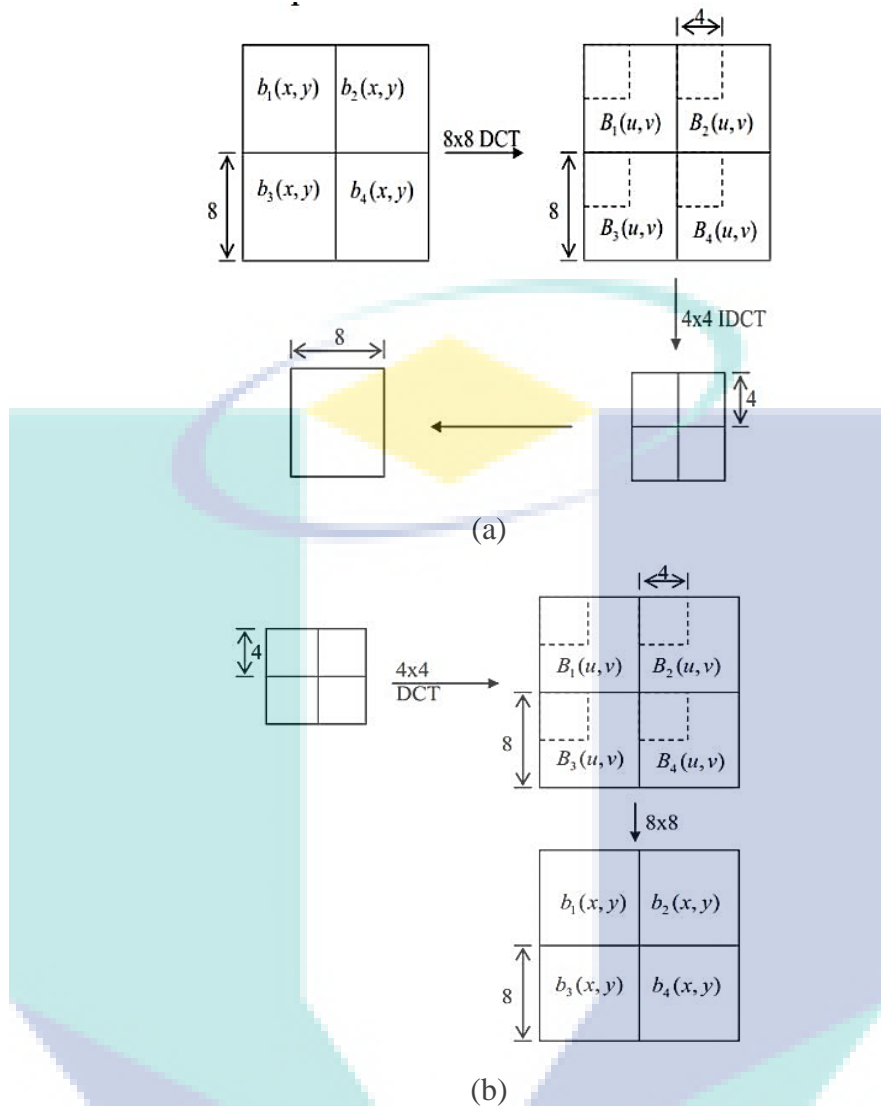


Figure 3.12 (a) Downsampling from 8x8 blocks to 4x4 blocks. (b) Upsampling from 4x4 blocks to 8x8 blocks.

Source: Singh & Rajput (2014)

In upsampling or expand function, image would be upsampled by two factors from 4x4 non-overlap blocks. High frequency region was treated as zero and low frequency region would be focused on. Low frequency region was converted into spatial domain by using 8x8 IDCT. Hence, four consecutive 4x4 blocks were converted into four consecutive 8x8 blocks. Figure 3.12(b) shows the upsampling from 4x4 blocks to 8x8 blocks.

The process for Laplacian Pyramid construction and reconstruction is shown in the figure 3.13. Image at the first level underwent downsampling to obtain half of the size of the image where both spatial density and resolution were reduced. The expand function

was also performed at the image construction level. For the following Laplacian level, the downsampling process was repeated. The construction of pyramid was formed by using the expand function and reduction function.

In image reconstruction, image fusion would be according to the image fusion rules. Pyramid construction would keep the error records in each image. In image reconstruction, the expand function was adopted here on the k level of pyramid. The magnitude comparison in between the output of every level of pyramid with the output of expand function in reconstruction stage was computed. The process was repeated until the level of pyramid ended. R is the reduction or downsampling method, E is the expand or upsampling method and z is the DCT coefficient

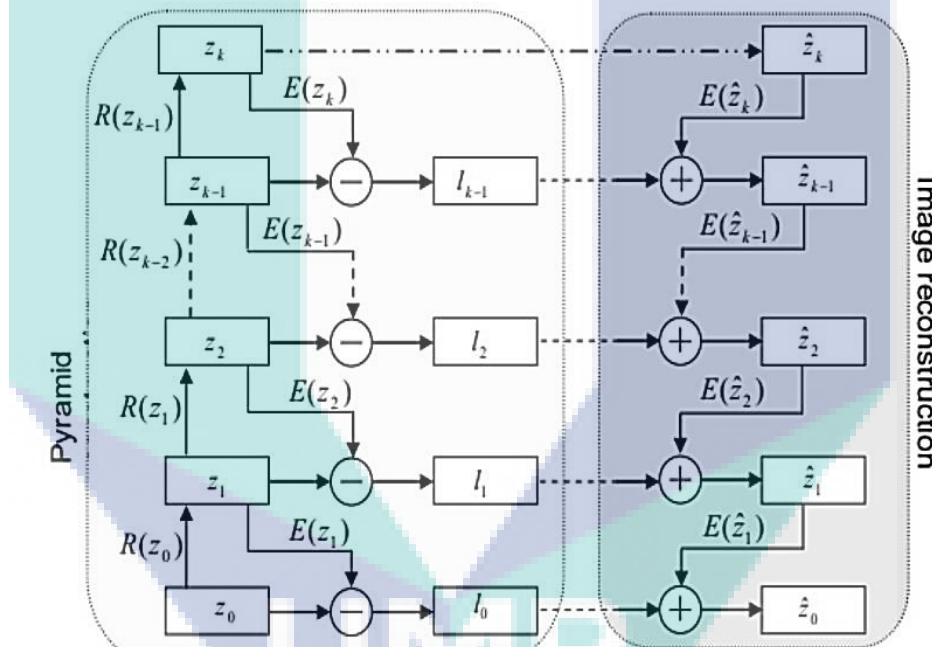


Figure 3.13 Laplacian Pyramid Construction and Reconstruction

Source: Singh & Rajput (2014)

3.4.2 Multi-resolution singular value decomposition (MSVD)

The method of MSVD is very similar to the wavelet transform in that its signal is filtered separately by low and high pass filters. The output was decimated by a factor of two that filter by low and high pass filters by achieving the first level of decomposition. The output of low pass filtered and high pass filtered would be filtered again with high and low pass filters with the decimated of factor by two for the next level decomposition. The process was repeated until the maximum level of decomposition was achieved. In

this multi-resolution singular value decomposition (MSVD), the FIR filter was replaced with the singular value decomposition (SVD).

2D MSVD is extended from the 1D MSVD for higher dimension. Image will be divided into 2x2 non-overlapping blocks. These blocks were arranged into 4x1 vector by forming a data matrix in columns form. The eigenvalue with the first row was considered as approximation component. The detail component that corresponded to edges or texture were represented in the remaining rows. Figure 3.14 shows the 2D MSVD with three decomposition levels.

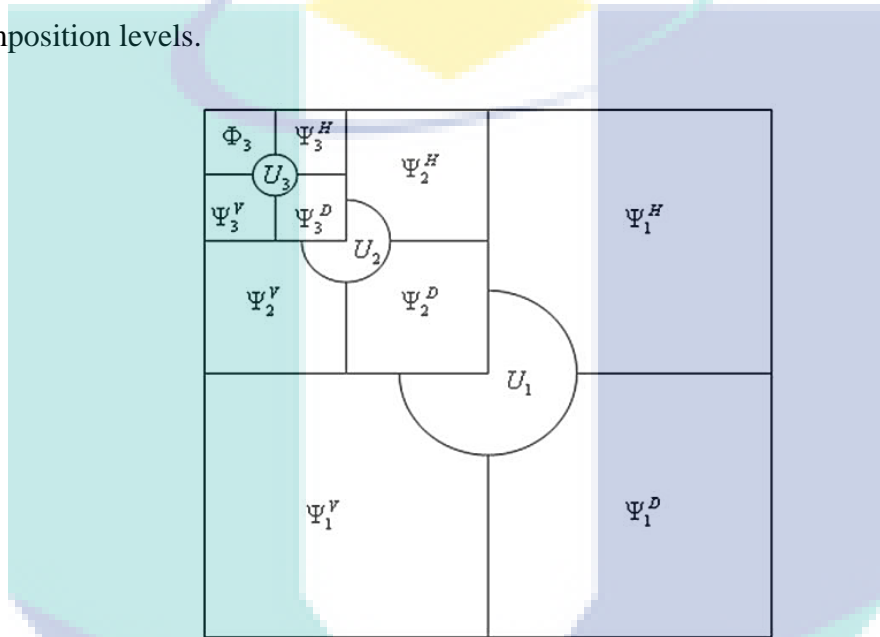


Figure 3.14 MSVD decomposition structures with three level of decomposition.

Source: Laboratories (2011)

In fusion stage, the fusion rule would select the largest value of two MSVD coefficients in image. Those coefficients corresponded to the sharper brightness changes in the images such as edges that would fluctuate at zero value. Once it reached the coarsest level, the fusion automatically took average of MSVD coefficients since the coefficients at this level were smoothed. The process was repeated until the level of coefficients ended. Figure 3.15 shows the schematic diagram for MSVD image fusion scheme.

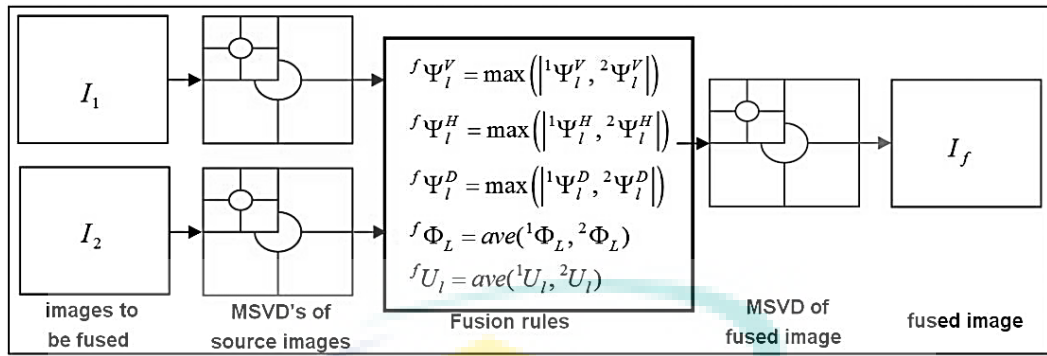


Figure 3.15 MSVD fusion scheme

Source: Laboratories (2011)

3.4.3 Energy of Laplacian (EOL)

Figure 3.16 shows the image fusion method based on EOL with guided filter and majority filter. Intensity of both images was normalized first and lie within the range from 0 to 1. EOL was computed by using the block diagram. The coefficient output was divided into 8x8 non-overlapping blocks and those blocks were computed independently. The coefficients in matrix form were compared to obtain a binary decision map. The focused image area produced higher EOL coefficient while defocused areas produced smaller EOL coefficients. Guided image filter was adopted to optimize the binary decision map. The fusion was in between the first original image and the decision map to the guidance image and the filtering image of the guided image filter respectively. Therefore, the fused image can be obtained by using the block diagram in Figure 3.16.

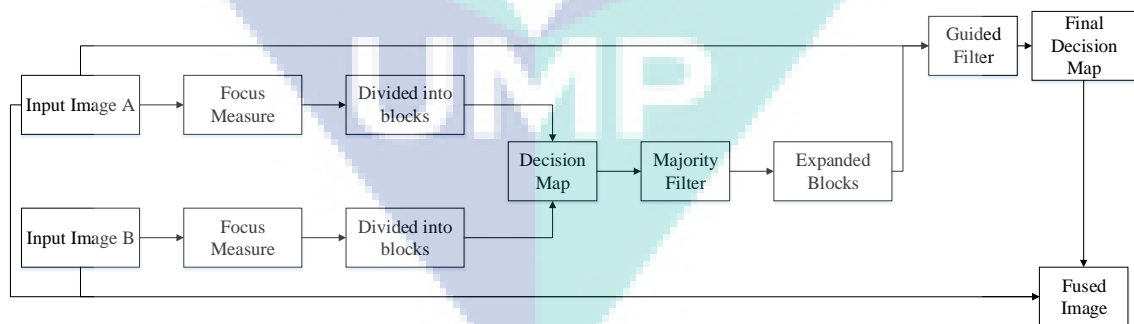


Figure 3.16 Schematic diagram of EOL based image fusion

Source: Zhan, Teng, Li, & Shi (2015)

3.4.4 Wavelet transform (WT)

In wavelet transform, wavelet based approach is used to get the fused image. Discrete Wavelet Transform (DWT) will decompose image into a different kind of coefficients by preserving the image information (Qiu, Kang, Tian, Jia, &Huang, 2017). Coefficients in both image were abstract and combined to become a new coefficients which means that the information in both images were appropriately collected and fused. After fusion, Inverse Discrete Wavelet Transform (IDWT) was achieved here so that the fused coefficients would be converted back to the final fused image which preserved the information. General equation of wavelet based fusion is shown in the Equation 3.3.

$$I_{FU} = idwt(\phi(dwt(I_1), dwt(I_2), \dots)) \quad 3.3$$

Haar wavelet at decomposition of level 2 was used for wavelet transform. In this work, “Min-Max” strategy was used as the fusion strategy (Barra, DeMarsico, Nappi, Narducci, &Riccio, 2018). Wavelet coefficients after DWT was obtained by computing a weighted average of the sources. This strategy was choosing the minimal approximation components in different channels as the fused components and maximal detail components as the fused detail components. Figure 3.17 shows the block diagram of wavelet based image fusion.

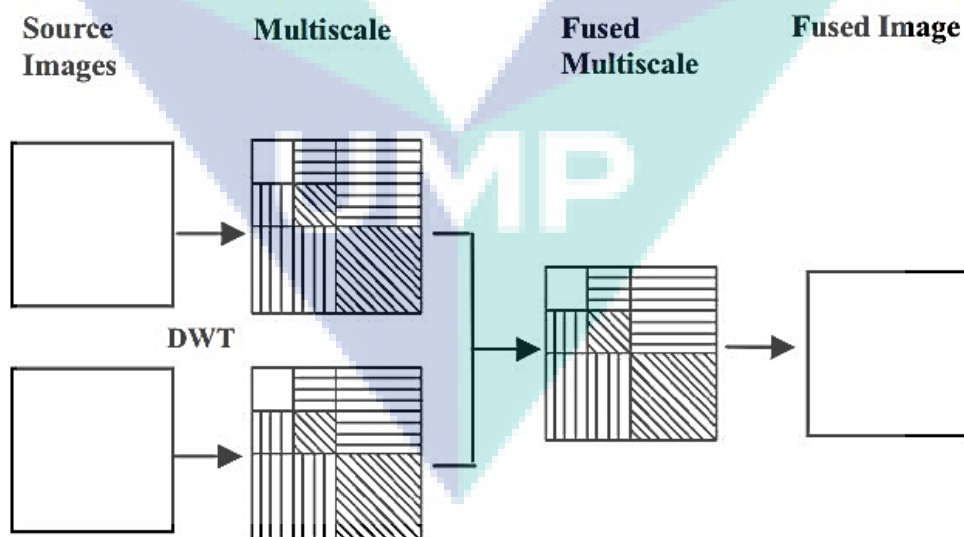


Figure 3.17 Block diagram of Wavelet based image fusion

Source: Kisku, Rattani, Gupta, Sing, & Hwang (2012)

3.5 Feature extraction

From all the feature extraction method, local invariant featured based method has been chosen for this research. Several method have been discussed in the literature review. All those methods can be categorized into four groups which are geometry based method, statistical based method, local invariant featured based method, and subspace method. By comparing the advantages and disadvantages from these few methods, local invariant featured based method seems to be the most perfect method for this research. Local invariant featured are not sensitive to scale, rotation, and translational changes. This method is the best feature extraction techniques that is appropriate for the contact free vein recognition.

3.5.1 Scale invariant feature transform (SIFT)

SIFT adopts the strategy for feature detection and description in the following steps: (1) scale-space extrema detection; (2) key-point localization; (3) orientation assignment; (4) generation of key-point descriptors; (5) the formation of several dimension descriptors to represent image features. Due to these features, this method would not be affected by any image which has rotation and scale changes. By using this method, issue on rotation could be solved.

Scale-space extrema detection is a scale space to detect the blob structure in an image (Giveki, Soltanshahi, &Montazer, 2017). The function is produced from the convolution of a variable-scale Gaussian with an input image. It is implemented effectively by using a Difference of Gaussian (DoG) algorithm to identify the potential key points that are not sensitive to scale and orientation changes. Gaussian function is produced from the convolution of a variable-scale Gaussian with an input image. Simple image subtraction computed in this function due to its efficient function and possibility in any case for scale space feature description. In Equation 3.4 and 3.5, it shows the Gaussian function with convolution of scale Gaussian with input image and image subtraction with down sampled of factor k respectively. In Figure 3.18, it shows the Difference of Gaussian obtained by using convolution on of each octave of scale space. The process was repeated by a down sampled of factor by 2 in the following octave scale.

$$L(x, z, \sigma) = G(x, y, \sigma) * I(x, y) \quad 3.4$$

$$D(x, z, \sigma) = (G(x, y, k\sigma) - G(x, y, \sigma)) * I(x, y) \quad 3.5$$

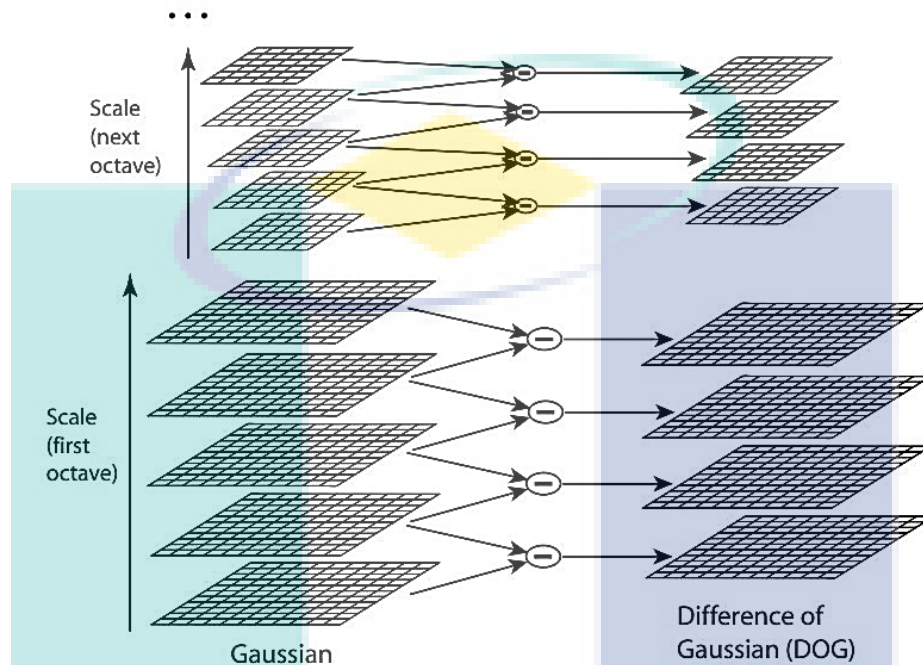


Figure 3.18 DoG obtained by using the simple subtraction of different scale Gaussian level

Source: Lowe (2004)

Key points were found by comparing a pixel to its neighbors. Key points were obtained by comparing the frequency in either spatial domain and also in scale domain. Figure 3.19 shows the key points detected by comparing a pixel with its neighbors in different space. Key points were fit in detailed for location, scale and ratio of principal curvatures. By using key point's localization, this algorithms evaluated the key points which were low contrast or poorly localized along the edge. This was because those points are very sensitive to noise. The threshold value was set as a parameter. The Gaussian value $G(x, y, \sigma)$ below that threshold would be recognized as low contrast and it would be removed directly. For stability of key points, 2x2 Hessian matrix was computed at the location and scale of the key point to produce principal curvatures.

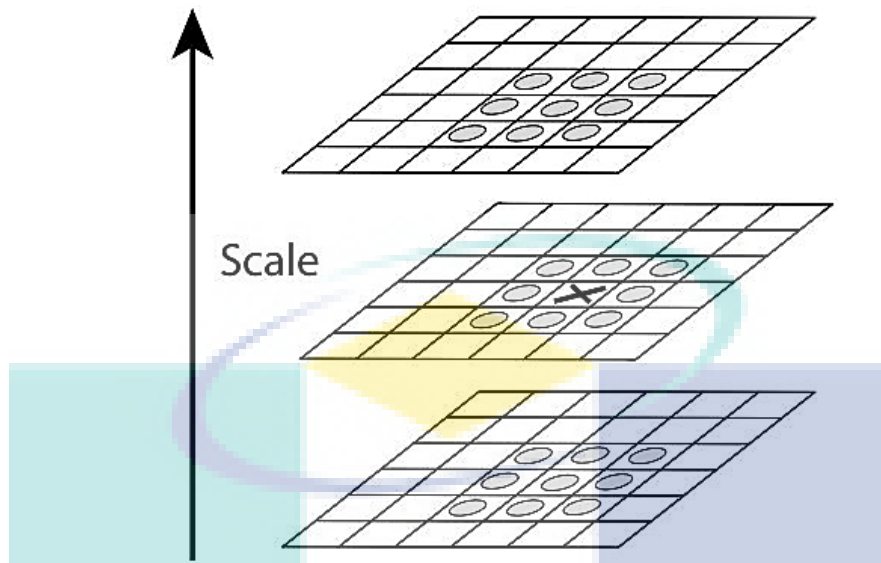


Figure 3.19 Key points located by comparing pixel with its neighbors.
Source: Lowe (2004)

Assigning consistent orientation to each key point made the key point achieve invariant to rotational changes and therefore represented relative to the orientation assignment. Orientation assignment had assigned one or more orientations based on local image gradients directions. All process were performed on image key points that had been transformed and thereby provide assigned orientation, scales and location for each feature that providing invariant to these transformations.

The scale of the key point was used to select the Gaussian smoothed image, L , with the closest scale, therefore all process were adopted in a scale-invariant manner. Equation 3.6 and 3.7 shows the scale, gradient magnitude, $m(x, y)$, and orientation, $\theta(x, y)$, computed using pixel differences for each image sample, $A(x, y)$. 36 bins covering 360 degree range of orientations was formed from the gradient orientations of sample points within a region around the key points.

$$m(x, y) = \sqrt{(A(x+1, y) - A(x-1, y))^2 + (A(x, y+1) - A(x, y-1))^2} \quad 3.6$$

$$\theta(x, y) = \tan^{-1} \left(\frac{A(x, y+1) - A(x, y-1)}{A(x+1, y) - A(x-1, y)} \right) \quad 3.7$$

Key point was generated by using the scale of the key point to select the level of Gaussian blur for the image. Figure 3.20 shows the descriptor generation from the key point locations. A Gaussian window was generated around the key point location which indicated gradient magnitude and orientation in each image sample points. The local image gradients at the selected scale in the region were measured around each key point. These transformations allowed for significant levels of local shape distortion and change in illumination. Results of 128 feature vector would be computed in SIFT algorithms.

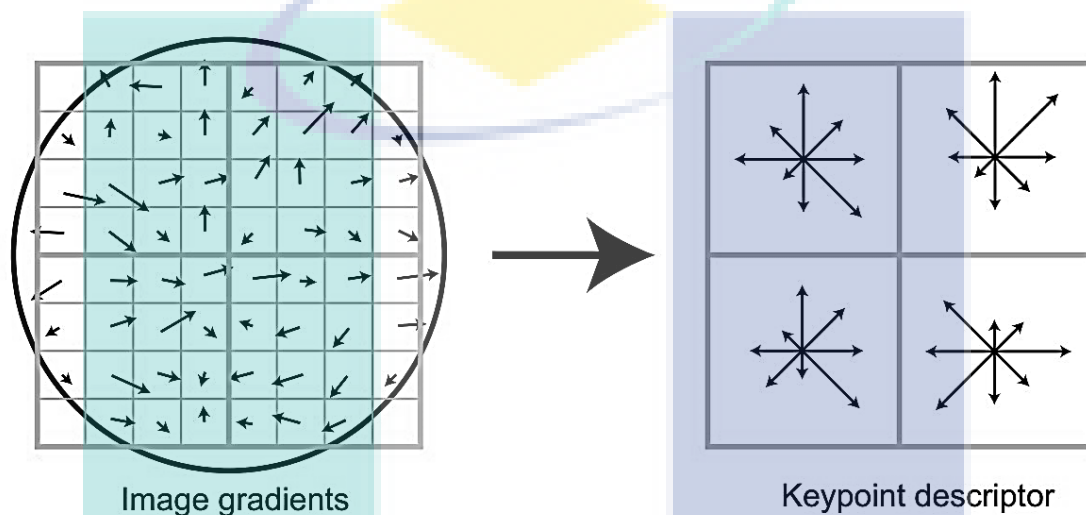


Figure 3.20 The key point descriptor generated by summarizing the contents in image gradients with the length of the arrow in eight directions.

Source: Lowe (2004)

3.5.2 Speed up robust feature (SURF)

Speed Up Robust Feature (SURF) is also the one of the local invariant features that uses existing algorithms. SURF algorithm would extract the feature vectors from the captured image. The feature vectors were formed by local pattern around the key points. Scaled up filter was applied to detect the key points. In SURF algorithms, there are also the key-point detector and descriptors.

Key-point descriptors was used by using Hessian matrix approximation. The box filter was applied on the Hessian matrix and finally the key points were localized in scale and image space by applying non-maximum suppression. SURF detected interest points by using Fast-Hessian detector that was based on Scale Space Theory. Hessian matrix was the detector of interest point in images. Determinant of Hessian matrix was used to

localize the interest points in images. Equation 3.8 and 3.9 defined Hessian matrix $H(X, \sigma)$ and Determinant of Hessian matrix in X at scale σ .

$$H(X, \sigma) = \begin{bmatrix} A_{XX}(X, \sigma) & A_{XY}(X, \sigma) \\ A_{XY}(X, \sigma) & A_{YY}(X, \sigma) \end{bmatrix} \quad 3.8$$

$$Det(H) = D_{XX}D_{YY} - (0.9 * D_{XY})^2 \quad 3.9$$

In SURF, a box filtered with these approximate second order of Gaussian derivative evaluated very fast using integral images. Figure 3.21 shows the 9x9 box filters approximate for Gaussian second order derivative. By approximating all X and Y directions, this yielded the determinant of Hessian matrix. Interest points were obtained in the maxima of Determinant of Hessian matrix. The discriminant value will be used to classify the maxima and minima of interest points.

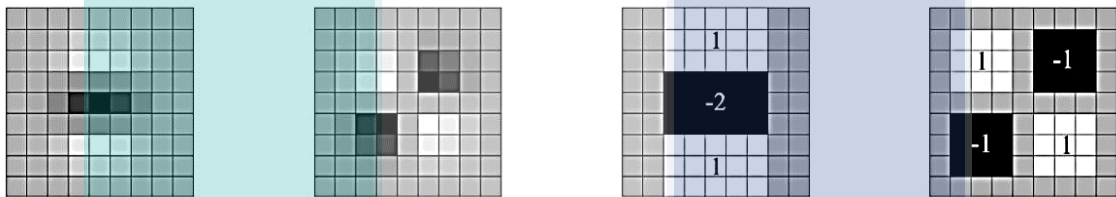


Figure 3.21 Gaussian second order derivative from left to right in x and y direction and approximations using box filters.

Source: Xu & Namit (2008)

Haar wavelet responses in x and y direction was calculated in orientation assignment. The side length of Haar wavelet was $4s$ while sampling step was scale dependent and defined as the s . The neighbor of the circle that surrounded the interest point was the center and its radius was $6s$. The wavelet responses were calculated and weighted with the Gaussian of $2.5s$ in the middle of the key points. The dominant orientation would calculate all responses in a sliding window covering all angles. Figure 3.22 shows the interest point detected in the picture and the use of the Haar wavelet to assign its own orientations.

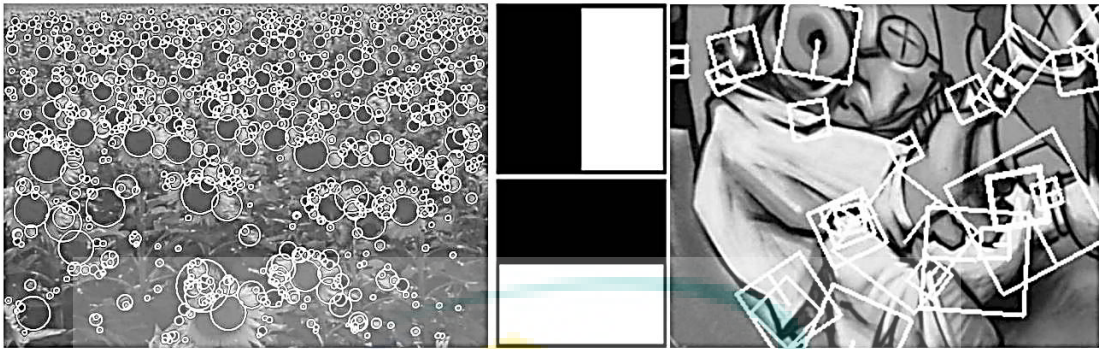


Figure 3.22 Interest point detected in left picture and orientation is assign in the right picture with Haar wavelet response in the middle.

Source: Xu & Namit (2008)

In descriptor component, a square region with size $20s$ was constructed in the center of the key points with all orientation selected. The region was split into 4×4 square sub regions with each sub region with $5s$ scale for Haar-wavelet response. Haar-wavelet responded in horizontal and vertical direction with weight of $3.3s$ in the center at the key points by increasing the geometric deformations robustness. 4 dimensional descriptor vector for each sub region was extracted. Therefore, 64 dimensional feature vector were extracted for every key point for all 4×4 square sub regions. Figure 3.23 shows the diagram for building the descriptor for every key points.

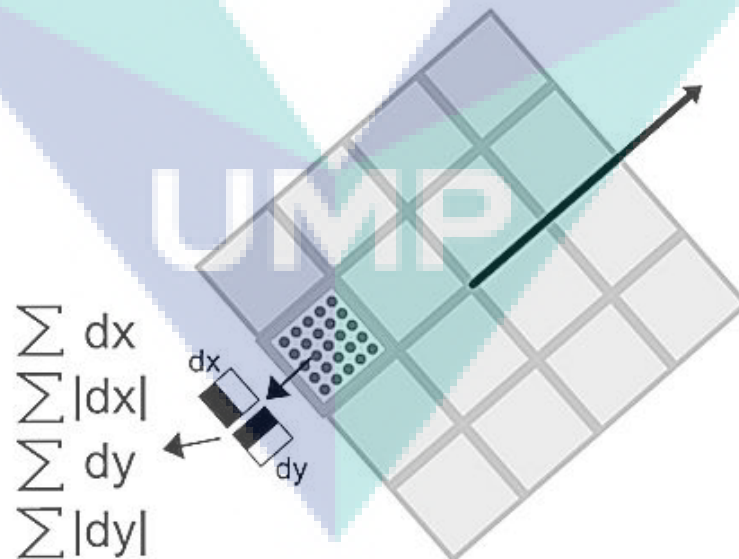


Figure 3.23 Diagram for building the descriptor in every interest points.

Source: Huijuan Zhang & Hu (2011)

3.6 Feature matching

Before going to feature matching, a mismatching removal tools have to be applied to reduce the mismatching point in SIFT and SURF algorithms. Random Sample Consensus (RANSAC) is an algorithm and estimator where user can select the threshold distance and iteration number. Random selection on the consensus set to obtain and calculate the parameter to find the highest consensus set (Y.Wu et al., 2015). A fundamental matrix was formed based on the number of SIFT matching results. SIFT matching results were randomly chosen to determine the epipolar lines and number of inliers. This process was repeated until the largest number of inlier was found (Vi & Vi, 2015). SIFT algorithms normally use point matching methods to decide on genuine and imposters. Hence, mismatching point that occurred in the SIFT algorithm were believed to be impact to the verification rate. Outliers are caused by image registration such as image fusion, image rotation, or image resize. Those outliers make the mismatching point on either genuine and imposter decision. It can be eliminated by estimating the geometrical transformation of the image.

In this works, Euclidean Distance classification for genuine or imposter was used in either SIFT or SURF feature extraction. Euclidean distance was compared with the database pattern to all test patterns. This is because Euclidean distance is the simplest classifier compared to other distance matrix classifier. Euclidean distance also achieve almost same EER rate compare to other classifier in other works. Genuine subjects would be recognized once the Euclidean Distance was obtained below the threshold value and vice versa. Euclidean distance, in other words, Pythagorean formula is the normal distance between the two points that can be measured with a ruler. Euclidean space becomes the Euclidean matrix by using the Pythagorean formula. The horizontal and vertical distance between the points was measured. With this small addition, a right-angled geometric shape with its legs or coordinates was obtained. By using the Pythagorean Theorem, length of the hypotenuse was obtained and that is the value of Euclidean Distance. This result was the same as the distance between the two points according to the distance formula.

Once the Euclidean Distance for each collection was obtained, the ratio of the Euclidean Distance between test samples with the database sample was obtained for feature point match between two images. The criterion of Equation is shown in Equation

3.10. Once the criterion in this Equation was accepted, it was recognized as matching pair, otherwise it would be rejected as an imposter.

$$\frac{d_{\min}}{d_{n-\min}} \leq 0.65 \quad 3.10$$

In order to obtain matching score, training and testing samples of each user were matched using Euclidean Distance (Pandey, Verma, &Kumar, 2018). Matching scores were referred as genuine scores if the testing and training was the same users, otherwise it would be referred to as imposter scores (Fang, Wu, &Kang, 2018). The minimum the matching scores, it would be taken as the genuine scores or otherwise the larger the matching scores, it would be taken as imposter scores. By generating Equal Error Rate (EER), threshold was drawn in comparison of both genuine and imposter scores. The threshold was decided by two different rate which was false rejection rate (FRR) and false acceptance rate (FAR). FRR is the percentage of the rejected genuine matching scores, while FAR is the percentage of accepted imposter scores. By generating Area under the Curve (AUC), the threshold was the one selected from ROC with the lowest FAR graph. Threshold of AUC determined the decision of acceptance and rejection in verification stage.

3.7 Summary

In this section, most of the methods had been discussed in detail. CASIA database was used for this work because of the popularity of usage of this database in previous works. Most of the works applied CLAHE, median filter and Otsu thresholding in most of the vein image enhancement techniques. Several types of image fusion techniques were applied after image enhancement. Image fusion was applied by fusing several images with different types of wavelength spectrum to form a new fused image. SIFT and SURF were the methods that were classified as invariant feature based method. These two algorithms will be discussed further in chapter four to identify which method would be able to obtain the best and most feature in the vein pattern images. Feature point were matched by using Euclidean distance to find the similarity of both images.

CHAPTER 4

RESULTS AND DISCUSSION

4.1 Introduction

This chapter will explain in detail all the results obtained from the beginning stage until the end of the stage of palm vein recognition system. Results of different type of palm vein feature extraction will be shown in the following sections. The most effective palm vein feature extraction techniques will be chosen and will proceed by using image fusion techniques. Overall image fusion techniques will be compared in Equal Error Rate. The most powerful image fusion techniques will be compared with the existing techniques to show that the effectiveness of the image fusion techniques to the palm vein recognition systems.

4.2 Pre-processing

In pre-processing stage, the middle of the palm image were obtained first by using the ROI extraction algorithms. However, there was a problem with the ROI extraction algorithm in extracting palm image in CASIA database. This algorithm didn't work for the majority images in CASIA database. The detected centroids were not compatible with the palm boundary detected. This caused the wrong rotation of the palm, hence the wrong ROI was taken in the middle of the palm. Besides that, the peak points were not the expected ones which was also one of the causes of the wrong ROI taken. In addition, this algorithm had computational error on matrix dimension and scalar distance when running the algorithms. However, the algorithm has been edited and adjusted. The morphological operation by using erosion and dilation has been added to the algorithms which makes the algorithms succeed in ROI extraction.

Figure 4.1 shows the full process of ROI extraction for a few samplers. Figure 4.1(a) shows the original image of palm image in CASIA database. The Otsu thresholding with smoothing filter was applied to obtain the black and white of palm image. Otsu thresholding separated the area in between background and palm region. By visual inspection in figure 4.1(b), there were some little noise or distortion in the images. That noise caused the ROI taken further away from the middle of the palm. Hence, the morphological operation was applied to remove all noises as shown in figure 4.1(c). The centroid of the palm was found by using the centroid of the function to find the centre point of the palm. By using the centre point, the ROI rotation would be based on the centre point of the palm.

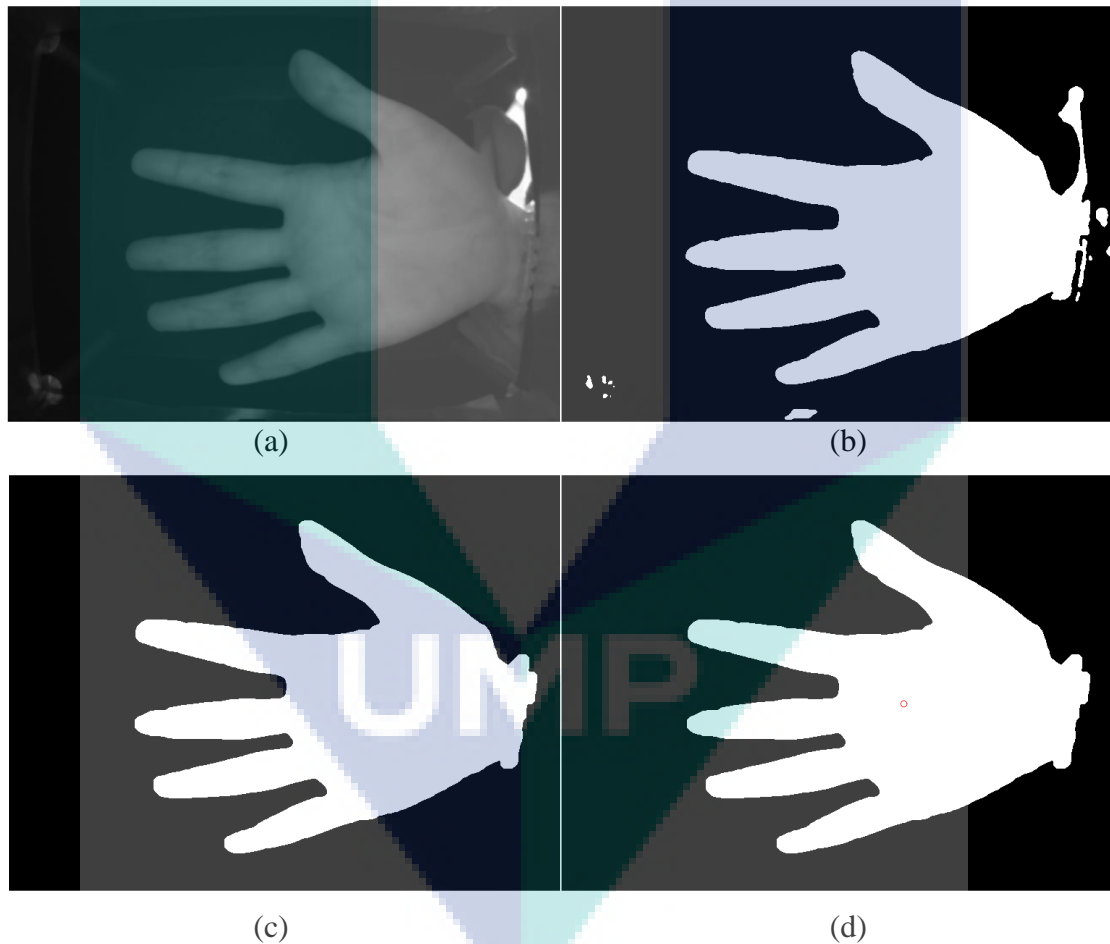


Figure 4.1 (a) Original Image, (b) Otsu Threshold, (c) Morphological Operation, (d) Centroid of the palm.

The web point in between middle with index finger and little with ring finger were obtained to draw the ROI extraction in the middle of the palm. The centroid of the palm was obtained and the ROI is drawn in the middle of the palm area. The ROI was extracted

with the size of 200x200. In Figure 4.2, different type of wavelength was extracted with the same rotational changes. By achieving the same rotational changes, the position of the ROI extraction in every image was similar.

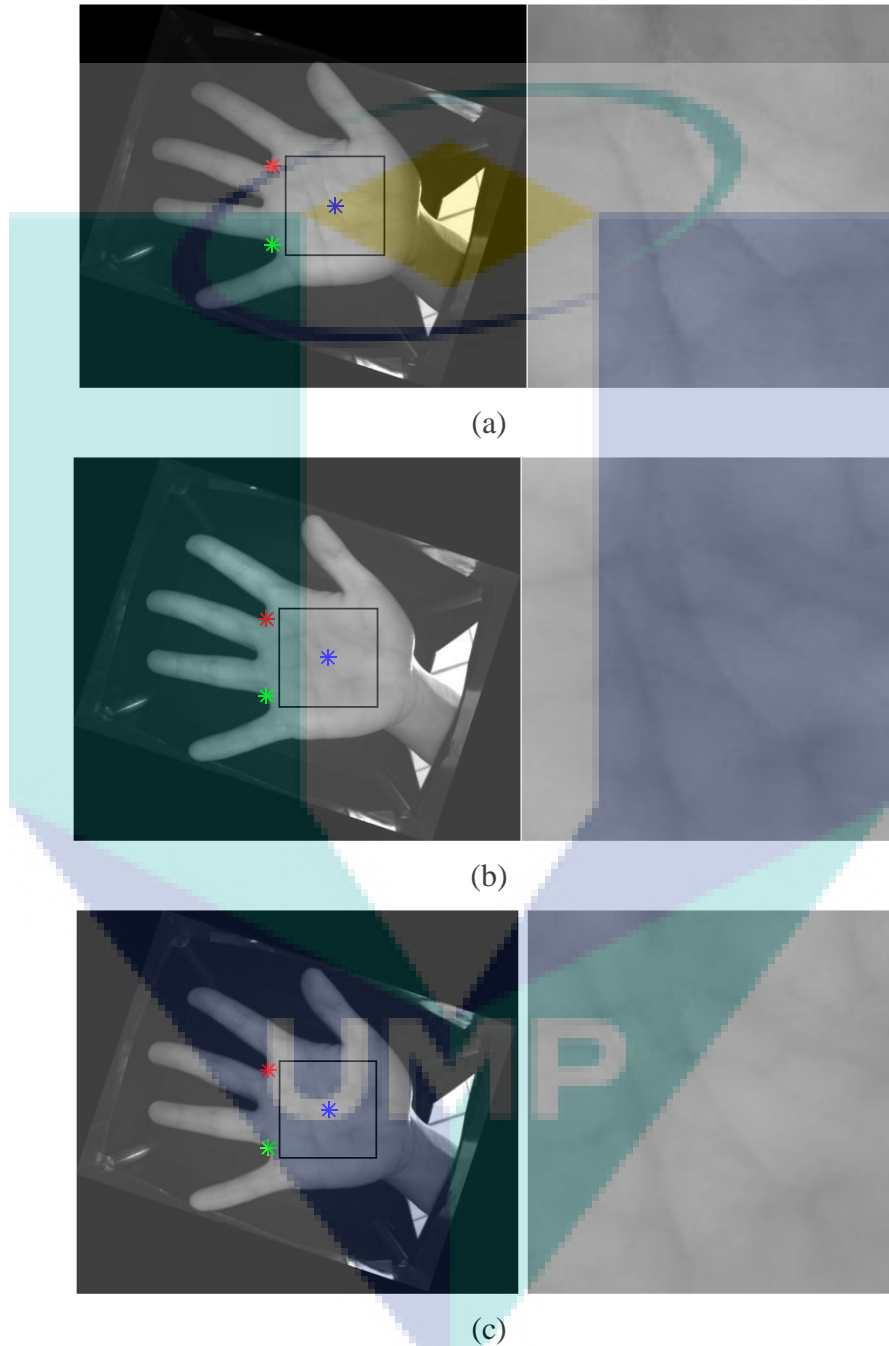


Figure 4.2 (a) ROI extraction in wavelength 700 nm, (b) ROI extraction in wavelength 850 nm, (c) ROI extraction in wavelength 940 nm.

In order to test for rotation effect, the artificial rotation has been done some samplers in 10°, 20° and 30° degree of rotation. Figure 4.3 shows one of the sample

rotation in 10° , 20° and 30° degree of rotation respectively. Distance in between 0° degree of rotation with 10° , 20° and 30° degree of rotation were calculated.

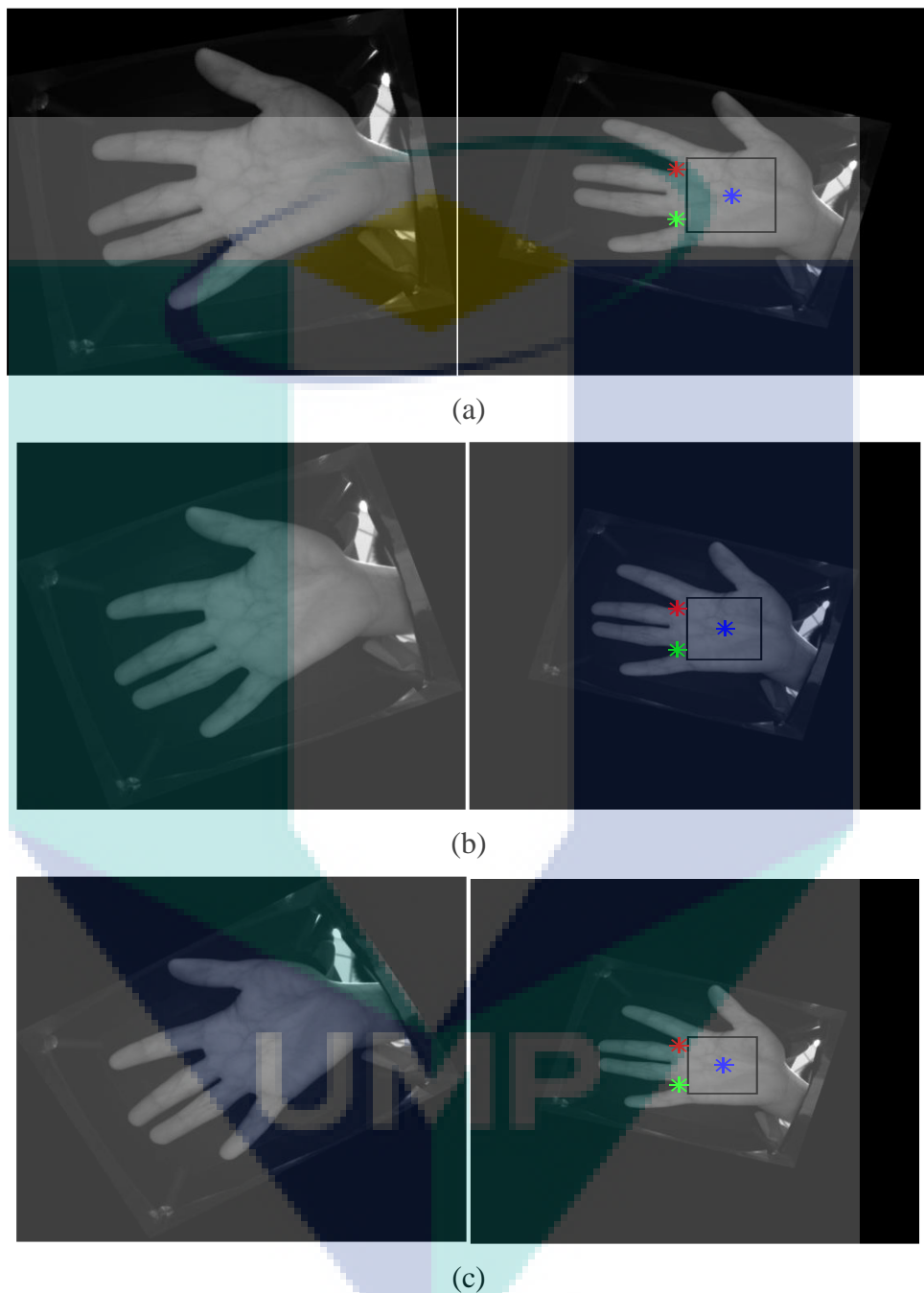


Figure 4.3 Artificial rotation in one sampler (a) 10 degree of rotation, (b) 20 degree of rotation, (c) 30 degree of rotation.

Euclidean Distance was calculated between rotation sample and sample without rotation. The lower the Euclidean distance that closer to zero the more similar in between two image. Hence, table 4.1 shows the Euclidean Distance in between 10° , 20° , and 30° degree of rotation to original image in 10 samples. It proved that the algorithm for ROI

extraction was suitable and to proceed to image fusion stage. It could be avoided for redundant or overlapped information or image in fused image when image fusion was applied.

Table 4.1 Euclidean Distance of 10 samplers 10°, 20°, and 30° degree of rotation

Number of sampler	10°	20°	30°
1	0.0274	0.0856	0.0193
2	0.0935	0.0724	0.0327
3	0.0252	0.1390	0.0186
4	0.0566	0.0457	0.0054
5	0.0219	0.0272	0.0443
6	0.0100	0.0566	0.0171
7	0.0599	0.0011	0.0910
8	0.0255	0.0123	0.0232
9	0.0183	0.0994	0.0210
10	0.0800	0.0503	0.0006

After ROI extraction, CLAHE and median filter were applied to enhance the images. Palm vein pattern could be observed visually after CLAHE was applied. However, there was little salt and pepper noise occurred in the images. Hence, median filter with 5x5 mask filter was applied to remove the noise that surrounded the palm vein area. Figure 4.4 shows the CLAHE and median filter applied to the ROI image in different type of wavelength respectively. CLAHE image is shown at the left hand side while median filter image is shown at the right hand side. It can be observed that the median filter image is able to achieve the smooth palm vein pattern compared to the CLAHE image.

By visual inspection of three different types of wavelength, the vein pattern could be observed clearly after CLAHE and median filter were applied. The difference of the three images could be observed in the bottom part of the image. The vein pattern shows most clearly in 850 nm image, followed by 940 nm image and 700 nm image. In 700 nm image, the vein pattern almost disappeared in the image which could lead to information loss to the feature extraction stage. Hence, those information in the image are believed that would be recovered once image fusion has been done.

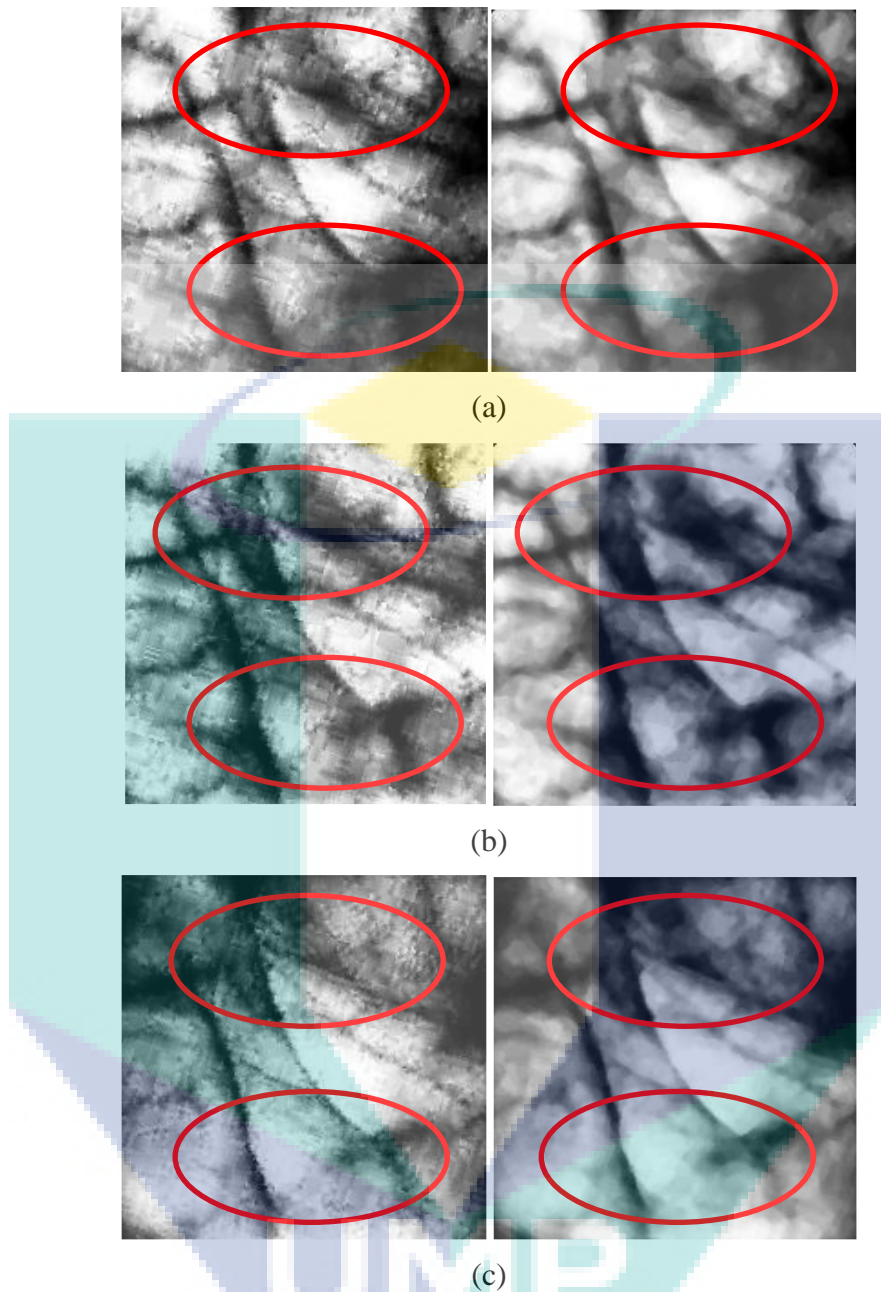


Figure 4.4 CLAHE filter (left) and Median Filter (right) in ROI extraction, (a) 940 nm palm vein image, (b) 850 nm palm vein image, (c) 700 nm palm vein image.

4.3 Feature extraction

This part will discuss the difference between SIFT and SURF feature extraction in palm vein images. These two methods are categorized under local invariant feature based methods. These two methods are popular in image recognition and image processing stages. However, these two methods have achieved different types of results in this work by using the CASIA database.

4.3.1 SIFT feature extraction

In section 3.5.1, total numbers of 128 feature vectors in each key point were extracted in SIFT algorithms. Orientation, scales and the centre of the frame were obtained for each key points. The octave and the number of level for SIFT descriptor has been selected as maximum as possible in order to obtain the most possible key point in the palm vein image. Figure 4.5 shows the example of a few samplers of SIFT feature extraction in palm vein image.

Figure 4.6 (a) and (b) shows the example of genuine matching using SIFT algorithm with and without adopted RANSAC mismatching removal. In SIFT matching, it could be observed that it has more than 50 matching point in genuine matching pairs. However, there was some mismatching point occurred due to the outliers problems. Outliers occurred are often caused by the image registration where this stage often occurred little or small axis, rotation and scales changes. Those mismatching points could be observed with the crossed line between two pairs of palm vein images. Mismatching line were obviously shown with the large distance in between two points. By reducing those problem, RANSAC mismatching point removal showed the perfect technique that minimizes the mismatching pair in genuine images. In imposter matching, it can be observed that imposter matching has lower number of matching point compared to genuine matching. The outlier could still be found and those mismatching point could still be removed by using RANSAC mismatching point removal.

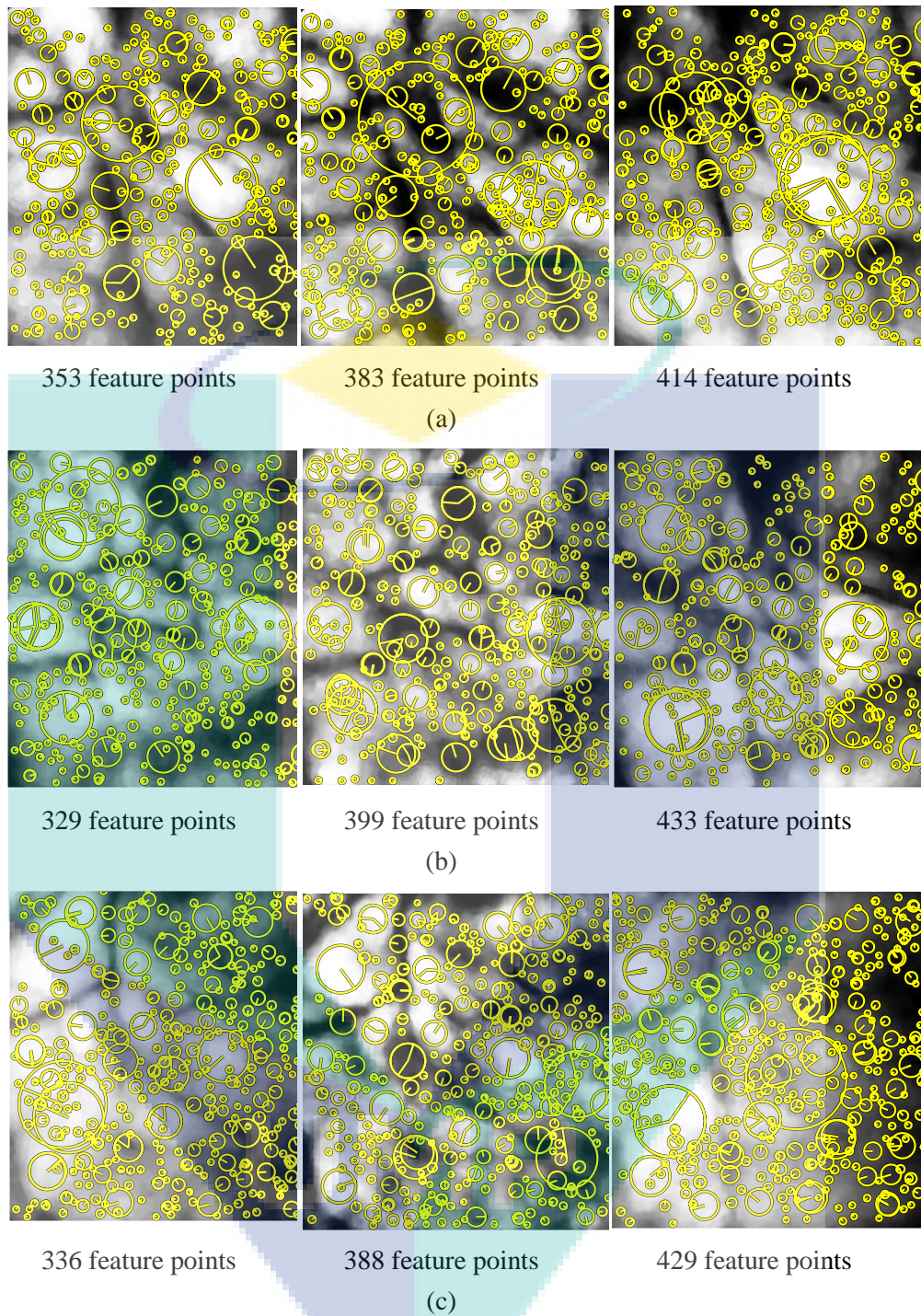


Figure 4.5 SIFT feature extraction with feature points for few sampler for 700 nm in the left, 850 nm in the middle and 940 nm in the right, a) sampler number 38, b) sampler number 88, c) sampler number 89

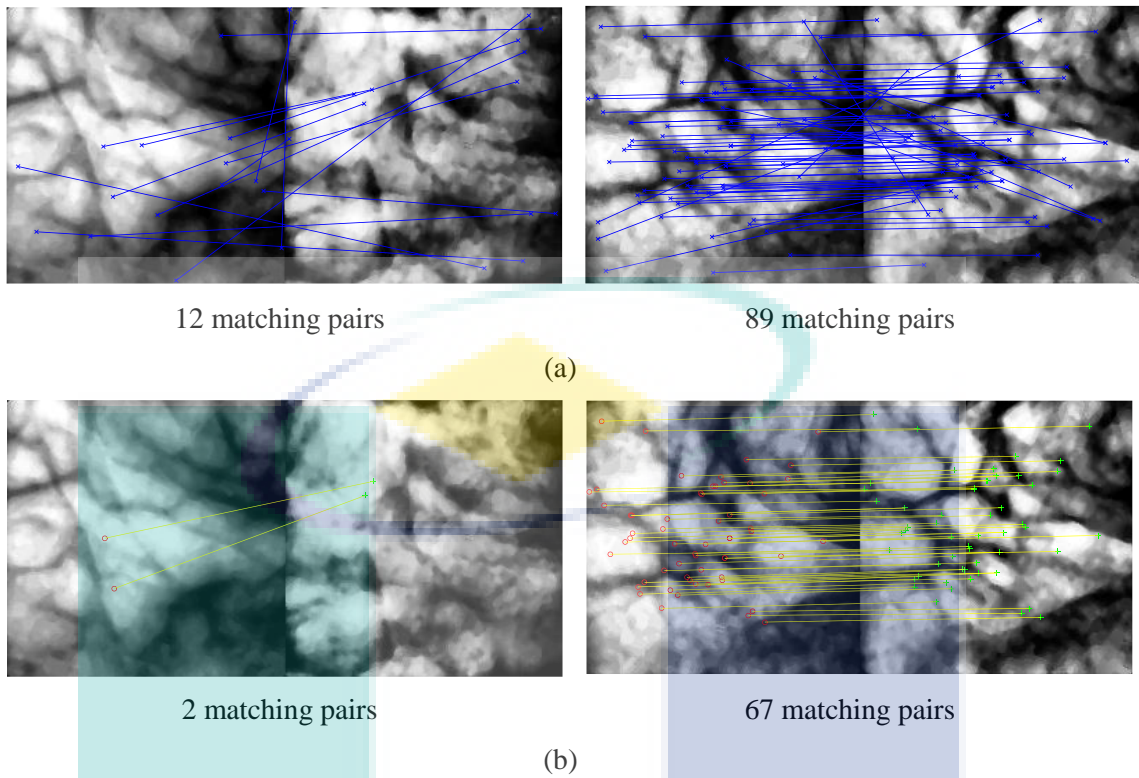


Figure 4.6 SIFT matching in genuine and imposter pair, (a) without RANSAC mismatching point removal, (b) after RANSAC mismatching point removal.

4.3.2 SURF feature extraction

In section 3.5.2, SURF feature extraction has been explained that 64 feature vector will be extracted in each key point. Orientation, scales and the centre of the frame were also obtained for each key point. The octave and the number of level for SURF descriptor were also selected as maximum as possible. Figure 4.7 shows the example of few sampler of SURF feature extraction in palm vein image. Figure 4.7 image left, middle and right refer to 700 nm, 850 nm, and 940 nm, respectively.

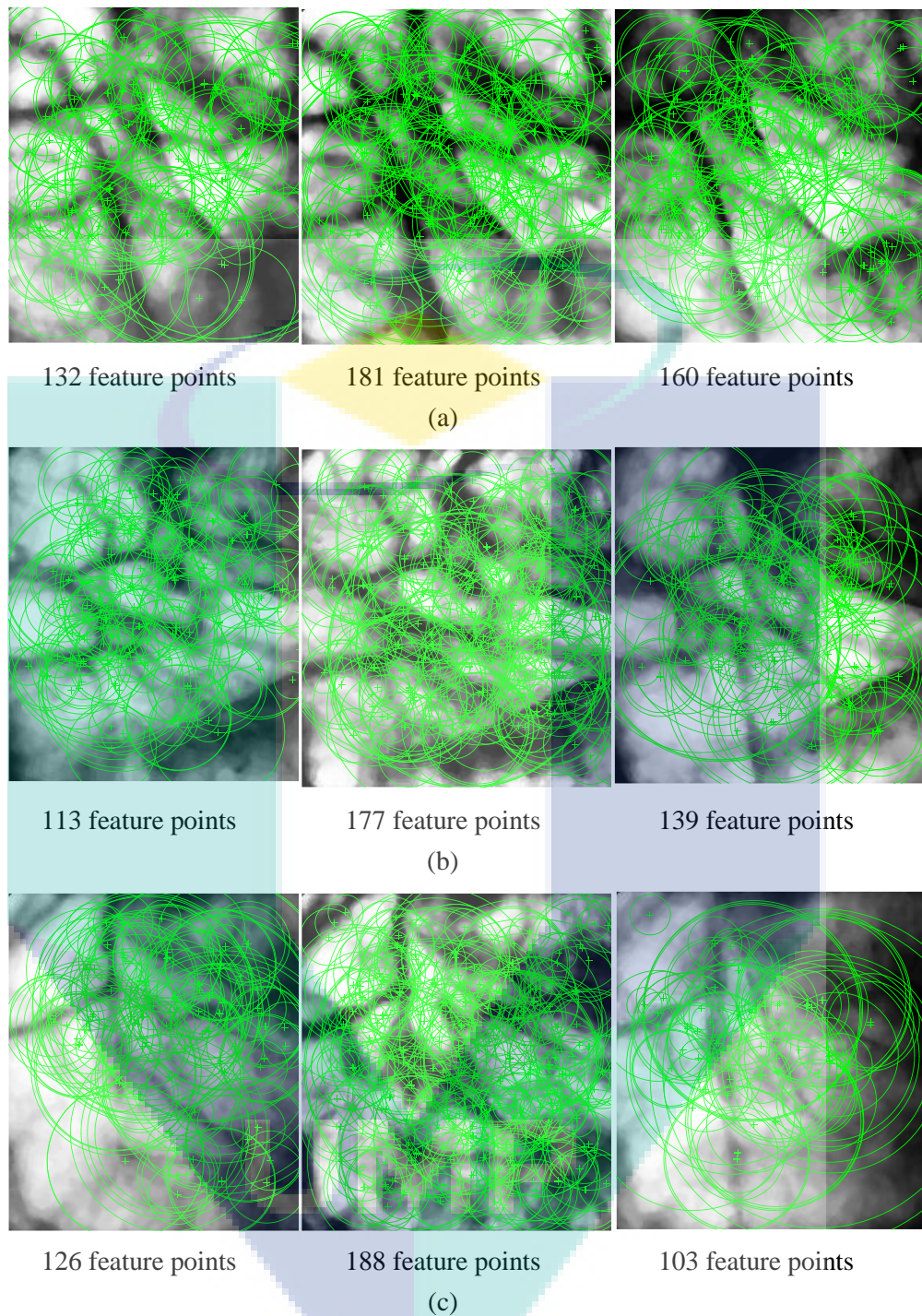


Figure 4.7 SURF feature extraction with feature points for few samplers for 700 nm in the left, 850 nm in the middle and 940 nm in the right, a) sampler number 38, b) sampler number 88, c) sampler number 89.

Figure 4.8 shows the example of SURF matching between two genuine pairs. SURF matching can be observed that it has less matching point in between genuine matching pairs. Because the feature point extracted is less, it impacted the matching pairs in between two palm vein images. Since the number of matching point was less,

RANSAC mismatching point removal were unable to remove most of the mismatching point in SURF matching.

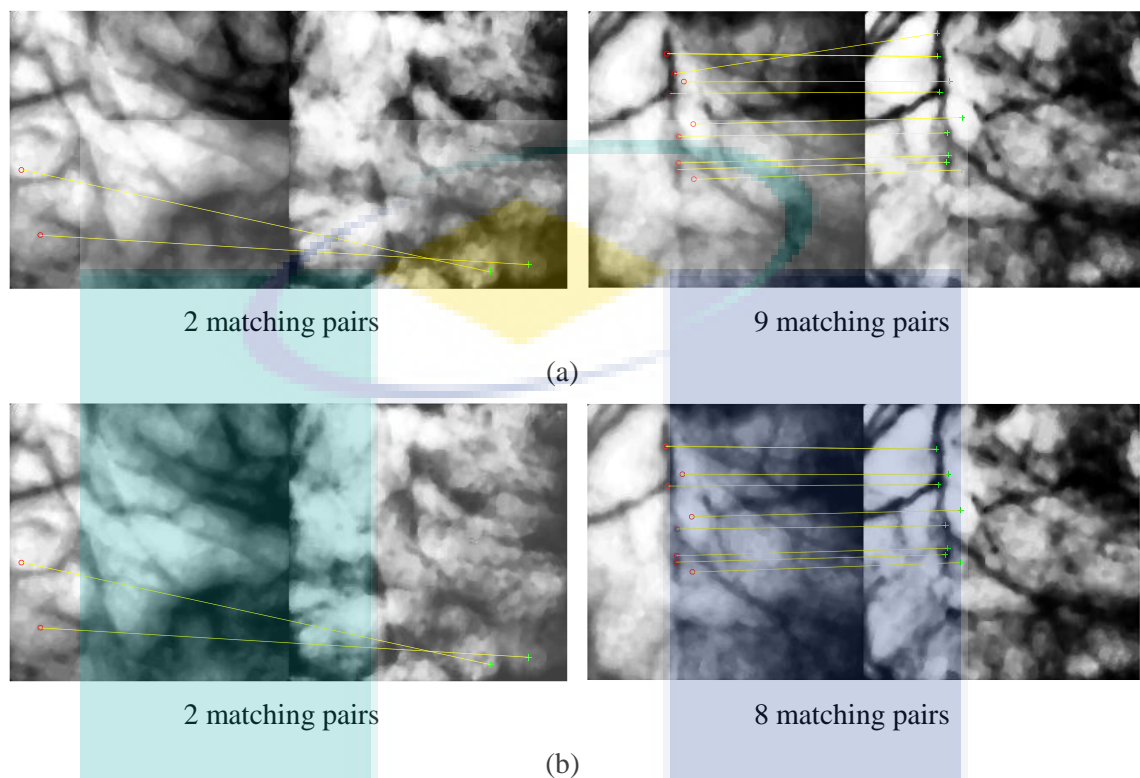


Figure 4.8 SURF matching in genuine pair, (a) without RANSAC mismatching point removal, (b) after RANSAC mismatching point removal.

In figure 4.8, one of the example shows that the number of matching pair in imposter pair using SURF algorithm were extremely low compared to genuine pair using SURF algorithm. RANSAC mismatching point removal were unable to work in imposter pair using SURF algorithm due to the extremely low matching point that made the RANSAC mismatching point unable to find the outliers.

4.4 Comparison with the feature extraction method

This section will discuss the comparison between the two types of feature extraction method. Although there were many experimental analysis has been done, this comparison is made to make sure that the feature extraction techniques chosen is effective in palm vein recognition and also in this CASIA database. Besides that, both methods will be using the same palm vein database which is CASIA database. Both feature extraction method will be compared in Equal Error Rate (EER) and also the matching

point of both palm vein images. The most effective techniques will be chosen to proceed and applied in the next stage.

Figure 4.9 shows the EER for the SIFT and SURF feature extraction between three different type of wavelength respectively. In both EER rate, 940 nm palm vein image achieve the lowest EER compared to 700 nm and 850 nm wavelength spectrum.

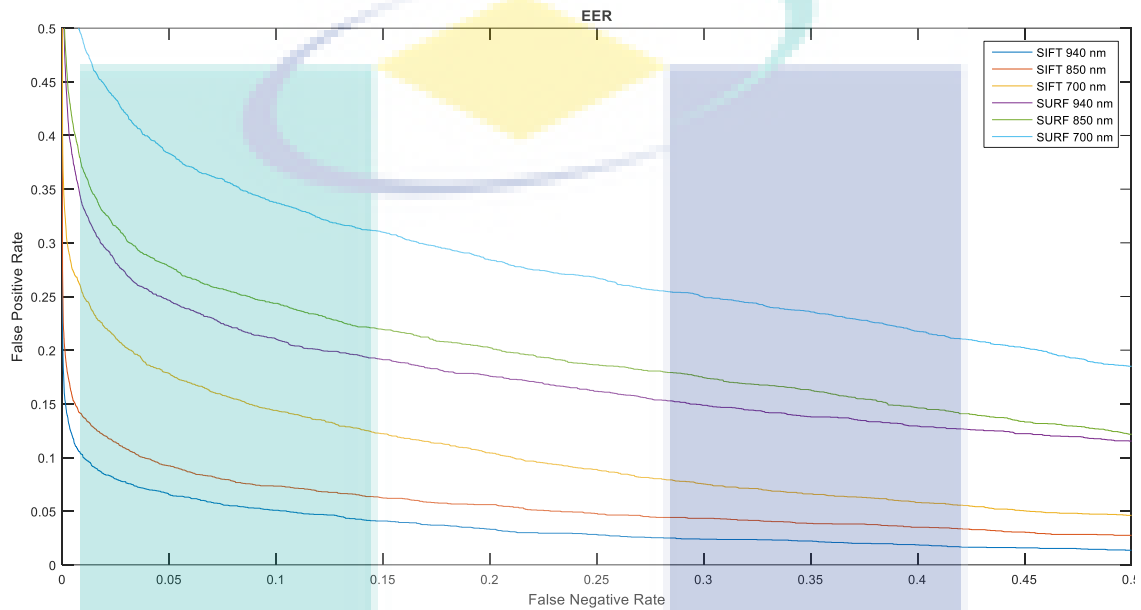


Figure 4.9 Equal Error Rate (EER) of SIFT and SURF matching in three different wavelength spectrum

Table 4.2 Equal Error Rate and Area Under Curve for three different wavelength using SIFT and SURF classifier in 700 nm, 850 nm and 940 nm image

Method	EER %		AUC %	
	SIFT	SURF	SIFT	SURF
700 nm	14.71	26.11	92.56	80.55
850 nm	12.50	20.14	93.90	86.64
940 nm	11.17	18.00	94.09	87.76

Note: Bold figure represent the lowest EER and highest AUC that represent the highest performance in recognition rate.

By referring to Table 4.2, it can be concluded that palm vein pattern feature extraction by using SIFT algorithm outperformed feature extraction by using SURF algorithm. EER rate decreased from 26% to 14% in 700 nm, 20% to 12.5% in 850 nm, and 18% to 11% in 940 nm by comparing SIFT algorithm with SURF algorithm. It can be concluded that SIFT algorithm achieved a better performance on palm vein pattern

feature extraction that cause a significant drop by 12% in 700 nm, 8% in 850 nm, and 7% in 940 nm.

A few papers also made the same comparison that SIFT algorithms outperform SURF algorithms. Yan, Kang et al. had proposed a palm vein recognition by using SIFT and SURF algorithms with feature level fusion (Yan, Kang, Deng, & Wu, 2015a). Before feature level fusion, they also tested the performance of SIFT and SURF algorithms separately. Their result showed that SIFT has a better recognition rate with an increase of number of feature point compare to SURF features. Pan and Kang also proposed a palm vein recognition by using local feature extraction algorithms (Pan & Kang, 2011). All local feature extraction algorithms achieved a satisfactory results, however SIFT outperformed other techniques in terms of recognition rate (Karami, Prasad, & Shehata, 2015) (Lakshmi & Vaithyanathan, 2017). In this paper, they had proven the feasibility and applicability of SIFT on palm vein recognition systems. Hence, SIFT has been proven to achieve better performance in recognition rate compared to SURF. SIFT algorithms were then applied and proceeded to apply the image fusion techniques.

4.5 Image fusion

Figure 4.10 shows one of the example of fusion techniques for three types of wavelength which were 700 nm, 850 nm and 940 nm palm vein image. Four different types of wavelength spectrum combination were formed which were fusion between 700 nm with 850 nm palm vein image, 700 nm with 940 nm palm vein image, 850 nm with 940 nm palm vein image and triple combination of wavelength palm vein image.

The impact of fusion techniques to the images can be clearly seen by using visual inspection. The original palm vein image in wavelength 850 nm has obtained a better vein pattern while 940 nm and 700 nm obtained a blur or unclear vein pattern in both left and right hand side. Those vein pattern was drawn by using a red circle. The effect of the fusion techniques can be easily seen by the red circle. Dark region especially in the right hand side has been de-blurred after fusion techniques applied. Fusion applied had enhanced the darkness area in region (c) by fusion of blur image in 700 nm and 940 nm with non-blur image of 850 nm palm vein image.

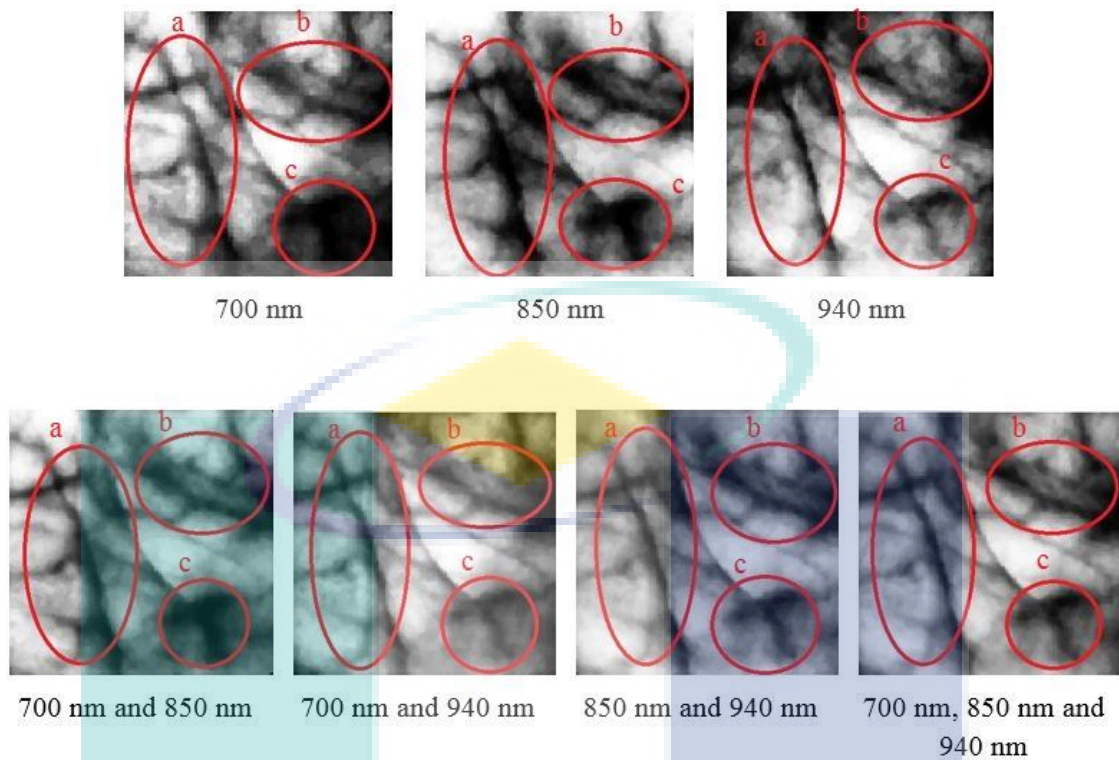


Figure 4.10 FPDCT image fusion for several types of combination

In overall visual inspection, region in left hand side in 850 nm palm vein image obtained a thick type of vein pattern while for 700 nm and 940 nm obtained a thin type of vein pattern or unclear vein pattern. Fusion image showed that the vein patterns in the left hand side had been enhanced. The vein patterns could be obtained in finer details and some of the dark region had also been removed by fusing several images. In several type of fusion techniques, it showed similar trend that improved the same side of the images. In Appendix A, it shows the fused image of every image fusion techniques of dual and triple types of different type of wavelength spectrum. Hence, fusion techniques are able to help enhance and preserve the information with less noises created. The fusion techniques are also able to recover the information and remove the dark region, improving the recognition rate in palm vein feature extraction.

4.6 Comparison with the image fusion method

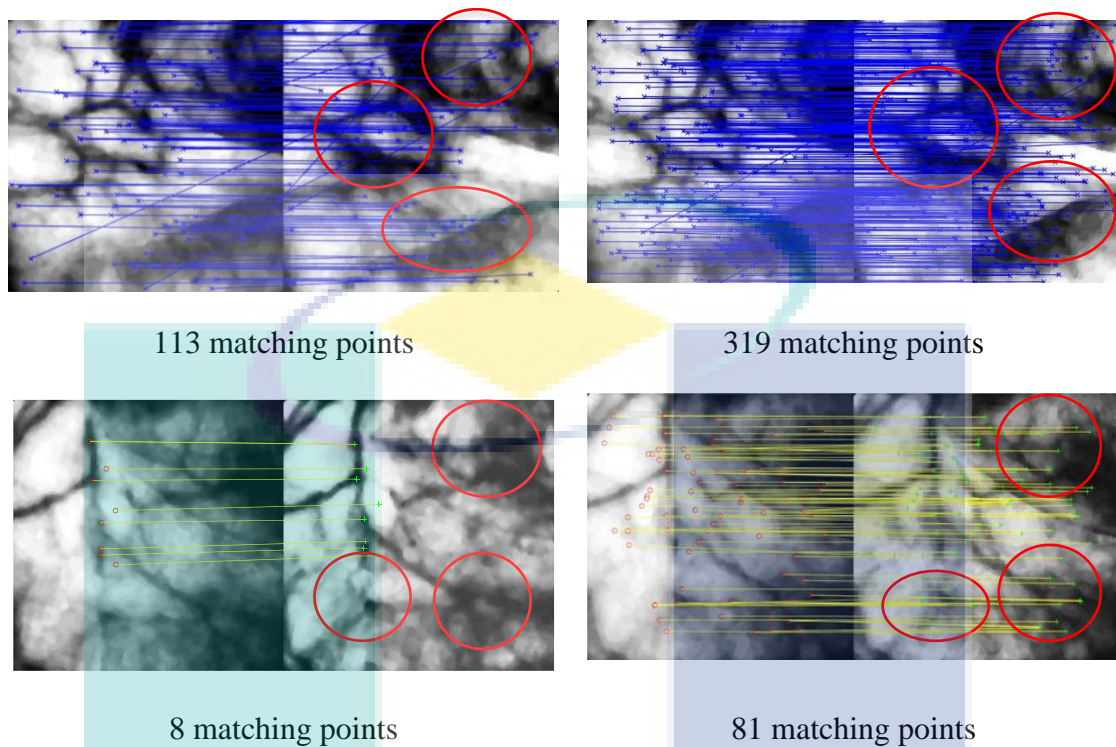
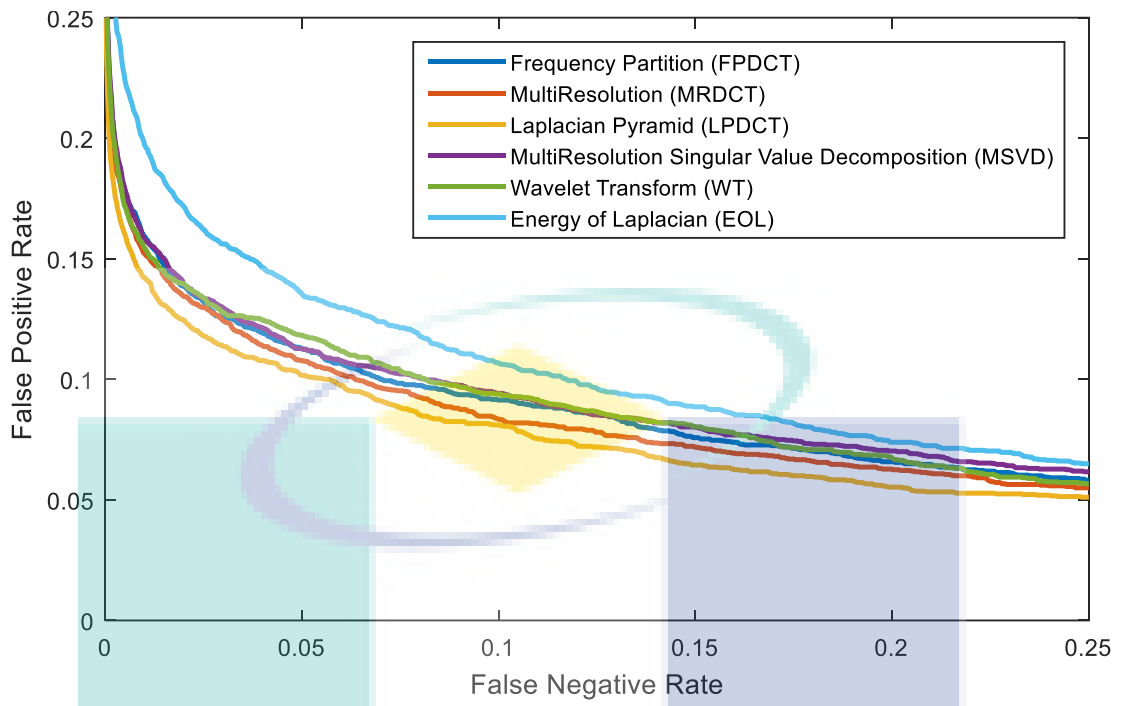


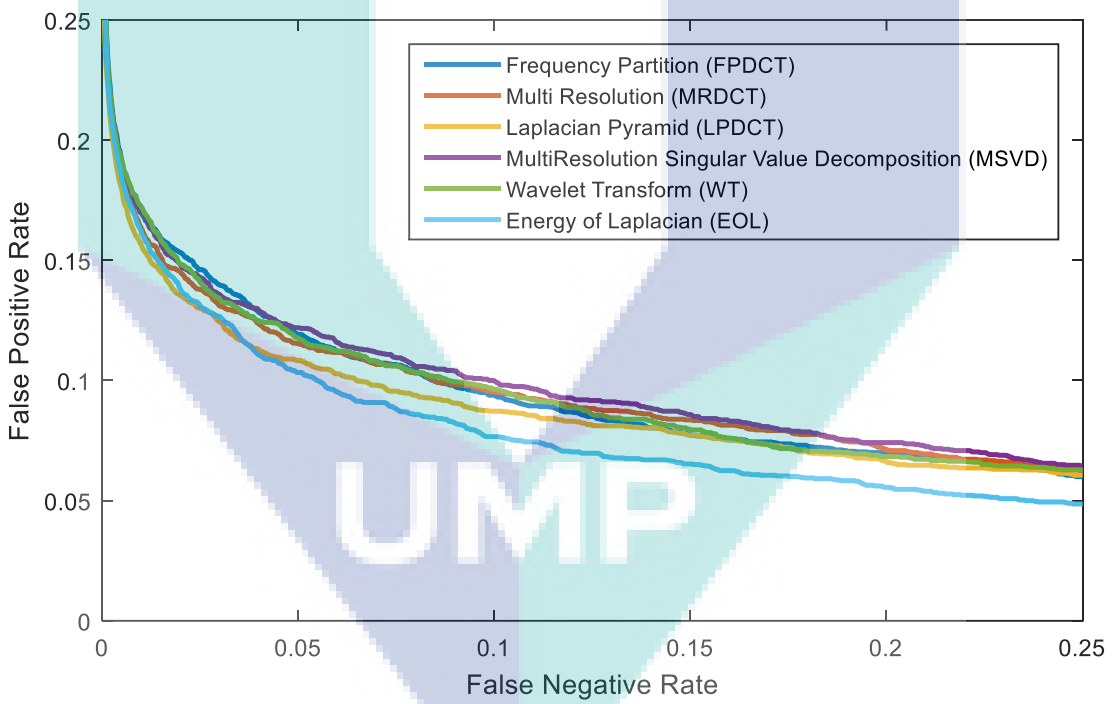
Figure 4.11 Effect of number of matching points before and after one of the image fusion applied.

In figure 4.11, the number of matching point had increased once the image fusion was applied. In every image fusion techniques, it shows similar trend that every image fusion technique has improved the possibility of matching pairs. It can be concluded that the matching performance will improve once the number of matching pair is improved. Hence, the possibility of genuine matching will be increased. Once the matching pair improved, the EER recognition rate will also improved.

Figure 4.12(a) to (c) shows the EER rate on overall techniques used between dual types of wavelength image fusion. In every combination of image fusion, every image fusion technique achieve different performance in dual types of image fusion. MRDCT and LPDCT achieved the highest performance in 850 nm with 940 nm image fusion and 700 nm with 850 nm image fusion respectively. Energy of Laplacian (EOL) achieved the highest performance fusion between 700 nm with 940 nm image. However, EOL has obtained the lowest performance fusion in between 700 nm with 850 nm wavelength image and also 850 nm with 940 nm wavelength image.



(a)



(b)

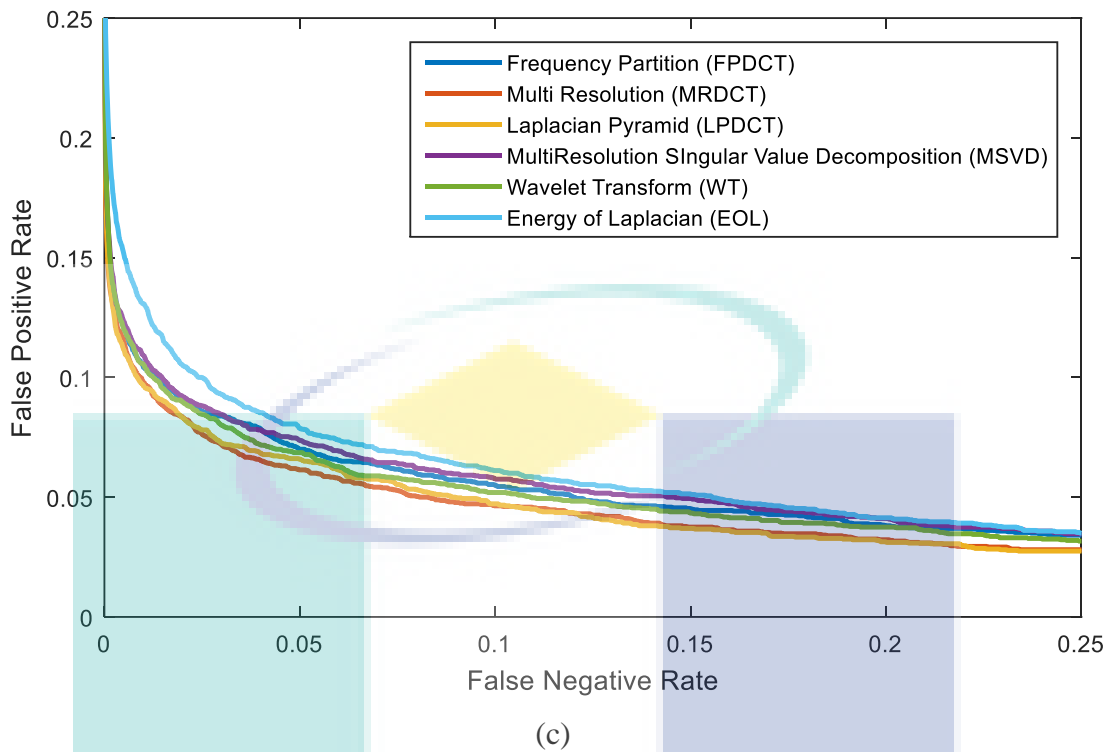


Figure 4.12 EER for dual type combination of wavelength spectrum, (a) 700 nm with 850 nm image, (b) 700 nm with 940 nm image, (c) 850 nm with 940 nm image

By comparing the fusion between 700 nm with 850 nm and 700 nm with 940 nm, the overall fusion techniques has a slightly degrade of 0.5 to 1% in EER rate. However, EOL image fusion achieved a different result that improved to 2% in compare with 700 nm with 850 nm and 700 nm with 940 nm. It shows that EOL image fusion achieved the highest EER rate in 700 nm with 940 nm image fusion. Table 4.4 and 4.5 shows the EER and AUC for every image fusion techniques in every combination of fusion.

In triple type of wavelength image fusion, the image fusion improved the low quality problems and focused the vein images which lead to more SIFT matching point while improving the recognition rate. Figure 4.13 and Table 4.5 shows the overall recognition rate by using different type of image fusion techniques matched with different wavelength spectrum. However, the performance showed that the fusion image for 850 nm with 940 nm was almost similar to triple types of image fusion while the performance was shown to be similar in 700 nm with 850 nm image fusion and also 700 nm with 940 nm image fusion.

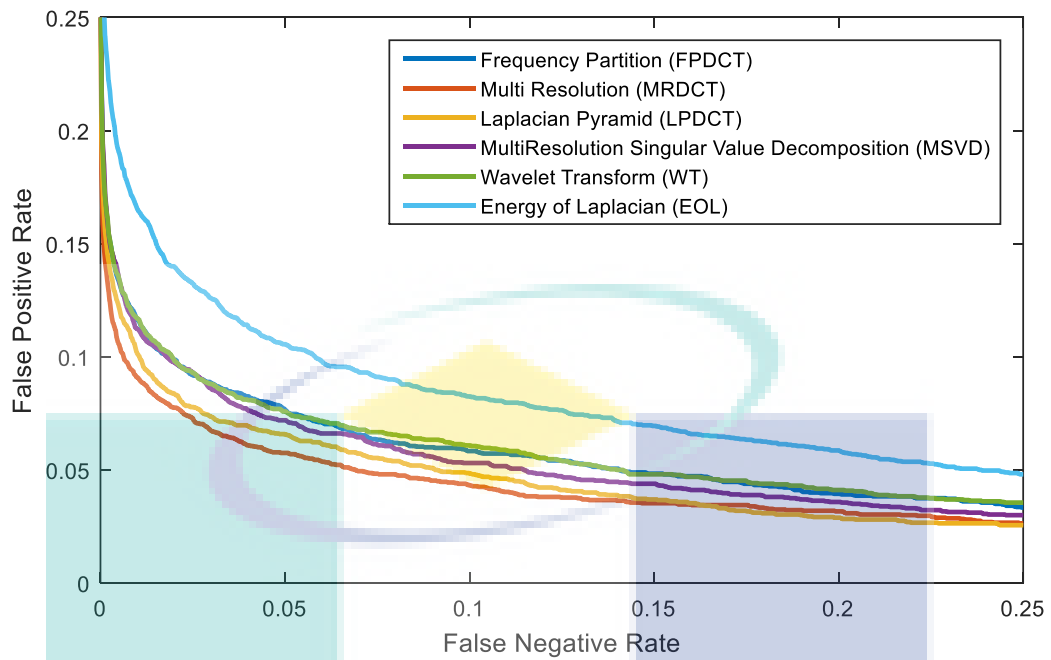


Figure 4.13 EER for triple combination of wavelength spectrum

The overall performance between 700 nm with 850 nm image fusion and 700 nm with 940 nm image fusion showed a difference in recognition rate at around 1%. For the fusion between 850 nm with 940 nm image fusion and triple combination of image fusion, the difference was also similar at around 1%. However, the triple combination of image fusion achieved a better recognition rate compared to dual types of image fusion. Appendix B to Appendix E shows the EER and AUC graph of dual and triple combination of wavelength spectrum.

LPDCT achieved the highest performance in overall techniques using image fusion between 700 nm with 850 nm while for EOL achieved the lowest performance which were 8.36% and 10.47% respectively. However, EOL achieved the different result in image fusion between 700 nm with 940 nm image fusion. EOL achieved the highest performance which is 8.47% overall in image fusion in between 700 nm with 940 nm image. In either 850 nm with 940 nm image fusion and triple combination type fusion, MRDCT achieved the highest result in these categories. The result is almost similar in these two categories which were 5.83% in 850 nm with 940 nm image fusion and 5.53% in triple combination wavelength. By comparing the AUC curve, the classification is better by using the MRDCT with triple type of image fusion that achieved the highest classification rate of 98.11% compared to others. It can be shown that MRDCT is the suitable technique to use for palm vein recognition with three types of image fusion.

Table 4.3 Equal Error Rate in 700 nm, 850 nm and 940 nm image

Method	700 nm and 850 nm	700 nm and 940 nm	850 nm and 940 nm	700 nm, 850 nm and 940 nm
MRDCT	8.83	9.65	5.83	5.53
FPDCT	9.33	9.56	6.47	6.76
LPDCT	8.36	9.06	6.08	6.11
MSVD	9.53	10	6.61	6.58
Wavelet	9.47	9.75	6.16	6.83
EOL	10.47	8.47	6.99	8.64

Note: Bold figure represent the lowest EER that represent the highest performance in recognition rate.

Table 4.4 Area Under Curve (AUC) in 700 nm, 850 nm and 940 nm image

Method	700 nm and 850 nm	700 nm and 940 nm	850 nm and 940 nm	700 nm,850 nm and 940 nm
MRDCT	96.23	95.77	97.91	98.11
FPDCT	95.95	95.90	97.61	97.57
LPDCT	96.44	95.96	98.01	98.1
MSVD	95.78	95.57	97.48	97.73
Wavelet	95.91	95.73	97.68	97.50
EOL	95.36	96.70	97.43	96.55

Note: Bold figure represent the lowest AUC that represent the highest performance in recognition rate.

4.7 Comparison with the conventional method

In overall fusion techniques, MRDCT with triple combination achieved the EER rate with 5.53% compare to others. MRDCT in triple types of image fusion obtained the highest performance compared to others. In table 4.6, the conventional method is the method of using the basic processing stage which is the SIFT algorithm in palm vein recognition system. MRDCT with triple combination of wavelength and basic method were using the same SIFT algorithm feature extraction and CASIA database. The EER image fusion in MRDCT improved by almost 9% compared with single 700 nm image, 7% in matching with single 850 nm image and 6 % in matching with single 940 nm image.

Table 4.5 EER in 700 nm, 850 nm and 940 nm image and MRDCT with triple combination of wavelength

Method	EER %	AUC %
700 nm SIFT	14.71	92.56
850 nm SIFT	12.50	93.90
940 nm SIFT	11.17	94.09
MRDCT with triple combination of wavelength	5.53	98.11

Note: Bold figure represent the lowest EER and highest AUC that represent the highest performance in recognition rate.

4.8 Summary

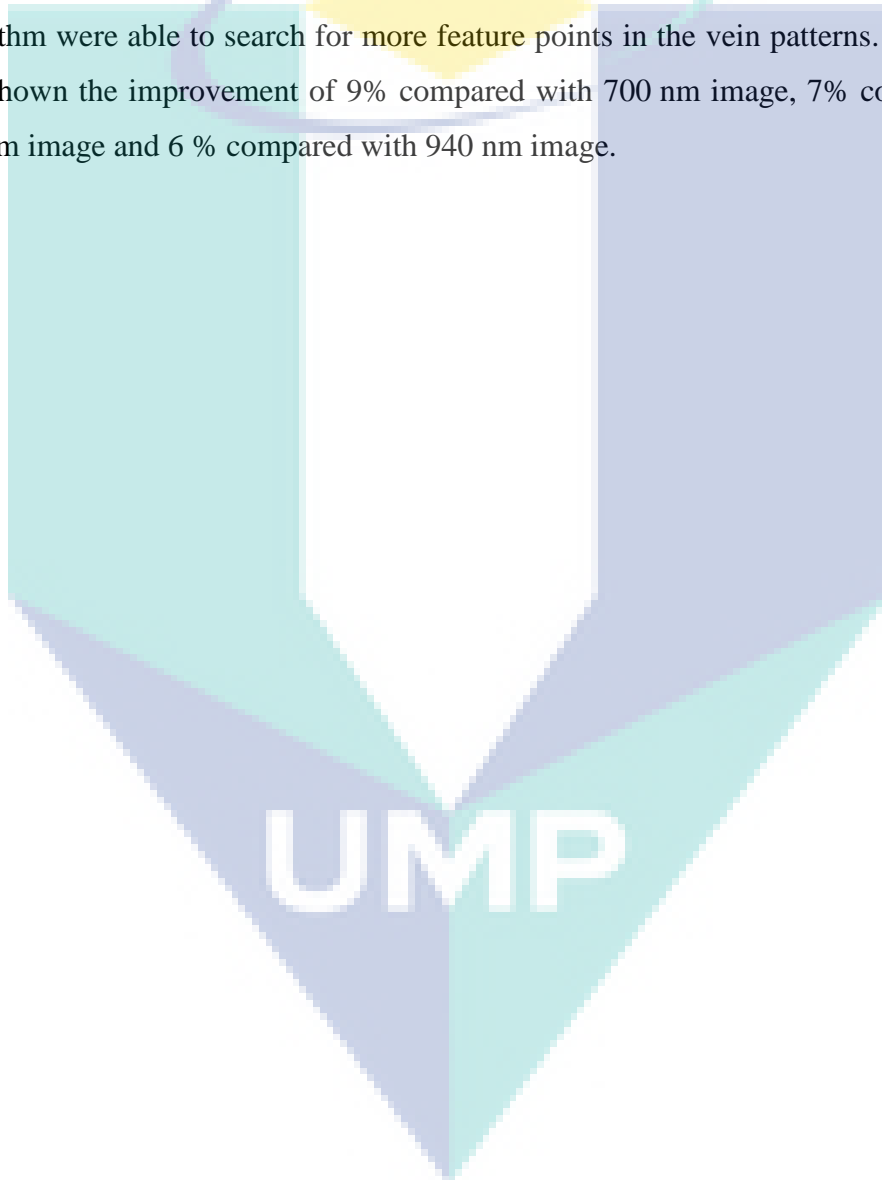
In this chapter, all experiment and analysis discussed for the whole process of vein recognition system. The result for every process was shown according to order by achieving all objectives. All objectives were achieved by referring to those results obtained.

By comparing SIFT and SURF palm vein feature extractions, SIFT algorithm achieved a better recognition rate in compared to SURF algorithm. SIFT algorithm achieved highest number of matching pair compared to SURF algorithm. Although SIFT and SURF algorithm had selected the maximum level of octave number and number of level of descriptor, SIFT was still able to find the most possible matching between both palm vein images. SIFT has also been proven and used in many works such as image processing. This method has been compared with several techniques that many works had proven to be the best and effective in most of the feature extraction techniques.

Image fusion techniques has been proven to be able to fuse several images to recover the information that was lost from some of the images. However, the issues of noise occurred after image fusion that caused impact to the image feature extraction. Several types of image fusion method has been discussed in this chapter. There were dual types of wavelength image fusion and triple types of wavelength image fusion done in this works. Result showed that triple types of wavelength image fusion has better

recognition rate compared to dual types of wavelength image fusion. More information has been fused such that SIFT algorithms will search for more feature points in the images.

Among several types of image fusion, MRDCT with triple types of wavelength image fusion has achieved the highest recognition rate. MRDCT with triple types of wavelength image fusion reached 5.53% in EER and 98.11% in AUC. The image after visual inspection in MRDCT shows better vein improvement and less distortions. SIFT algorithm were able to search for more feature points in the vein patterns. MRDCT has also shown the improvement of 9% compared with 700 nm image, 7% compared with 850 nm image and 6 % compared with 940 nm image.



CHAPTER 5

SUMMARY AND FUTURE WORK

5.1 Introduction

In this work, palm vein verification system using image fusion techniques is proposed. For feature extraction techniques, the work has investigated SURF and SIFT algorithm and it found that SIFT was able to extract more feature point in each palm vein image compared to SURF. Extracting more feature point will lead to more matching pair in between both vein image thus increasing the accuracy of the system. Multi-resolution DCT, Laplacian Pyramid DCT and Frequency Partition DCT techniques has been tested using the SIFT feature extraction with CASIA database. Overall, MRDCT achieved the best performance compared to other techniques in both visual inspection and the recognition rate.

5.2 Summary of the work

There were three objectives achieved in this study. The first objective of this work is to investigate and implement image fusion technique using different wavelength spectrum for a palm vein recognition system. The objective successfully achieved by testing several types of image fusion techniques. By referring to the fused image, the palm vein pattern has been improved with finer detail with also less generation of noises. Fused image in every image fusion techniques shows similar trend in the vein patterns. Fused image also improved in matching pair's link in between both images. More feature points are extracted using SIFT algorithm. The comparison of dual and triple combination types of wavelength were also tested in this works. Triple combination types of wavelength image fusion achieved the highest recognition rate in EER and AUC compare to dual combination types of wavelength image fusion. Besides that, MRDCT in triple

combination types of wavelength image fusion achieved the highest EER rate with 5.53% and AUC with 98.11%.

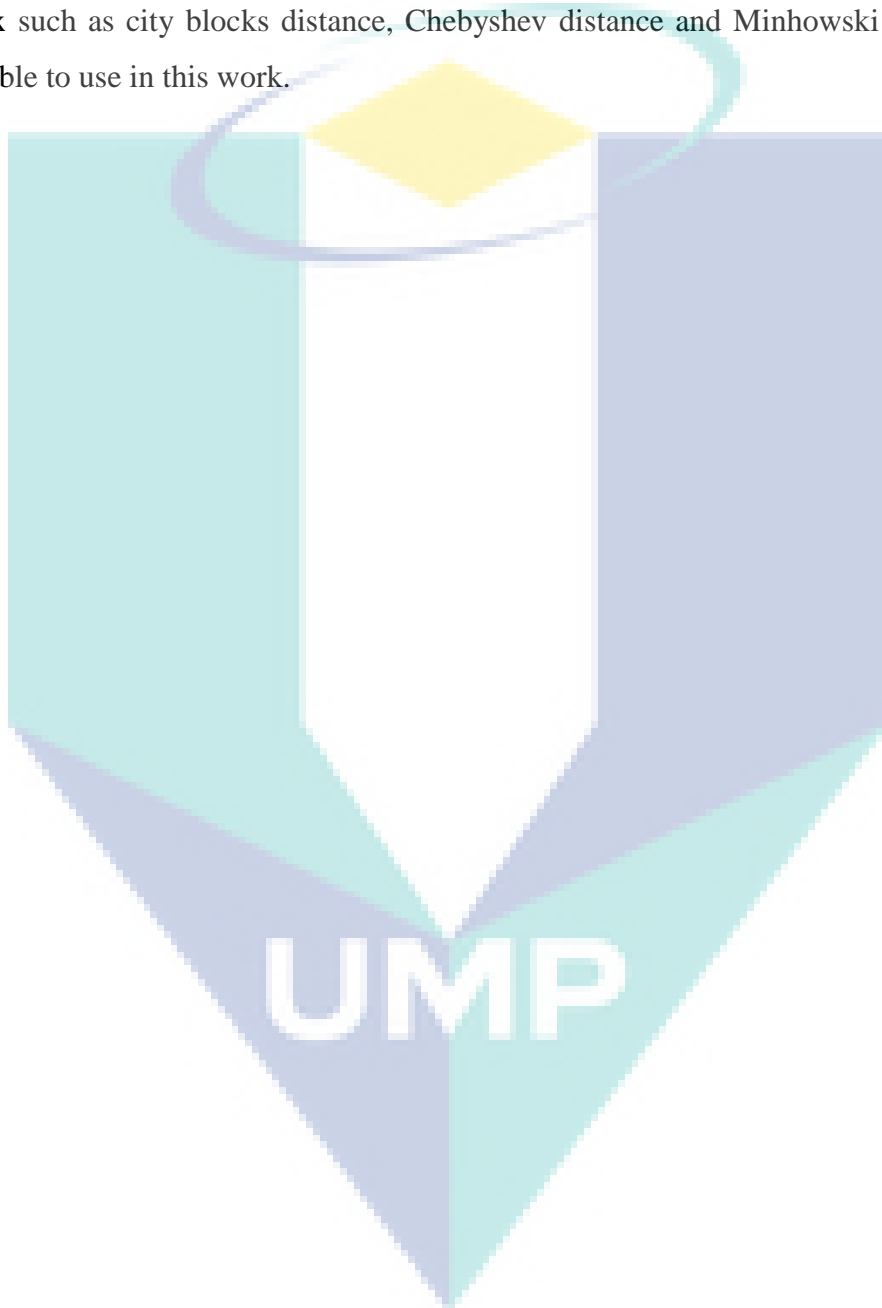
The second objective of this work is to develop features extraction algorithms that is able to handle orientation changes in palm vein pattern. The objective was achieved through the comparison in between SIFT and SURF algorithm. SIFT algorithm are able to extract more feature point than SURF algorithm. Feature point extracted will impact the matching pairs between genuine and imposter images. Hence, the more feature points extracted, the more matching pairs will be linked between both images. Besides that, SIFT algorithm achieved higher EER rate compared to SURF algorithm in three different types of wavelength. SIFT algorithm achieved a significant drop in EER rate by 12% in 700 nm, 8% in 850 nm, 7% in 940 nm compared with the SURF algorithm. Most of the previous work also proved that SIFT algorithm works more effectively than SURF algorithm.

The last objective in this work is to evaluate and validate the effectiveness of image fusion techniques and the robustness of the proposed feature extraction in this study. MRDCT in triple combination types of wavelength image fusion was compared with the conventional method in palm vein recognition systems. The conventional method of using SIFT algorithm had obtained the EER rate of 14.71% in 700 nm, 12.5% in 850 nm, and 11.17% in 940 nm wavelength images. Throughout the works, the EER image fusion in MRDCT has improved by almost 9% compared with 700 nm image, 7% in matching with 850 nm image and 6% in matching with 940 nm image. MRDCT in triple types of image fusion obtained the highest performance compared to others.

5.3 Future work

There is still room for further improvement in this work in order to improve recognition rate effectively. In this work, there is only single fusion techniques applied for the palm vein recognition systems which is the image fusion techniques applied on the input image. There are still several fusion techniques available in different stages which are feature level fusion, decision level fusion and signal level fusion. Fusion techniques are able to improve the recognition rate for the recognition systems. Hence, hierarchical fusion techniques can be further studied for better analysis and evaluation of the recognition rate.

Besides from that, this work only applied Euclidean distance for classifier distance matrix techniques. There are other distance matrix techniques that applied in other works that also in other fields. This work can be extended by using several type of distance matrix techniques to make a comparison or effect in EER rate by using difference types of distance matrix in palm vein recognition system. Difference type of distance matrix such as city blocks distance, Chebyshev distance and Minhowski Distance are available to use in this work.



REFERENCES

- Aghagolzadeh, A. (2018). Multi-Focus Image Fusion in DCT Domain using Variance and Energy of Laplacian and Correlation Coefficient for Visual Sensor Networks, *6*(2), 233–250. <https://doi.org/10.22044/JADM.2017.5169.1624>
- Aishwarya, V.V, &Devipriyanga, V. (2016). Multibiometrics By Combining Left and Right Palmprint Images using SIFT Features, *2*(18), 186–197.
- Akbar, A. F., Wirayudha, T. A. B., &Sulistiyo, M. D. (2016). Palm vein biometric identification system using local derivative pattern. *2016 4th International Conference on Information and Communication Technology (ICoICT)*, *4*(c), 1–6. <https://doi.org/10.1109/ICoICT.2016.7571956>
- Article, R. (2014). Available Online at www.jgrcs.info A Survey On Biometric Authentication Techniques Using Palm, *5*(8), 2010–2013.
- Barra, S., DeMarsico, M., Nappi, M., Narducci, F., &Riccio, D. (2018). A hand-based biometric system in visible light for mobile environments. *Information Sciences*, *0*, 1–14. <https://doi.org/10.1016/j.ins.2018.01.010>
- Bharathi, S., &Sudhakar, R. (2018). Biometric recognition using finger and palm vein images. *Soft Computing*. <https://doi.org/10.1007/s00500-018-3295-6>
- B . K . Shreyamsha Kumar , M . N . S . Swamy (2013). Multiresolution Dct Decomposition For Multifocus Image Fusion, IEEE Department of Electrical and Computer Engineering , Concordia University , Montreal , Canada, 1–4.
- Daugman, J. G. (1993). High confidence visual recognition of persons by a test of statistical independence. *IEEE Transactions on Pattern Analysis and Machine Intelligence*, *15*(11), 1148–1161.
- Elnasir, S., &Shamsuddin, S. M. (2014). Palm Vein Recognition based on 2D-Discrete Wavelet Transform and Linear Discrimination Analysis, *6*(3).
- Fang, Y., Wu, Q., &Kang, W. (2018). A novel finger vein verification system based on two-stream convolutional network learning. *Neurocomputing*, *290*, 100–107. <https://doi.org/10.1016/j.neucom.2018.02.042>

- Giveki, D., Soltanshahi, M. A., &Montazer, G. A. (2017). A new image feature descriptor for content based image retrieval using scale invariant feature transform and local derivative pattern. *Optik*, 131, 242–254.
<https://doi.org/10.1016/j.ijleo.2016.11.046>
- Gurunathan, V., Sathiyapriya, T., &Sudhakar, R. (2016). Multimodal biometric recognition system using SURF algorithm. *2016 10th International Conference on Intelligent Systems and Control (ISCO)*, 1–5.
<https://doi.org/10.1109/ISCO.2016.7727020>
- Han, D., Guo, Z., &Zhang, D. (2008). Multispectral palmprint recognition using wavelet-based image fusion. *International Conference on Signal Processing Proceedings, ICSP*, 2074–2077. <https://doi.org/10.1109/ICOSP.2008.4697553>
- Han, W. Y., &Lee, J. C. (2012). Palm vein recognition using adaptive Gabor filter. *Expert Systems with Applications*, 39(18), 13225–13234.
<https://doi.org/10.1016/j.eswa.2012.05.079>
- Huang, D.-S., Jia, W., &Zhang, D. (2008). Palmprint verification based on principal lines. *Pattern Recognition*, 41(4), 1316–1328.
- Huang, W., &Jing, Z. (2007). Evaluation of focus measures in multi-focus image fusion, 28, 493–500. <https://doi.org/10.1016/j.patrec.2006.09.005>
- Kang, W., Liu, Y., Wu, Q., &Yue, X. (2014a). Contact-free palm-vein recognition based on local invariant features. *PLoS ONE*, 9(5).
<https://doi.org/10.1371/journal.pone.0097548>
- Kang, W., Liu, Y., Wu, Q., &Yue, X. (2014b). Contact-Free Palm-Vein Recognition Based on Local Invariant Features, 9(5).
<https://doi.org/10.1371/journal.pone.0097548>
- Kang, W., &Wu, Q. (2014). Contactless palm vein recognition using a mutual foreground-based local binary pattern. *IEEE Transactions on Information Forensics and Security*, 9(11), 1974–1985.
<https://doi.org/10.1109/TIFS.2014.2361020>
- Kang, W. X., &Deng, F. Q. (2009). Vein image enhancement and segmentation based on maximal intra-neighbor difference. *Acta Opt Sin*, 29, 1830–1837.

- Karami, E., Prasad, S., & Shehata, M. (2015). Image Matching Using SIFT , SURF , BRIEF and ORB : Performance Comparison for Distorted Images Image Matching Using SIFT , SURF , BRIEF and ORB : Performance Comparison for Distorted Images, (February 2016). <https://doi.org/10.13140/RG.2.1.1558.3762>
- Kaur, V., & Kaur, J. (2015). Frequency Partitioning Based Image Fusion for, *6*(4), 3968–3972.
- Kisku, D. R. (2010). Multispectral Palm Image Fusion for Person Authentication using Ant Colony Optimization.
- Kisku, D. R., Rattani, A., Gupta, P., Sing, J. K., & Hwang, C. J. (2012). Human Identity Verification Using Multispectral Palmprint Fusion. *Journal of Signal and Information Processing*, *3*(May), 263–273. <https://doi.org/10.4236/jsip.2012.32036>
- Laboratories, N. A. (2011). Image Fusion Technique using Multi-resolution Singular Value Decomposition, *61*(5), 479–484. <https://doi.org/10.14429/dsj.61.705>
- Ladoux, P.-O., Rosenberger, C., & Dorizzi, B. (2009). Palm vein verification system based on SIFT matching. In *International Conference on Biometrics* (pp. 1290–1298). Springer.
- Ladoux, P. O., Rosenberger, C., & Dorizzi, B. (2009). Palm vein verification system based on SIFT matching. *Lecture Notes in Computer Science (Including Subseries Lecture Notes in Artificial Intelligence and Lecture Notes in Bioinformatics)*, *5558 LNCS*, 1290–1298. https://doi.org/10.1007/978-3-642-01793-3_130
- Lakshmi, K. D., & Vaithyanathan, V. (2017). Image Registration Techniques Based on the Scale Invariant Feature Transform. *IETE Technical Review*, *34*(1), 22–29. <https://doi.org/10.1080/02564602.2016.1141076>
- Lee, J. C. (2012). A novel biometric system based on palm vein image. *Pattern Recognition Letters*, *33*(12), 1520–1528. <https://doi.org/10.1016/j.patrec.2012.04.007>
- Li, W. (2018). Multiple palm features extraction method based on vein and palmprint. *Journal of Ambient Intelligence and Humanized Computing*, *0*(0), 0. <https://doi.org/10.1007/s12652-018-0699-1>
- Lowe, D. G. (2004). Distinctive image features from scale-invariant keypoints. *International Journal of Computer Vision*, *60*(2), 91–110.

- Lu, G.-M., Wang, K.-Q., & Zhang, D. (2004). Wavelet based independent component analysis for palmprint identification. In *Machine Learning and Cybernetics, 2004. Proceedings of 2004 International Conference on* (Vol. 6, pp. 3547–3550). IEEE.
- Lu, G., Zhang, D., & Wang, K. (2003). Palmprint recognition using eigenpalms features. *Pattern Recognition Letters*, 24(9), 1463–1467.
- Lu, L., Zhang, X., Xu, X., & Shang, D. (2017). Multispectral image fusion for illumination-invariant palmprint recognition. <https://doi.org/10.1371/journal.pone.0178432>
- Lu, W., Li, M., & Zhang, L. (2016). Palm Vein Recognition Using Directional Features Derived from Local Binary Patterns, 9(5), 87–98.
- Mallat, S. (1999). *A wavelet tour of signal processing*. Academic press.
- Manmohan, Saxena, J., Teckchandani, K., Pandey, P., Dutta, M. K., Travieso, C. M., & Alonso-Hernandez, J. B. (2015). Palm Vein Recognition using Local Tetra Patterns. *IWOBI 2015 - 2015 International Work Conference on Bio-Inspired Intelligence: Intelligent Systems for Biodiversity Conservation, Proceedings*, 151–156. <https://doi.org/10.1109/IWOBI.2015.7160159>
- Michael, G., Connie, T., Teoh, A., Connie, T., & Teoh, A. (2011). A Contactless Biometric System Using Palm Print and Palm Vein Features. *Image (Rochester, N.Y.)*. <https://doi.org/10.5772/19337>
- Mikolajczyk, K., & Schmid, C. (2005). A performance evaluation of local descriptors. *IEEE Transactions on Pattern Analysis and Machine Intelligence*, 27(10), 1615–1630.
- Mirmohamadsadeghi, L., & Drygajlo, A. (2011). Palm vein recognition with Local Binary Patterns and Local Derivative Patterns. *2011 International Joint Conference on Biometrics, IJCB 2011*. <https://doi.org/10.1109/IJCB.2011.6117804>
- Mishra, D. (2015). Image Fusion Techniques : A Review, 130(9), 7–13.
- Miura, N., Nagasaka, A., & Miyatake, T. (2004). Feature extraction of finger-vein patterns based on repeated line tracking and its application to personal identification. *Machine Vision and Applications*, 15(4), 194–203.

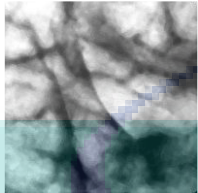
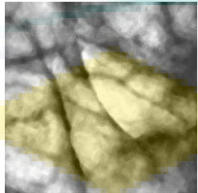
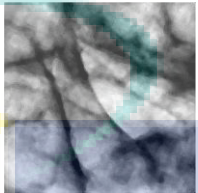
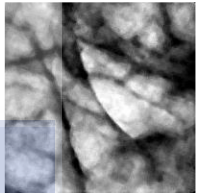
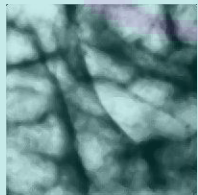
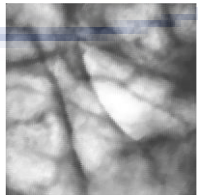
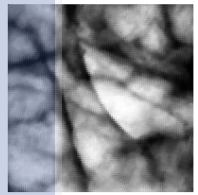
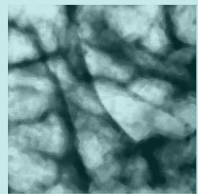
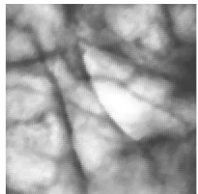
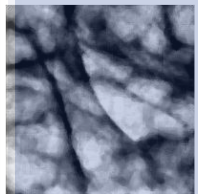
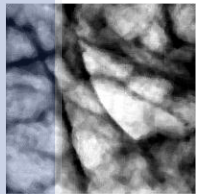
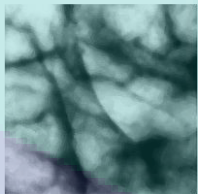
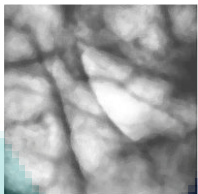
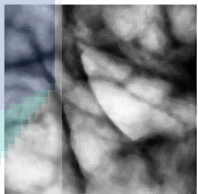
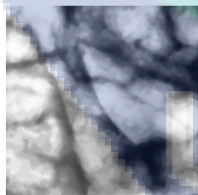
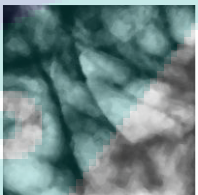
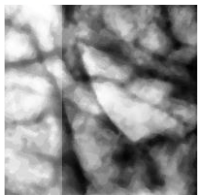
- Miura, N., Nagasaka, A., & Miyatake, T. (2007). Extraction of finger-vein patterns using maximum curvature points in image profiles. *IEICE TRANSACTIONS on Information and Systems*, 90(8), 1185–1194.
- Multispectral Palm Image Fusion For Accurate Contact-Free Palmprint Recognition
National Laboratory of Pattern Recognition , Institute of Automation , CAS.
(2008), 281–284.
- Naidu, V. P. S. (2010). Discrete cosine transform-based image fusion. *Defence Science Journal*, 60(1), 48.
- Naidu, V. P. S. (2013). Novel Image Fusion Techniques using DCT, 5(1), 1–18.
- Naidu, V. P. S., Aerospace, N., & Naidu, V. P. S. (2015). Discrete Cosine Transform-based Image Fusion Discrete Cosine Transform-based Image Fusion, (September). <https://doi.org/10.14429/dsj.60.105>
- Ojala, T., Pietikainen, M., & Maenpaa, T. (2002). Multiresolution gray-scale and rotation invariant texture classification with local binary patterns. *IEEE Transactions on Pattern Analysis and Machine Intelligence*, 24(7), 971–987.
- Palmprint, C. M., & Database, I. (2012.). Note on CASIA Multi-Spectral Palmprint Database, 1–4.
- Pan, M., & Kang, W. (2011). Palm Vein Recognition Based on Three Local Invariant Feature Extraction Algorithms *, 116–124.
- Pandey, N., Verma, P. O. P., & Kumar, A. (2018). A Hand-Based Biometric Verification System Using Ant Colony Optimization, 7(2), 693–717.
- Piciuccio, E., Maiorana, E., & Campisi, P. (2017). Biometric Fusion for Palm-Vein-Based Recognition Systems BT - Digital Communication. Towards a Smart and Secure Future Internet. In A. Piva, I. Tinnirello, & S. Morosi (Eds.) (pp. 18–28). Cham: Springer International Publishing.
- Qiu, X., Kang, W., Tian, S., Jia, W., & Huang, Z. (2017). Finger Vein Presentation Attack Detection Using Total Variation Decomposition. *IEEE Transactions on Information Forensics and Security*, 13(2), 465–477. <https://doi.org/10.1109/TIFS.2017.2756598>
- Rahul, R. C., & Cherian, M. (2015). A Novel MF-LDTP approach for contactless palm vein Recognition, 793–798.

- Rivera, A. R., Castillo, J. R., &Chae, O. (2015). Local directional texture pattern image descriptor. *Pattern Recognition Letters*, 51, 94–100.
- Roopa, B., &Manvi, S. S. (2014). Image Fusion Techniques for Wireless Sensor Networks : Survey.
- Saxena, J., Tec, K., Travieso, C. M., &Alonso-hernández, B. (2015). Palm Vein Recognition using Local Te etra Patterns, 151–156.
- Sharma, M. (2016). A Review : Image Fusion Techniques and Applications, 7(3), 1082–1085.
- Singh, S., &Rajput, R. (2014). Multiple Image Fusion Using Laplacian Pyramid, 3(12), 9442–9446.
- Smorawa, D., &Kubanek, M. (2013.). Biometric Systems Based on Palm Vein Patterns.
- Soh, S. C., Ibrahim, M. Z., &Yakno, M. (2018). A Review: Personal Identification Based on Palm Vein Infrared Pattern. *Journal of Telecommunication, Electronic and Computer Engineering (JTEC)*, 10(1–4), 175–180.
- Soh, S. C., Ibrahim, M. Z., Yakno, M. B., &Mulvaney, D. J. (2018). Palm Vein Recognition Using Scale Invariant Feature Transform with RANSAC Mismatching Removal. In *IT Convergence and Security 2017* (pp. 202–209). Springer.
- Sun, X., Ma, X., Wang, C., Zu, Z., Zheng, S., &Zeng, X. (2017). An Adaptive Contrast Enhancement Method for Palm Vein Image BT - Biometric Recognition. In J.Zhou, Y.Wang, Z.Sun, Y.Xu, L.Shen, J.Feng, ...S.Yu (Eds.) (pp. 240–249). Cham: Springer International Publishing.
- Thamri, E., Aloui, K., &Naceur, M. S. (2018). New approach to extract palmprint lines. *2018 International Conference on Advanced Systems and Electric Technologies (IC_ASET)*, 432–434. <https://doi.org/10.1109/ASET.2018.8379895>
- Vi, C., &Vi, W. G. (2015). An Integrated Ransac And Graph Based Mismatch Elimination Approach For Wide-Baseline Image Matching, *XL*, 23–25. <https://doi.org/10.5194/isprsarchives-XL-1-W5-297-2015>

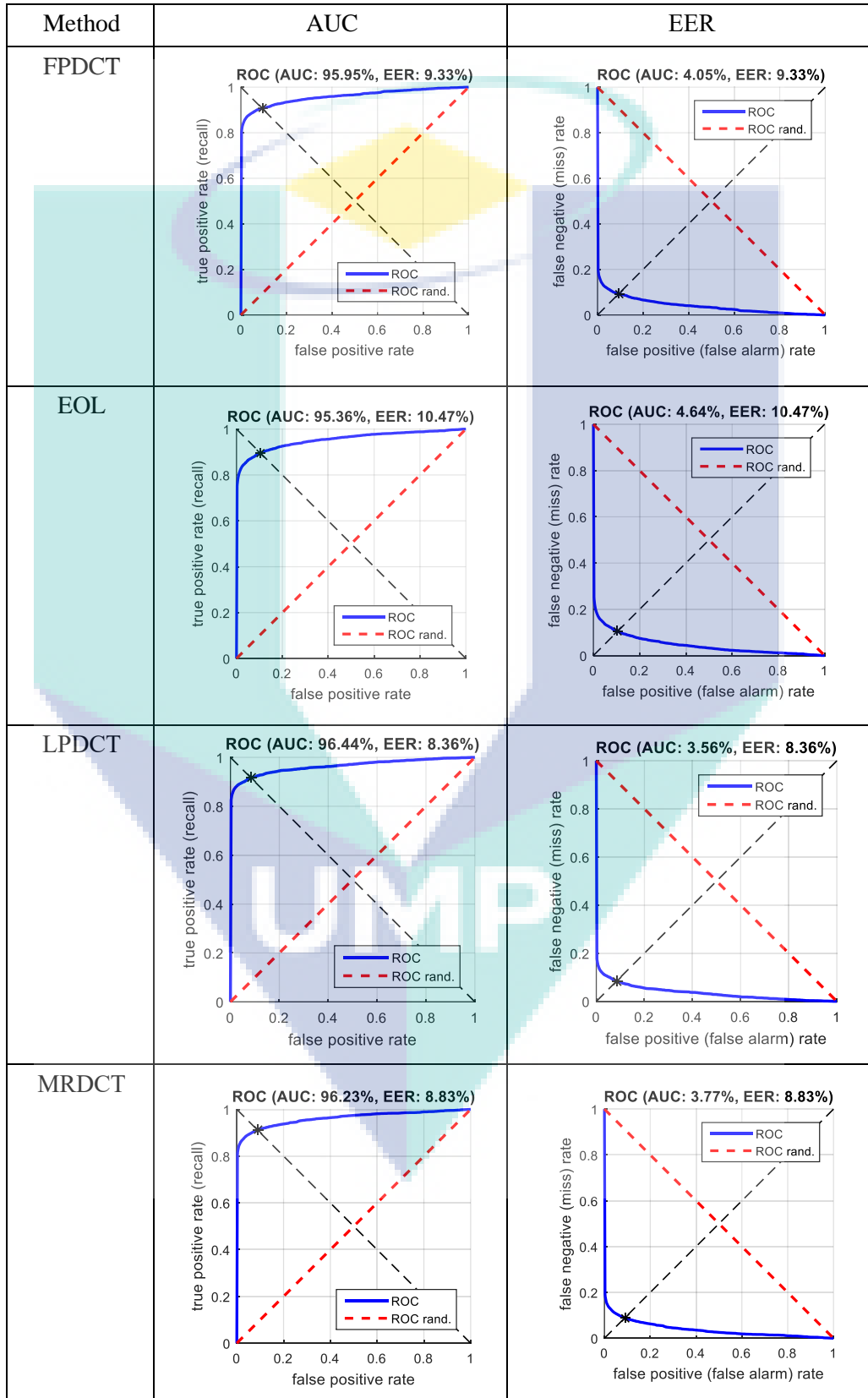
- Victy, Y. A., &Amutha, R. (2014). Discrete Cosine Transform based fusion of multi-focus images for visual sensor networks. *Signal Processing*, 95, 161–170. <https://doi.org/10.1016/j.sigpro.2013.09.001>
- Wang, C., Zeng, X., Sun, X., Dong, W., &Zhu, Z. (2017). Quality assessment on near infrared palm vein image. *Proceedings - 2017 32nd Youth Academic Annual Conference of Chinese Association of Automation, YAC 2017*, 0(1), 1127–1130. <https://doi.org/10.1109/YAC.2017.7967580>
- Wang, L., Leedham, G., &Siu-Yeung Cho, D. (2008). Minutiae feature analysis for infrared hand vein pattern biometrics. *Pattern Recognition*, 41(3), 920–929. <https://doi.org/10.1016/j.patcog.2007.07.012>
- Wu, X., Wang, K., &Zhang, D. (2004a). A novel approach of palm-line extraction. In *Image and Graphics (ICIG'04), Third International Conference on* (pp. 230–233). IEEE.
- Wu, X., Wang, K., &Zhang, D. (2004b). Palmprint recognition using directional line energy feature. In *Pattern Recognition, 2004. ICPR 2004. Proceedings of the 17th International Conference on* (Vol. 4, pp. 475–478). IEEE.
- Wu, X., Zhang, D., &Wang, K. (2003). Fisherpalms based palmprint recognition. *Pattern Recognition Letters*, 24(15), 2829–2838.
- Wu, Y., Ma, W., Gong, M., Su, L., Jiao, L., &Member, S. (2015). A Novel Point-Matching Algorithm Based on Fast Sample Consensus for Image Registration, *12*(1), 43–47.
- Xin, Y., Kong, L., Liu, Z., Wang, C., Zhu, H., Gao, M., ...Xu, X. (2018). Multimodal Feature-Level Fusion for Biometrics Identification System on IoMT Platform. *IEEE Access*, 6, 21418–21426. <https://doi.org/10.1109/ACCESS.2018.2815540>
- Xu, A., &Namit, G. (2008). SURF : Speeded - Up Robust Features. *European Conference on Computer Vision*, 1–30. https://doi.org/10.1007/11744023_32
- Yan, X., Deng, F., &Kang, W. (2015). Palm vein recognition based on multi-algorithm and score-level fusion. *Proceedings - 2014 7th International Symposium on Computational Intelligence and Design, ISCID 2014*, 1, 441–444. <https://doi.org/10.1109/ISCID.2014.93>
- Yan, X., Kang, W., Deng, F., &Wu, Q. (2015a). Neurocomputing Palm vein recognition based on multi-sampling and feature-level fusion. *Neurocomputing*, 151, 798–807. <https://doi.org/10.1016/j.neucom.2014.10.019>

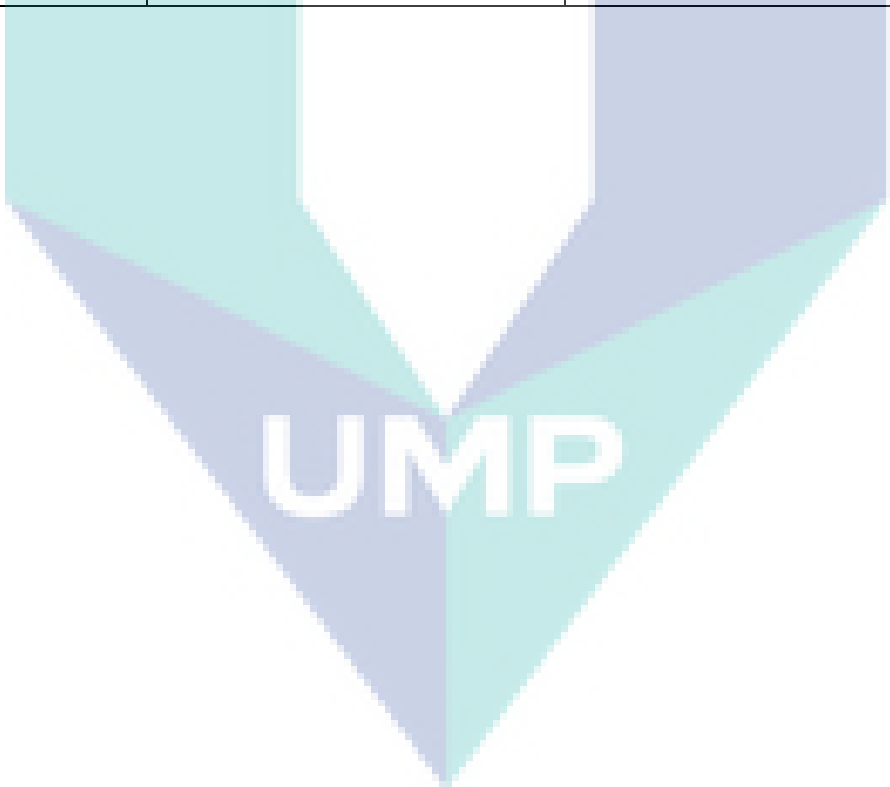
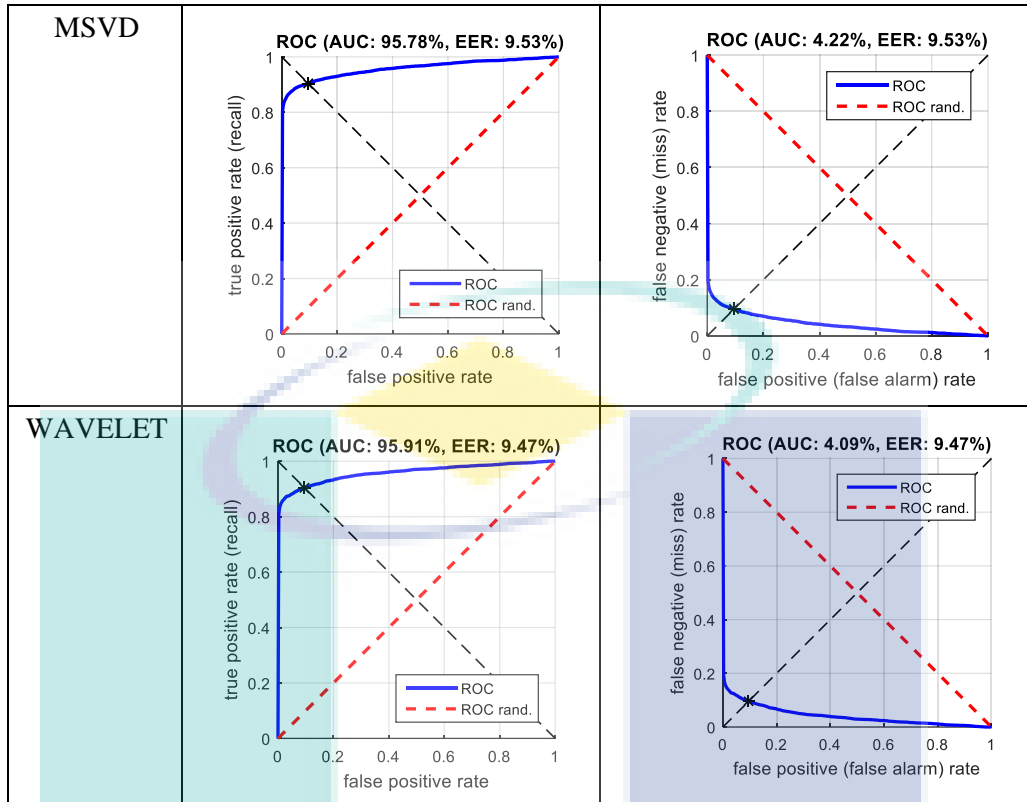
- Yan, X., Kang, W., Deng, F., &Wu, Q. (2015b). Palm vein recognition based on multi-sampling and feature-level fusion. *Neurocomputing*, *151*, 798–807.
<https://doi.org/10.1016/j.neucom.2014.10.019>
- You, J., Li, W., &Zhang, D. (2002). Hierarchical palmprint identification via multiple feature extraction. *Pattern Recognition*, *35*(4), 847–859.
- Zhan, K., Teng, J., Li, Q., &Shi, J. (2015). A novel explicit multi-focus image fusion method A Novel Explicit Multi-focus Image Fusion Method, (January).
- Zhang, D., Kong, W.-K., You, J., &Wong, M. (2003). Online palmprint identification. *IEEE Transactions on Pattern Analysis and Machine Intelligence*, *25*(9), 1041–1050.
- Zhang, H., &Hu, Q. (2011). Fast image matching based-on improved SURF algorithm. *2011 International Conference on Electronics, Communications and Control, ICECC 2011 - Proceedings*, (1), 1460–1463.
<https://doi.org/10.1109/ICECC.2011.6066546>
- Zhang, H., Tang, C., Li, X., Wai, A., &Kong, K. (2015.). A Study of Similarity between Genetically Identical Body Vein Patterns.
- Zhang, X., &Gao, Y. (2009). Face recognition across pose: A review. *Pattern Recognition*, *42*(11), 2876–2896.
- Zhang, Z., &Blum, R. S. (1999). *A Categorization of Multiscale-decomposition-based Image Fusion Schemes with a Performance Study for a Digital Camera Application*.
- Zhou, Y., Kumar, A., &Member, S. (2011). Human Identification Using Palm-Vein Images, *6*(4), 1259–1274.

APPENDIX A
IMAGE FUSION TECHNIQUES IN DUAL COMBINATION OF DIFFERENT
TYPE OF WAVELENGTH SPECTRUM

Method	700 nm with 850 nm	700 nm with 940 nm	850 nm with 940 nm	700 nm, 850 nm and 940 nm
MRDCT				
MSVD				
LPDCT				
WAVELET				
EOL				

APPENDIX B
EER AND AUC FOR IMAGE FUSION IN DUAL COMBINATION OF 700 NM
AND 850 NM WAVELENGTH SPECTRUM



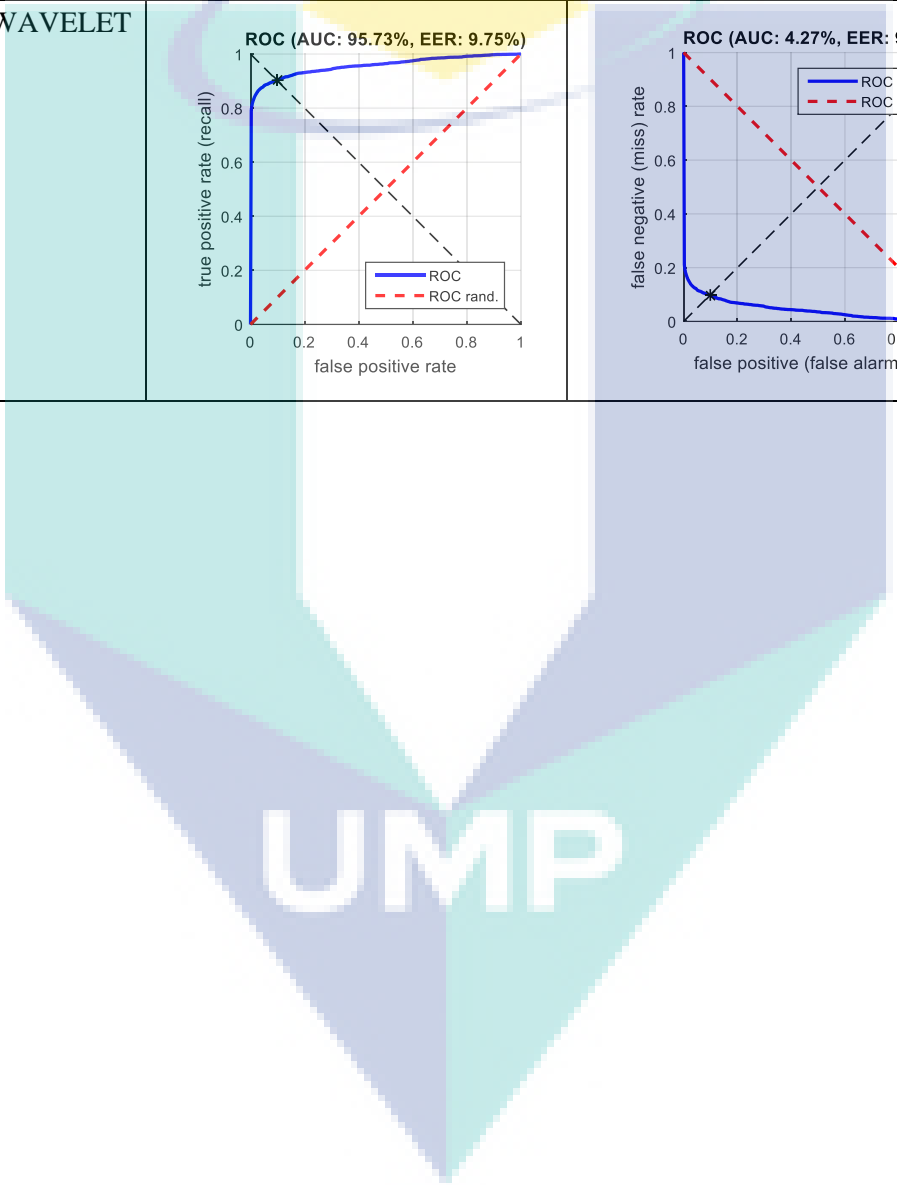
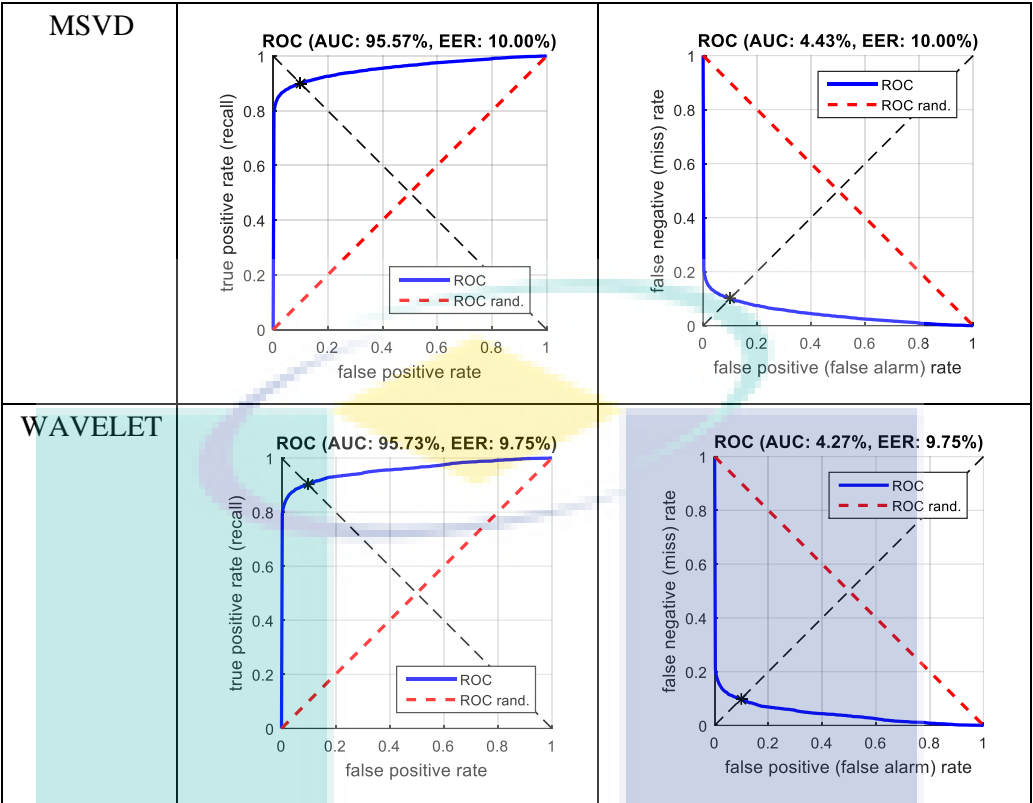


UMP

APPENDIX C

EER AND AUC FOR IMAGE FUSION IN DUAL COMBINATION OF 700 NM AND 940 NM WAVELENGTH SPECTRUM

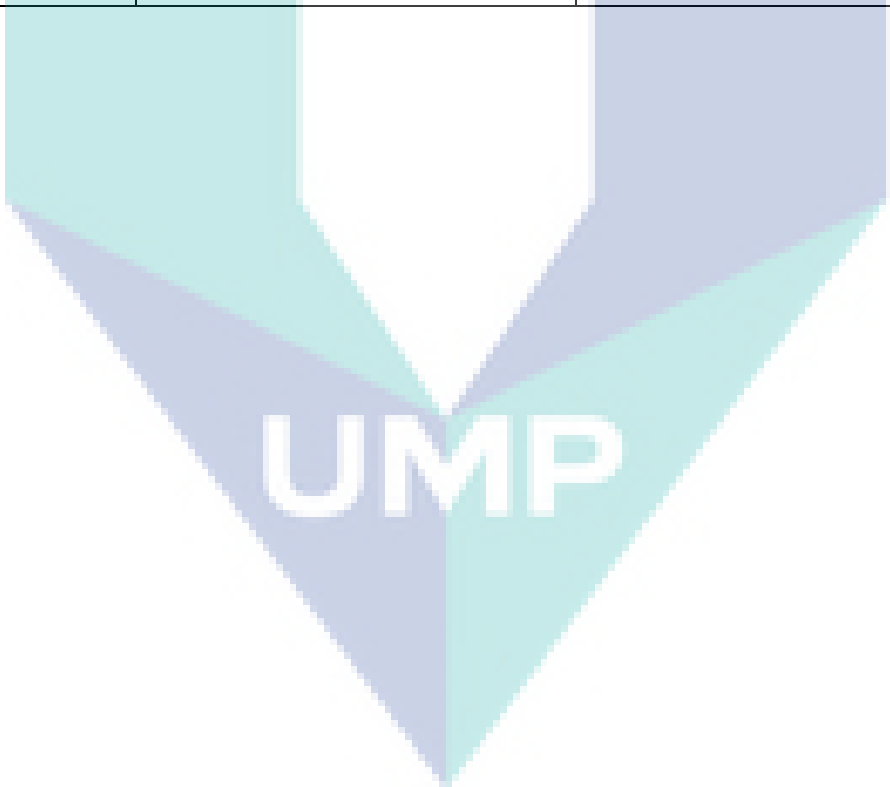
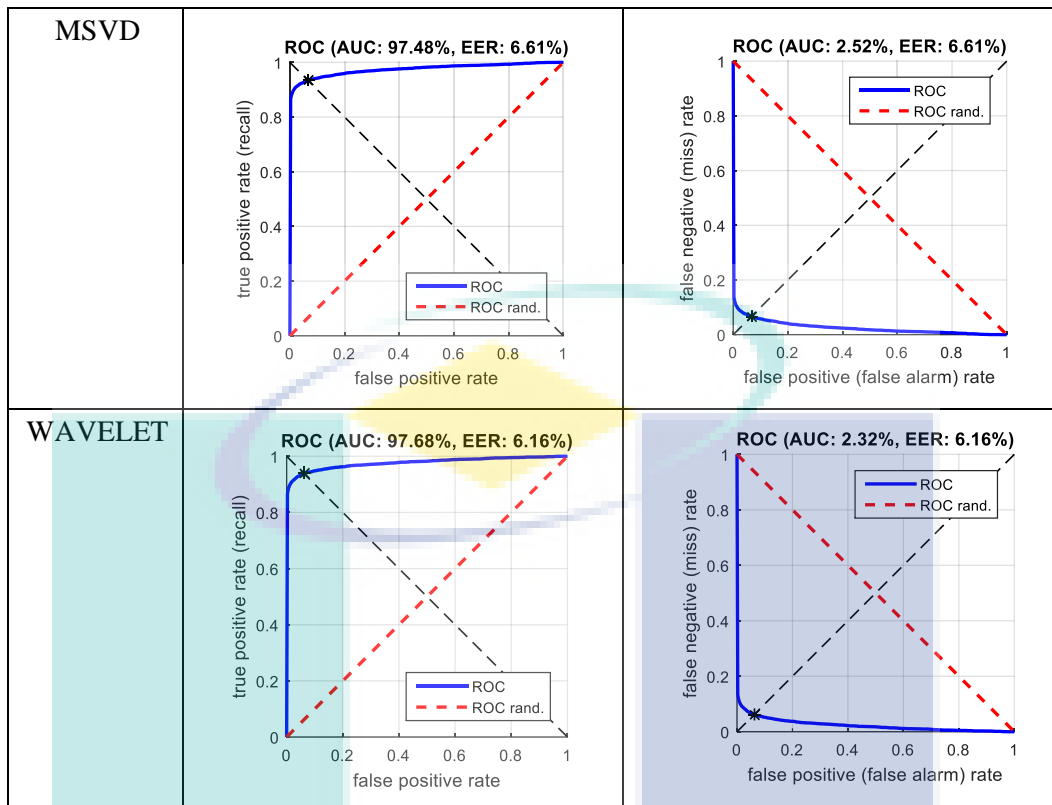
Method	AUC	EER
FPDCT	<p>ROC (AUC: 95.90%, EER: 9.56%)</p> <p>Y-axis: true positive rate (recall)</p> <p>X-axis: false positive rate</p> <p>Legend: ROC (solid blue), ROC rand. (dashed red)</p>	<p>ROC (AUC: 4.10%, EER: 9.56%)</p> <p>Y-axis: false negative (miss) rate</p> <p>X-axis: false positive (false alarm) rate</p> <p>Legend: ROC (solid blue), ROC rand. (dashed red)</p>
EOL	<p>ROC (AUC: 96.70%, EER: 8.47%)</p> <p>Y-axis: true positive rate (recall)</p> <p>X-axis: false positive rate</p> <p>Legend: ROC (solid blue), ROC rand. (dashed red)</p>	<p>ROC (AUC: 3.30%, EER: 8.47%)</p> <p>Y-axis: false negative (miss) rate</p> <p>X-axis: false positive (false alarm) rate</p> <p>Legend: ROC (solid blue), ROC rand. (dashed red)</p>
LPDCT	<p>ROC (AUC: 95.96%, EER: 9.06%)</p> <p>Y-axis: true positive rate (recall)</p> <p>X-axis: false positive rate</p> <p>Legend: ROC (solid blue), ROC rand. (dashed red)</p>	<p>ROC (AUC: 4.04%, EER: 9.06%)</p> <p>Y-axis: false negative (miss) rate</p> <p>X-axis: false positive (false alarm) rate</p> <p>Legend: ROC (solid blue), ROC rand. (dashed red)</p>
MRDCT	<p>ROC (AUC: 95.77%, EER: 9.65%)</p> <p>Y-axis: true positive rate (recall)</p> <p>X-axis: false positive rate</p> <p>Legend: ROC (solid blue), ROC rand. (dashed red)</p>	<p>ROC (AUC: 4.23%, EER: 9.65%)</p> <p>Y-axis: false negative (miss) rate</p> <p>X-axis: false positive (false alarm) rate</p> <p>Legend: ROC (solid blue), ROC rand. (dashed red)</p>



UMP

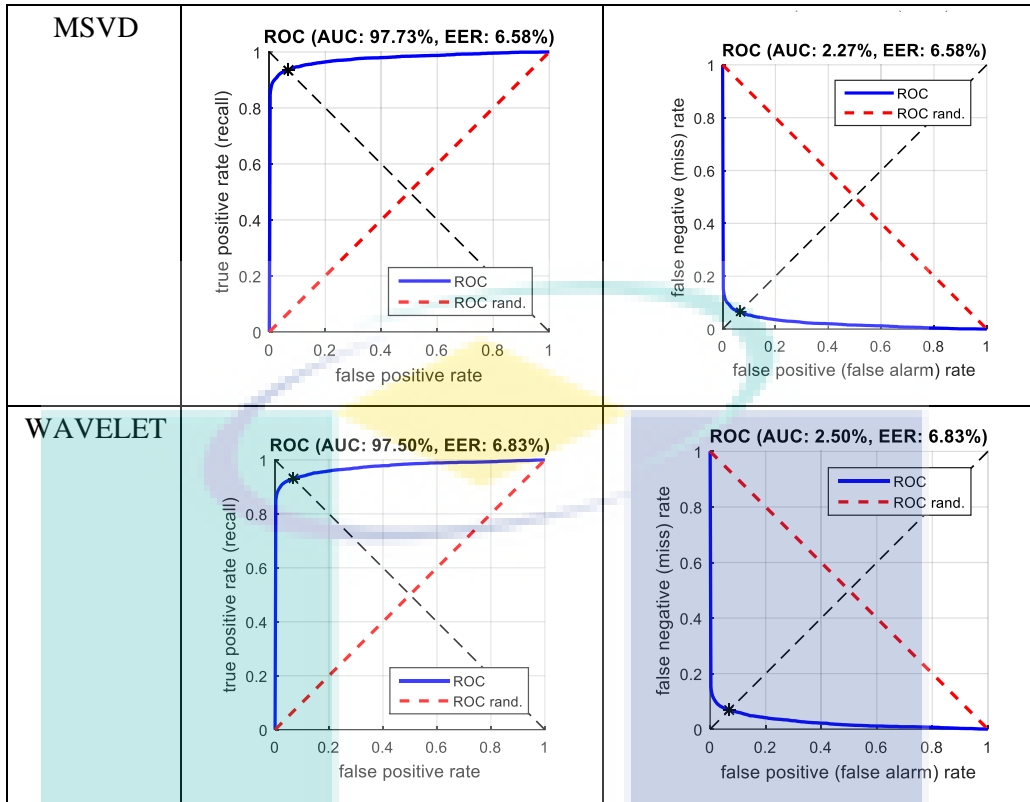
APPENDIX D
EER AND AUC FOR IMAGE FUSION IN DUAL COMBINATION OF 850 NM
AND 940 NM WAVELENGTH SPECTRUM

Method	AUC	EER
FPDCT	<p>ROC (AUC: 97.61%, EER: 6.47%)</p> <p>Y-axis: true positive rate (recall) X-axis: false positive rate</p>	<p>ROC (AUC: 2.39%, EER: 6.47%)</p> <p>Y-axis: false negative (miss) rate X-axis: false positive (false alarm) rate</p>
EOL	<p>ROC (AUC: 97.43%, EER: 6.99%)</p> <p>Y-axis: true positive rate (recall) X-axis: false positive rate</p>	<p>ROC (AUC: 2.57%, EER: 6.99%)</p> <p>Y-axis: false negative (miss) rate X-axis: false positive (false alarm) rate</p>
LPDCT	<p>ROC (AUC: 98.01%, EER: 6.08%)</p> <p>Y-axis: true positive rate (recall) X-axis: false positive rate</p>	<p>ROC (AUC: 1.99%, EER: 6.08%)</p> <p>Y-axis: false negative (miss) rate X-axis: false positive (false alarm) rate</p>
MRDCT	<p>ROC (AUC: 97.91%, EER: 5.83%)</p> <p>Y-axis: true positive rate (recall) X-axis: false positive rate</p>	<p>ROC (AUC: 2.09%, EER: 5.83%)</p> <p>Y-axis: false negative (miss) rate X-axis: false positive (false alarm) rate</p>



APPENDIX E
EER AND AUC FOR IMAGE FUSION IN TRIPLE COMBINATION OF
700 NM , 850 NM AND 940 NM WAVELENGTH SPECTRUM

Method	AUC	EER
FPDCT	<p>ROC (AUC: 97.57%, EER: 6.76%)</p>	<p>ROC (AUC: 2.43%, EER: 6.76%)</p>
EOL	<p>ROC (AUC: 96.55%, EER: 8.64%)</p>	<p>ROC (AUC: 3.45%, EER: 8.64%)</p>
LPDCT	<p>ROC (AUC: 98.10%, EER: 6.11%)</p>	<p>ROC (AUC: 98.10%, EER: 6.11%)</p>
MRDCT	<p>ROC (AUC: 98.11%, EER: 5.53%)</p>	<p>ROC (AUC: 1.89%, EER: 5.53%)</p>



UMP

